On the role of the random density fluctuations in the generation of the type III solar radio bursts

Anna Tkachenko

UNIVERSITÉ D'ORLÉANS

ÉCOLE DOCTORALE ÉNERGIE, MATÉRIAUX, SCIENCES DE LA TERRE ET DE L'UNIVERS

Laboratoire de Physique et Chimie de l'Environnement et l'Espace (LPC2E)

THÈSE présentée par :

Anna Tkachenko

soutenue le : **28 mai 2021**

pour obtenir le grade de : **Docteur de l'Université d'Orléans**

Discipline/ Spécialité : Sciences de l 'Univers

Le rôle des fluctuations aléatoires de densité dans la génération des sursauts radio solaires de type III

THÈSE dirigée par :

M. Krasnoselskikh Vladimir	Directeur de recherche émérite, LPC2E / CNRS

RAPPORTEURS :

M. Voitenko Yuriy	Senior Scientist, Royal Belgian Institute for Space Aeronomy
M. Zimbardo Gaetano	Professeur associé, Università della Calabria

---

JURY :

M. Bale Stuart	Professeur, University of California
M. Dudok de Wit Thierry	Professeur, LPC2E / CNRS, Universté d'Orléans
M. Krasnoselskikh Vladimir	Directeur de recherche émérite, LPC2E / CNRS
M. Kretzschmar Matthieu	Maître de conférences, LPC2E / CNRS, Université d'Orléans
M. Maksimovic Milan	Directeur de recherche, LESIA / Observatoire de Paris
M. Voitenko Yuriy	Senior Scientist, Royal Belgian Institute for Space Aeronomy
M. Zimbardo Gaetano	Professeur associé, Università della Calabria

To Eugene

Abstract

Type III solar radio bursts are among the most intense radio emissions in the solar system. The production of a such emission is a multi-stage process which includes the generation of the Langmuir waves by the energetic electron beam and further conversion of the Langmuir waves into electromagnetic emission at a fundamental frequency or its harmonic by means of various mechanisms. Random density fluctuations in solar wind plasma are ubiquitous and play an important role in the processes that determine the generation of an electromagnetic emission associated with type III (and type II) solar radio bursts. In the current manuscript we have attempted to summarize various contributions as well as introduce some new results in order to cover the problem of the role of density fluctuations in the formation of type III radio emissions in the most complete manner.

First we start with the theory of beam-plasma interaction, and provide unambiguous arguments that density fluctuations may alter the interaction of the electron beam and plasma waves in such a way that the predictions of the theory come to a good agreement with the observations. We emphasize that the recent probabilistic model of a beam-plasma interaction allows to obtain plausible predictions of the energy density of the Langmuir waves that are typically observed at 1 a.u. by making use of the probability distributions of plasma density fluctuations.

Several mechanisms have been suggested in order to explain the subsequent generation of radio emission at a fundamental frequency. We consider them in detail and show that according to the recent findings the linear mode conversion of the Langmuir wave into electromagnetic wave that occurs during the reflection of the Langmuir wave from density inhomogeneities, may be a dominant process in the framework of the fundamental type III emission.

But the reflections from the density inhomogeneities may be very important for the generation harmonic emission as well, as it requires the presence of the forwards and backwards moving Langmuir waves. We revisit the conventional mechanism of coalescence of a primarily generated and a back-scattered Langmuir waves in a quasihomogeneous plasma and show that the resulting harmonic emissions are significantly more intense than found in previous studies. Additionally, we propose and investigate another mechanism: the nonlinear coupling of incident and reflected Langmuir waves inside localized regions with higher plasma density, in the close vicinity of the reflection point. We use the results of a probabilistic model of beam–plasma interaction and evaluate the efficiency of energy transfer from Langmuir waves to the harmonic electromagnetic emission. The efficiency of Langmuir wave conversion into electromagnetic harmonic emission is inferred to be higher at large heliospheric distances for the mechanism operating in quasihomogeneous plasma and at small heliocentric distances for the one operating in inhomogeneous plasma. The evaluation of emission intensity in a quasihomogeneous plasma may also be applied to type II solar radio bursts. The radiation pattern in both cases is quadrupolar, and we show that emission from density inhomogeneities may efficiently contribute to the visibility of harmonic radio emission, what comes in a good agreement with the observations.

And finally, we analyze the density fluctuations, measured *in situ* inside the source regions of the type III radio bursts by a Parker Solar Probe spacecraft. We investigate various statistical properties of such density fluctuations.

Résumé

Les sursauts radio solaires de type III sont parmi les émissions radio les plus intenses du système solaire. La production d'une telle émission est un processus en plusieurs étapes qui comprend la génération des ondes de Langmuir par le faisceau d'électrons énergétiques et la conversion ultérieure des ondes de Langmuir en émission électromagnétique à une fréquence fondamentale ou son harmonique au moyen de divers mécanismes. Les fluctuations aléatoires de la densité du plasma du vent solaire sont omniprésentes et jouent un rôle important dans les processus qui déterminent la génération d'une émission électromagnétique associée aux sursauts radio solaires de type III (et de type II). Dans le présent manuscrit, nous avons tenté de résumer diverses contributions ainsi que d'introduire de nouveaux résultats afin de couvrir le problème du rôle des fluctuations de densité dans la formation des émissions radio de type III de la manière la plus complète.

Tout d'abord, nous commençons par la théorie de l'interaction faisceau-plasma et fournissons des arguments sans équivoque selon lesquels les fluctuations de densité peuvent modifier l'interaction du faisceau d'électrons et des ondes de plasma de telle sorte que les prédictions de la théorie s'accordent bien avec les observations. Nous soulignons que le modèle probabiliste récent d'une interaction faisceau-plasma permet d'obtenir des prédictions plausibles de la densité d'énergie des ondes de Langmuir qui sont typiquement observées à 1 u.a. en utilisant les distributions de probabilité des fluctuations de densité du plasma.

Plusieurs mécanismes ont été suggérés pour expliquer la génération ultérieure d'émission radio à une fréquence fondamentale. Nous les examinons en détail et montrons que, selon les découvertes récentes, la conversion de mode linéaire de l'onde de Langmuir en onde électromagnétique qui se produit lors de la réflexion de l'onde de Langmuir à partir des inhomogénéités de densité, peut être un processus dominant dans le cadre d'émission fondamentale de type III.

Mais les réflexions provenant des inhomogénéités de densité peuvent également être très importantes pour l'émission harmonique de génération, car elles nécessitent la présence d'ondes de Langmuir se déplaçant vers l'avant et vers l'arrière. Nous revisitons le mécanisme conventionnel de coalescence des ondes de Langmuir principalement générées et rétrodiffusées dans un plasma quasi homogène et montrons que les émissions harmoniques résultantes sont significativement plus intenses que celles trouvées dans les études précédentes. De plus, nous proposons et étudions un autre mécanisme: le couplage non linéaire des ondes de Langmuir incidentes et réfléchies à l'intérieur de régions localisées avec une densité de plasma plus élevée, à proximité immédiate du point de réflexion. Nous utilisons les résultats d'un modèle probabiliste d'interaction faisceau-plasma et évaluons l'efficacité du transfert d'énergie des ondes de Langmuir vers l'émission électromagnétique harmonique. On déduit que l'efficacité de la conversion des ondes de Langmuir en émission harmonique est plus élevée à de grandes distances héliosphériques pour le mécanisme fonctionnant dans un plasma quasi homogène et à de petites distances héliocentriques pour celui fonctionnant dans un plasma inhomogène. L'évaluation de l'intensité d'émission dans un plasma quasi homogène peut également s'appliquer aux sursauts radio solaires de type II. Le diagramme de rayonnement dans les deux cas est quadrupolaire, et nous montrons que l'émission des inhomogénéités de densité peut contribuer efficacement à la visibilité de l'émission radio harmonique, ce qui est en bon accord avec les observations.

Et enfin, nous analysons les fluctuations de densité, mesurées *in situ* à l'intérieur des régions sources des sursauts radio de type III par la sonde spatiale Parker Solar Probe. Nous étudions diverses propriétés statistiques de ces fluctuations de densité.

Acronyms and Super/Subscripts

a.u.	astronomical unit	l / t	refers to Langmuir wave / EM wave
EM	electromagnetic		
PDF	probability density function	e / i / b	refers to electrons, ions, electron beam
PSD	power spectral density		
QLT	quasi-linear theory	$homog$ / $inhom$	refers to a homogeneous / inhomogeneous plasma
SGT	stochastic growth theory		
LMC	linear mode conversion	i / r	refers to incident / reflected Langmuir wave
HOA	head-on approximation		
PSP	Parker Solar Probe	ω_{p_e} / $2\omega_{p_e}$	refers to a fundamental / harmonic EM emission

Symbols

ω_{p_e} / ω_l / ω_t	electron plasma frequency / Langmuir wave frequency / EM wave frequency
n / n_e $\{n_0\}$ / n_b	number density of plasma / electrons {average on a given interval} / electron beam
λ_D ; N_D	Debye length ; number of particles in Debye sphere
T / T_e / T_i	temperature of plasma / electrons / ions
k_l / k_t	wavenumber of Langmuir wave / EM wave
δn $\{\langle \Delta n \rangle\}$; $P_{\delta n}(\delta n)$	density fluctuation {its standard deviation} ; its PDF
$f(v)$ $\{f(v_e)\}$	distribution function of particles {electrons} in a velocity space
E / H ; J ; A	amplitude of the electric / magnetic field ; current density ; vector potential of magnetic field
v_T / v_b $\{\Delta v_b\}$	electron thermal velocity / initial electron beam velocity {its thermal spread}
ψ ; $P_\psi(\psi)$	angle between Langmuir wave wavevector and magnetic field direction or density gradient direction (often equivalent) ; its PDF
L $\{L_{sc}\}$; $P_L(L)$	characteristic spatial scale of a density gradient inside density fluctuations {characteristic scale of a PDF of scales L, inferred from observations}; its PDF
V_{ph} / V_{gr}	phase velocity / group velocity of a Langmuir wave
N_l / N_t	number of wave quanta of Langmuir waves / EM waves
W_l / W_t	energy density of Langmuir waves / EM waves
γ ; D	growth rate of the waves; coefficient of diffusion of particles in velocity space
P_{ref}	the probability of the reflection of the Langmuir wave in an inhomogeneous plasma
$K_{\omega_{p_e}}$ / $K_{2\omega_{p_e}}$	efficiency of Langmuir waves conversion into EM emission at fundamental / harmonic frequency

CGS units were used throughout the manuscript unless other specified

Contents

Chapter 1

Introduction

This manuscript is dedicated to the investigation and general outlook on the role of the ubiquitous plasma density fluctuations in the formation of the radio emission of type III, and where applicable, type II solar radio bursts. We trace all the main stages that constitute the process of generation of type III emission. First we start with the electron beam, that is generated by an eruptive solar event, and propagates into the inner heliosphere exciting the plasma waves. We mention numerous studies that have contributed to the discovery of the physical picture of this process, both theoretical and observational; and after we discuss one of the latest models that allows to describe this phenomenon most closely to the observational evidence and takes into account the presence of density fluctuations in solar wind. After we give a credit to the studies that have been performed in order to illustrate the generation of the electromagnetic (EM) emission on the fundamental frequency by the plasma waves, notably those which have accounted for the variations of the background density of plasma. And finally we dedicate two Chapters of the current manuscript to the new investigation, performed in the framework of a study of the harmonic radio emission by plasma waves in presence of the random density fluctuations. The conclusions, made at the end of the manuscript aim to sum up the contributions to the theory of the formation of type III solar radio bursts in a

turbulent inhomogeneous plasma.

1.1 Type III radio bursts

1.1.1 General definition

Type III solar radio bursts are among to the most intense radio emissions in solar system. They are associated with the electron beam that is accelerated at the reconnection sites during the solar flare and propagates away from the Sun along an opened magnetic field line. On the way the kinetic energy of the electrons in the beam is partially converted to EM radio emission at a local electron plasma frequency ω_{p_e}, often referred to as $f_{p_e} = \omega_{p_e}/2\pi$ (fundamental), or at $2\omega_{p_e}$ and higher (harmonic). For this reason in observations the radiation starts at high frequencies and quickly descends to lower frequencies. The starting and stopping frequencies of type IIIs are varying from burst to burst. The total frequency extend is between $\sim$ GHz and $\sim$ 10 kHz, where 20 kHz corresponds to plasma frequency at around 1 a.u. Those bursts that are observed at frequencies lower then $\sim$ 1 MHz ($\approx 7R_\odot$) are considered as interplanetary. Type IIIs are characterized by extremely fast average frequency drift rate df/dt and the duration of the bursts varies as a function of the inverse frequency. Thus they are typically observed during dozens of minutes (e.g. see Fig.1.1) but may also extend up to a few days as a radio storm, i.e. when multiple faint bursts are observed quasi-continuously (Reid & Ratcliffe, 2014).

There is a big observational base of radio bursts of type III, made by spacecrafts (e.g. *WIND, STEREO, PSP*), as well as by ground-based radio telescopes (e.g. LOFAR, Nançay), which cover various frequency ranges. Type IIIs, due to their mechanism of generation, are a powerful tool for diagnostics of coronal and solar wind plasma, as well as for tracking energetic electron beams (Mann et al., 2018).

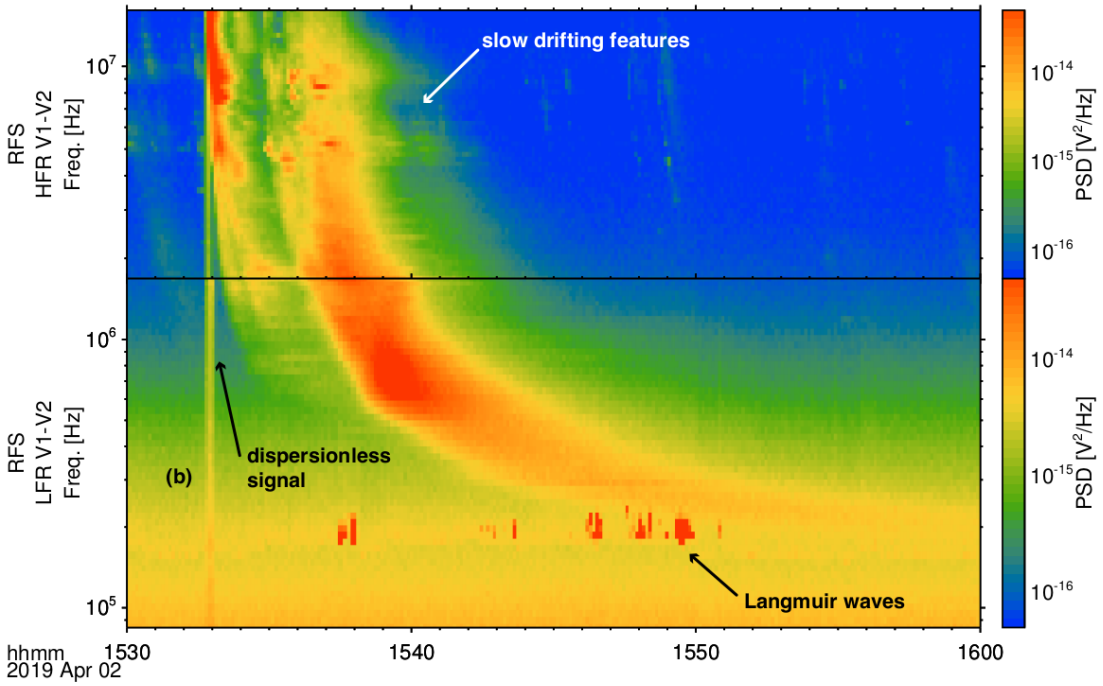

Figure 1.1: A type III solar radio burst observed by Parker Solar Probe during in April 2019 (Pulupa et al., 2020).

1.1.2 Harmonic structure

In their majority, type IIIs exhibit harmonic structure. If observed simultaneously, fundamental (F) and harmonic (H) components may be distinguished at decametric or shorter wavelengths (coronal plasma frequency range). There F component is normally more intense and has a 2-3 times higher degree of circular polarization than H component (Dulk & Suzuki, 1980). Above around 100 MHz type IIIs generally do not show two separate components and the emission is thought to be purely harmonic. For interplanetary bursts it is almost impossible to distinguish components in time and frequency or by polarization (Krupar et al., 2020) except for rare cases when electron beams are observed *in situ* by spacecrafts (Kellogg, 1980; Dulk et al., 1998).

1.1.3 Mechanisms of emission

Radio emissions in the inner heliosphere, associated with extreme space weather events, such as solar flares, are generated via plasma emission mechanism first suggested by Ginzburg & Zheleznyakov (1958). Generally, it can be described as consisting of two steps: a beam of electrons, accelerated at the reconnection sites of solar flare or excited by coronal mass ejections (CMEs) driven shockwaves, is propagating from the Sun along the opened magnetic field line. On its way it interacts with ambient plasma, generating Langmuir waves via the *bump-on-tail* instability. These waves in their turn, may transfer part of their energy into EM radio emission (see Fig.1.2). This two-step process is widely recognized as the one responsible for generation of type II and type III solar radio bursts (Reid & Ratcliffe, 2014).

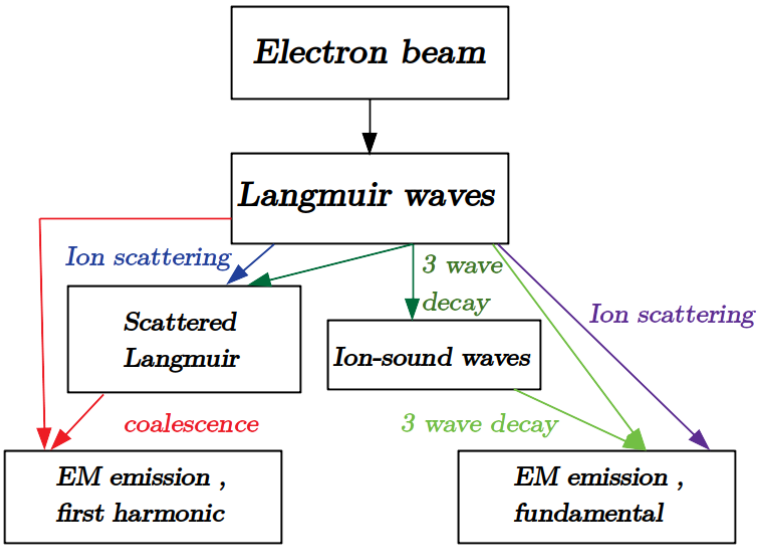

Figure 1.2: A flow diagram indicating the possible mechanisms and stages of production of EM emission in plasma according to an updated version of the original plasma emission theory (adapted from (Reid & Ratcliffe, 2014; Melrose, 2008)).

1.1.4 Electron beams in solar wind

The early *in situ* simultaneous observations of electron beams, associated plasma waves and radio emissions of type III solar radio bursts have shown that type IIIs are

generated by $\sim 1 \div 10^2$ keV electrons (Lin et al., 1981; Lin, 1985; Ergun et al., 1998; Malaspina & Ergun, 2008; Krucker et al., 2009). Observations have revealed that the spatial electron distributions in such beams are highly anisotropic and are directed along the background magnetic field lines. Interestingly, these beams are typically bi-directional at the moment of generation, triggering the hard X-ray bremsstrahlung emission in the direction of movement towards the Sun and a radio emission moving outwards. The beams often exhibit a scatter-free velocity dispersion, making the faster particles arrive earlier than the slower ones (see Fig.1.3). The presence of the beam in a plasma perturbs the equilibrium state and leads to an instability, when the unbalanced electron distribution function triggers the growth of the Langmuir waves well above the thermal noise level.

1.1.5 Langmuir waves

Langmuir waves are the most ubiquitous and common type of waves naturally present in plasma. In a plasma being a mixture of electrons, ions, neutral particles, electric and magnetic fields, various oscillations are occurring all the time as it tends to remain quasi-neutral. For instance, any small deviation from the equilibrium state may cause a change in a self-consistent electric field, which, in turn, will force the particles (especially and notably electrons, as they are the lightest) to be displaced from their initial positions (here the term 'initial' is very nominal, as particles and fields in plasma constantly tend to remain in equilibrium with one another and thus compensate to any deviations from it; for this reason in plasma there are always numerous modes of oscillations present at a thermal noise level). After the displacement of the electrons the local separation of charges will generate an electric field that will force the electrons to come back, but, due to their momentum they will overshoot the equilibrium position and consequently generate an opposite directed electric field. The procedure will repeat again and again and a propagating version of such longitudinal electrostatic oscillations, triggered by the variations of

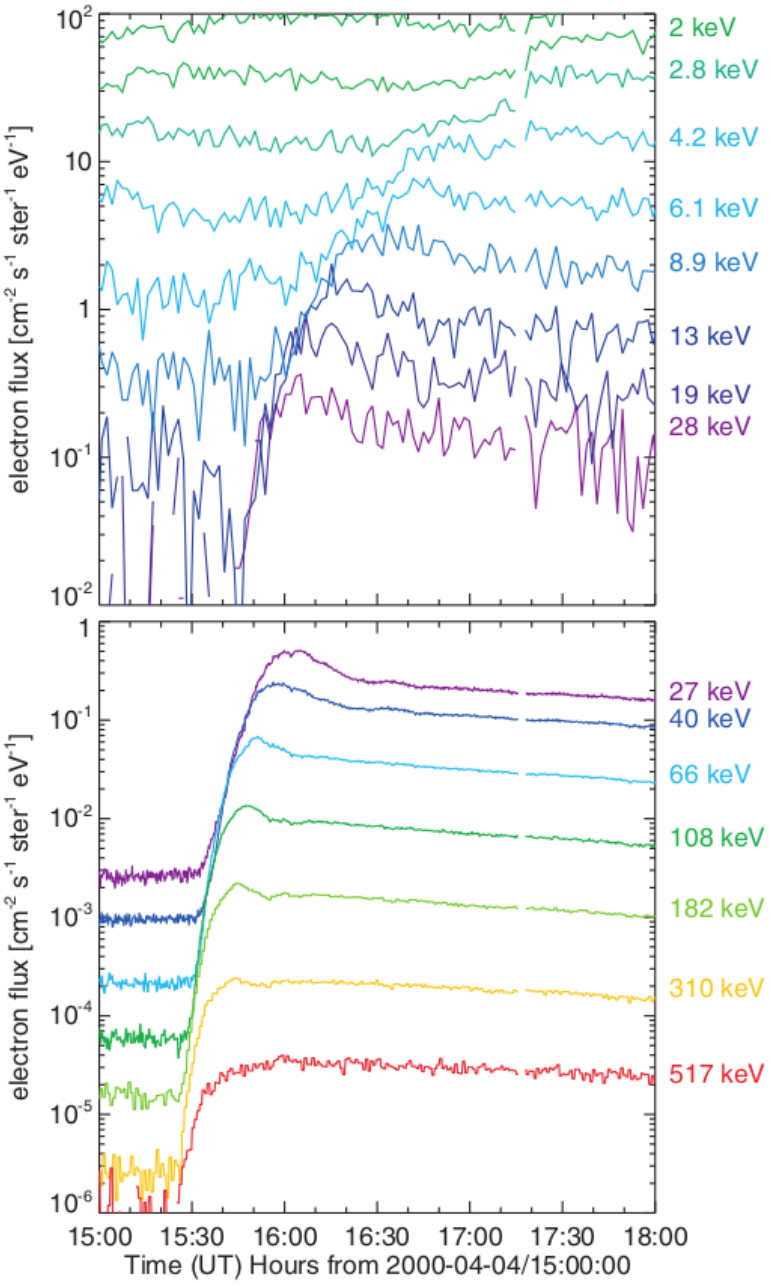

Figure 1.3: Example of a typical solar impulsive electron event observed by two different instruments on board the *WIND* spacecraft. Time profiles at different energies as indicated with colors. The top panel shows data from the electrostatic analyzer, and the bottom panel shows data from the solid-state telescope (with much higher sensitivity) (Krucker et al., 2009).

plasma's electron density is called the Langmuir wave. Its dispersion relation is:

$$\omega_l^2 = \omega_{p_e}^2 + 3k_l^2 v_T^2, \tag{1.1}$$

where ω_l is the angular frequency of the Langmuir wave, v_T is the thermal velocity of electrons in plasma, k_l is the module of a wavevector (wavenumber) of the wave. As the $3k_l^2 v_T^2$ term, which is called *dispersion* of the waves, is very often much smaller than the plasma frequency, a simplified version of a dispersion relation is normally used, namely

$$\omega_l^2 = \omega_{p_e}^2(1 + 3k_l^2\lambda_D^2) \rightarrow \omega_l \approx \omega_{p_e}\sqrt{1 + \frac{3}{2}k_l^2\lambda_D^2}, \tag{1.2}$$

here we have used the definition of the electron Debye radius $\lambda_D = v_T/\omega_{p_e}$, and the fact that $3k_l^2\lambda_D^2 \ll 1$, which we will mention many times throughout this manuscript. In the case of a 'cold' plasma when electron thermal velocity is small, the dispersion term in Eq.(1.2) can be omitted, and it is said that the Langmuir waves oscillate with a plasma frequency. This approximation will be used as well in some of our calculations presented here.

1.1.6 Parametric instability

Plasma as a medium consists not only of a large number of charged particles, but also of a large number of elementary modes of oscillations, which are characterized by their own wavenumber and frequency. In equilibrium state of plasma, these oscillations exist on the level of thermal fluctuations. When the deviations from the equilibrium state occur (electric current in plasma, a beam of fast particles etc.) some oscillations may be amplified to a significant level as a result of a certain instability. If the amplitudes of oscillations are small, they can be considered as harmonic and independent one from another. But when the amplitude becomes large enough, the nonlinear effects are no longer negligible and a connection between the

modes of oscillations occurs. One of the forms of such connection is the parametric instability (or *parametric decay*).

Let us say that there is an oscillation with a finite amplitude above the thermal level, excited in plasma. Such wave is called a pump wave (or a driver). In this case, small oscillations (perturbations) in plasma may be amplified due to the presence of the pump wave, if the resonance conditions, similar to the conditions of parametric resonance in mechanics, are satisfied. In this case the pump wave transfers its energy to two daughter waves and thus it is considered as a decay of a pump wave, however, in general the energy can be transferred both ways. If the pump wave has a frequency ω_0 and a wavevector $\mathbf{k}_0$, the two waves with frequencies ω_1 and ω_2 and wavevectors $\mathbf{k}_1$ and $\mathbf{k}_2$, may be amplified if

$$\begin{cases} \omega_0 = \omega_1 + \omega_2, \\ \mathbf{k}_0 = \mathbf{k}_1 + \mathbf{k}_2. \end{cases} \tag{1.3}$$

In fact, more than two waves might be amplified, but with the increasing number of waves, it becomes much harder to simultaneously satisfy both the resonance conditions. The Eqs.(1.3) may be also interpreted as the laws of energy and momentum conservation, if we treat the oscillation modes as the quasi-particles with the energy $\epsilon = \hbar\omega$ and momentum $\mathbf{p} = \hbar\mathbf{k}$.

1.1.7 Generation of fundamental electromagnetic emission

According to conventional plasma emission mechanism, the EM emission at a fundamental frequency is generated due to the Reyleigh scattering of Langmuir waves by plasma thermal ions (Ginzburg & Zheleznyakov, 1958). However, some of the observed properties of the type III radio emissions were not fully explained by the plasma emission mechanism. This has led to numerous revisions of the initial theory

(e.g., see the review by Reid & Ratcliffe (2014)).

Several mechanisms were proposed, aiming to cover the properties of the fundamental emissions. Among them - the nonlinear wave-wave interaction of Langmuir, ion sound, and EM waves: $l \pm s \rightarrow t$. The ion sound wave may be generated by the parametric decay of the primary Langmuir wave to another backward propagating Langmuir wave and ion sound wave ($l \rightarrow l^{'} + s$).

Another mechanism that may explain the EM emissions at fundamental frequency is the linear mode conversion (LMC) of Langmuir waves directly into EM waves in presence of an increasing density gradient. The important role of the encounter of Langmuir waves with the higher density regions in the generation of EM waves was pointed out by Hinkel-Lipsker et al. (1992); Krasnoselskikh et al. (2019) and extensively studied by Mjølhus (1983, 1990); Kim et al. (2007, 2008, 2009, 2013); Schleyer et al. (2013, 2014) in the presence of a background magnetic field. It was shown that even a simple reflection of Langmuir waves from a density inhomogeneity can result in an efficient generation of fundamental EM emission.

1.1.8 Generation of harmonic electromagnetic emission

It is widely accepeted that the harmonic EM emission in plasma is generated by the coalescence of two Langmuir waves $l + l^{'} \rightarrow t$. Since the moment of suggestion of the plasma emission mechanism, the harmonic emission was attributed to the Reyleigh scattering of beam-driven Langmuir waves on thermal ions and subsequent coalescence of the forward-moving and scattered waves. However, a few decades later this process has been revised as insufficient to be consistent with the brightness temperatures of type IIIs, observed in corona (e.g., (Melrose, 1980a)). This has lead to the investigation of the role of ion sound waves in producing the back-scattered Langmuir waves via the electrostatic decay process $l \rightarrow l^{'} + s$ (e.g., see (Cairns, 1987) and the references therein). Based on this idea, Willes et al. (1996) have derived the analytical solutions to describe the $l + l^{'} \rightarrow t$ process for a broad class of

Langmuir waves spectra, including the case of almost anti-parallel waves (a head-on approximation).

Among the other mechanisms, suggested to explain harmonic emissions in plasma, there is the radiation by localized bunches of Langmuir waves (Galeev & Krasnoselskikh, 1976; Brejzman & Pekker, 1978; Papadopoulos & Freund, 1978; Goldman et al., 1980; Ergun et al., 2008; Malaspina et al., 2012), which considers a radiation by nonlinear currents at twice the plasma frequency, driven by plasma oscillations (antenna-type radiation).

1.2 Density fluctuations in a solar wind

1.2.1 Spectrum of density fluctuations

Random density fluctuations within the solar wind and solar corona are a well-known feature of the heliospheric plasma. The spectral characteristics of density fluctuations have been extensively studied by many authors (e.g., (Neugebauer, 1975; Celnikier et al., 1983, 1987; Goldstein et al., 1995; Shaikh & Zank, 2010; Chen et al., 2012)), and have demonstrated a several-power law dynamics throughout a broad frequency interval. Recent observation have allowed to measure a particularly large frequency expand (in the reference frame of a spacecraft), which lies within the interval between $\sim 10^{-3}$ Hz and $\sim 10^{2} \div 10^{3}$ Hz. The largest frequencies correspond to the smallest scales that are resolved. Typically in the frequency domain from the smallest frequencies to $\sim 10^{-1}$ Hz the spectrum corresponds to a Kolmogorov turbulent cascade with the spectral index -5/3. The spectrum of the density fluctuations in a solar wind will be considered in more detail in Section 2.5.4.

1.2.2 Probability density function of density fluctuations

An interesting issue is the probability density function (PDF) of the density fluctuations in a solar wind and its deviations from Gaussianity, as in numerous studies it is

assumed to be Gaussian by default. Chen et al. (2014) have investigated the PDFs of the ion density fluctuations on the kinetic scales measured by *Spectr-R* spacecraft. They have found that such PDFs are highly non-Gaussian. Reconstructing synthetic density data from the specra of density fluctuations, measured in solar wind by various spacecrafts, Voshchepynets & Krasnoselskikh (2015) have deduced that the PDF of density variation obeys rather a Pearson type II distribution than a Gaussian. However, the question requires more studies with a high temporal resolution data, since numerous recent theoretical investigations of physical phenomena related to type III radio bursts rely on the assumptions about the statistical properties of density fluctuations and are in demand of a strong observational evidence (Voshchepynets et al., 2015; Voshchepynets & Krasnoselskikh, 2015; Krasnoselskikh et al., 2019; Tkachenko et al., 2021).

1.2.3 Observed amplitudes of density fluctuations

The average level of background density fluctuations in the solar wind at around 1 a.u. was measured *in situ* already in 1970s-1980s and was shown to reach several percent of the average background density (see, for example (Celnikier et al., 1983)). Recent observations as well as *in situ* measurements by *Parker Solar Probe* (*PSP*) spacecraft have confirmed that the level of density fluctuations in the solar wind can go up to seven percent of the average background density at $\sim 36\ R_{\odot}$, and the analysis based on comparison of Monte Carlo simulations with *PSP* observations of decay times of the type III bursts predicts a growth of the level of density fluctuations towards the Sun, reaching up to twenty percent in the high corona (Krupar et al., 2020). These turbulent structures strongly affect the propagation and observed properties of radio emissions in coronal and solar wind plasma (Reid & Ratcliffe, 2014), as well as the process of the generation of such emission on each stage: beginning from the beam-plasma instability, followed by excitation of the plasma waves and finishing with the conversion of the plasma waves into a radio emission.

1.3 General structure of the manuscript

The goal of the current manuscript is to revisit the theory of the generation of the EM emissions in plasma, especially in relation with the type III solar radio bursts, by taking into account the presence of the random density fluctuations in the solar wind.

In the current Chapter we have given a general outlook of the type III solar radio bursts, their observational characteristics, established mechanism of generation and discussions around different stages of formation of such emission. The electron beam, being an initial trigger of the type III emission, generates the plasma waves which in turn will convert into EM waves at fundamental or harmonic frequency, observed later as radio bursts. At each of these multiple stages the ubiquitous density fluctuations in solar wind plasma may affect and alter the physical processes that determine the type III emission. Thus we provide a short insight to the observations of the plasma density fluctuations in the solar wind.

In Chapter 2 we will revise step by step the theory of beam-plasma interaction, that explains how the beam that propagates inside the plasma generates the plasma waves. We will re-examine a classical quasi-linear theory and the ideas that were suggested in order to make the theory fit better the observations. Further we will stop on the observational evidence of the presence of the density fluctuations in the solar wind and the way they manifest themselves. After we will consider in detail the probabilistic model of beam-plasma interaction that takes into account the random density fluctuations in plasma, and allows to obtain plausible predictions of plasma wave intensities and particle distributions at the final stages of a beam relaxation. We emphasize the estimations of the energy density of the Langmuir waves obtained within the framework of this model as we will use them further in our calculations. We also dedicate one Section of Chapter 2 for an outlook on the generation of the EM emission at the fundamental frequency under conditions of a randomly inhomogeneous plasma. We will revise the mechanisms suggested earlier

and will provide the most recent results.

After having revised the beam-plasma interaction and the generation of the fundamental emission in a randomly inhomogeneous plasma, we proceed to the main focus of the current manuscript - the harmonic EM emission in a plasma with density fluctuations. It is widely accepted that for the generation of the harmonic emission the necessary process is the coalescence of two almost opposite directed Langmuir waves. Various theories have suggested several approaches to explain the presence of the population of back-scattered Langmuir waves, among them the scattering by ions and the parametric decay of the pump Langmuir wave into a back-scattered Langmuir wave and an ion sound wave. We will discuss the role of these phenomena and will suggest another possible explanation in terms of density fluctuations. In this case density clumps will be considered as the 'mirrors' where the reflection of the Langmuir waves occurs and consequently the population of back-scattered Langmuir waves is created. We will divide our consideration into two main parts: the coalescence that occurs on a large distance from the reflection point where plasma can be considered as quasi-homogeneous, and the coalescence in the close vicinity of the reflection point, inside the localized density inhomogeneity.

The coalescence of the Langmuir waves in a quasi-homogeneous plasma will be described in Chapter 3. This problem has a very similar structure to the one already studied in the literature, with the only difference that the spectrum of the back-scattered Langmuir waves is attributed to the reflections from the density fluctuations and not to the parametric decay of a pump Langmuir wave. We will perform the analytical calculations and will evaluate the energy density of such harmonic emission.

The coalescence of the Langmuir waves inside the localized space of the density inhomogeneity in the close vicinity of the reflection point will be considered in Chapter 4. We will perform a set of analytical calculations in order to evaluate the energy density of the harmonic emission produced in this case.

In Chapter 5 we provide the preliminary results of the statistical analysis of the plasma density measurements performed by Parker Solar Probe spacecraft at a heliocentric distance around 0.2 a.u within 12 hours during Encounter 5 phase. We approximately estimate the level of the electron density fluctuations on the given time interval and establish future objectives of the analysis.

After we will conclude our results in Chapter 6 and perform a quantitative estimations and comparison of the results obtained in Chapters 3 and 4. We will evaluate the efficiency of the wave conversion for each of two mechanisms and will also highlight the differences between the radiation patterns of such emissions, showing that with both mechanisms working, we may explain some of the observed properties of the harmonic type III emission.

The description of the two mechanisms of the generation of harmonic radio emission of type III radio bursts in a randomly inhomogeneous plasma, together with the main results presented in this manuscript were recently published in (Tkachenko et al., 2021).

1.4 Résumé en français

Le but du manuscrit actuel est de revisiter la théorie de la génération des émissions électromagnétique dans le plasma, notamment en relation avec les sursauts radio solaires de type III, en tenant compte de la présence des fluctuations aléatoires de densité dans le vent solaire.

Dans le présent Chapitre, nous avons donné une vue d'ensemble des sursauts radio solaires de type III, de leurs caractéristiques d'observation, du mécanisme de génération établi et des discussions autour des différentes étapes de formation d'une telle émission. Le faisceau d'électrons, étant un déclencheur initial de l'émission de type III, génère les ondes de plasma qui à leur tour se convertiront en ondes radio électromagnétiques à fréquence fondamentale ou harmonique, observées plus tard

sous forme de sursauts radio. À chacune de ces étapes multiples, les fluctuations de densité omniprésentes dans le plasma du vent solaire peuvent affecter et modifier les processus physiques qui définissent l'émission de type III. Ainsi, nous donnons un bref aperçu des observations des fluctuations de densité du plasma dans le vent solaire.

Dans le Chapitre 2 nous réviserons pas à pas la théorie de l'interaction faisceau-plasma, qui explique comment le faisceau qui se propage à l'intérieur du plasma génère les ondes de plasma. Nous réexaminerons une théorie quasi-linéaire classique et les idées qui ont été suggérées afin de mieux adapter la théorie aux observations. De plus, nous nous arrêterons sur les preuves d'observation de la présence des fluctuations de densité dans le vent solaire et de la façon dont elles se manifestent. Ensuite, nous examinerons en détail le modèle probabiliste de l'interaction faisceau-plasma qui prend en compte les fluctuations aléatoires de densité dans le plasma, et permet d'obtenir des prédictions plausibles des fréquences d'onde du plasma et des distributions de particules aux étapes finales d'une relaxation de faisceau. Nous soulignons les estimations de la densité d'énergie des ondes de Langmuir obtenues dans le cadre de ce modèle car nous les utiliserons plus loin dans nos calculs. Nous dédions également une section du Chapitre 2 pour une perspective sur la génération de l'émission électromagnétique à la fréquence fondamentale dans les conditions d'un plasma aléatoirement inhomogène. Nous réviserons les mécanismes suggérés précédemment et fournirons les résultats les plus récents.

Après avoir révisé l'interaction faisceau-plasma et la génération de l'émission fondamentale dans un plasma aléatoirement inhomogène, nous passons à l'objectif principal du manuscrit actuel - l'émission électromagnétique harmonique dans un plasma avec des fluctuations de densité. Il est largement admis que pour la génération de l'émission harmonique, le processus nécessaire est la coalescence de deux ondes de Langmuir dirigées presque opposées. Diverses théories ont suggéré plusieurs approches pour expliquer la présence de la population d'ondes de Langmuir rétrod-

iffusées, parmi lesquelles la diffusion par les ions et la désintégration paramétrique de l'onde de pompe de Langmuir en une onde de Langmuir rétrodiffusée et une onde sonore ionique. Nous discuterons du rôle de ces phénomènes et proposerons une autre explication possible en termes de fluctuations de densité. Dans ce cas, les touffes de densité seront considérés comme les «miroirs» où se produit la réflexion des ondes de Langmuir et par conséquent la population d'ondes de Langmuir rétrodiffusées est créée. Nous diviserons notre réflexion en deux parties principales: la coalescence qui se produit à grande distance du point de réflexion où le plasma peut être considéré comme quasi homogène, et la coalescence au voisinage immédiat du point de réflexion, à l'intérieur de l'inhomogénéité de densité localisée.

La coalescence des ondes de Langmuir dans un plasma quasi homogène sera décrite au Chapitre 3. Ce problème a une structure très similaire à celle déjà étudiée dans la littérature, à la seule différence que le spectre des ondes de Langmuir rétrodiffusées est attribué aux réflexions des fluctuations de densité et non à la décroissance paramétrique d'une onde de Langmuir pompe. Nous effectuerons les calculs analytiques et évaluerons la densité d'énergie d'une telle émission harmonique.

La coalescence des ondes de Langmuir à l'intérieur de l'espace localisé de l'inhomogénéité de densité au voisinage immédiat du point de réflexion sera considérée dans le Chapitre 4. Nous effectuerons un ensemble de calculs analytiques afin d'évaluer la densité d'énergie de l'émission harmonique produite dans ce cas.

Dans le chapitre 5, nous fournissons les résultats préliminaires de l'analyse statistique des mesures de densité de plasma effectuées par l'engin spatial Parker Solar Probe à une distance héliocentrique d'environ 0,2 u.a. en 12 heures pendant la phase de rencontre 5. Nous estimons approximativement le niveau des fluctuations de densité électronique sur l'intervalle de temps donné et établissons les objectifs futurs de l'analyse.

Ensuite, nous conclurons nos résultats dans le Chapitre 6 et effectuerons une estimation quantitative et une comparaison des résultats obtenus dans les Chapitres

3 et 4. Nous évaluerons l'efficacité de la conversion d'onde pour chacun des deux mécanismes et mettrons également en évidence les différences entre les diagrammes de rayonnement de telles émissions, montrant qu'avec les deux mécanismes fonctionnant, nous pouvons expliquer certaines des propriétés observées de l'émission harmonique de type III.

La description des deux mécanismes de génération d'émission radio harmonique de sursauts radio de type III dans un plasma aléatoirement inhomogène, ainsi que les principaux résultats présentés dans ce manuscrit ont été récemment publiés dans (Tkachenko et al., 2021).

Chapter 2

Beam-plasma interaction

2.1 Introduction

In this Chapter we are going to make an overview of the development of the theory around the beam-plasma interaction, with connection to the type III solar radio bursts. First we will start with a classical approaches that were used in early investigations and will follow their development that made the theory fit better the observations.

We will start with description of the classical quasi-linear theory of wave-particle interaction in a homogeneous plasma, providing the basic equations and their solutions in the framework of one-dimensional problem. We will explain with the help of this theory how the energy exchange between particles and waves in plasma is enabled what allows the plasma waves to grow significantly above the thermal noise level. Together with this we will provide the arguments in favor of one-dimensional consideration of the problem based on the *in situ* observations of various spacecrafts. After, there will follow a discussion of discrepancies between the observations and predictions of the quasi-linear theory for the case of beam-plasma interaction under the typical conditions related to the type III radio bursts.

Next we will highlight the ideas that were suggested to modify the quasi-linear

theory in order to describe more plausibly the solar wind plasma, in particular, the consideration of a decreasing density profile in the direction of the propagation of the electron beam. We will also discuss a role of a random density fluctuations in plasma, how they manifest themselves in observations and measurements and also how they affect each stage of the generation of the type III emission, starting with the excitation of Langmuir waves by electron beams and their further conversion into fundamental EM emission, both discussed in current Chapter, and the formation of harmonic EM emission brought up in the two following Chapters. Alongside with this, we will mention some of the relevant models and theories, that found a support in some observational properties but failed to reproduce the other ones.

And finally we will present the essentials of a probabilistic model of beam-plasma interaction that, based on equations of a quasi-linear theory, incorporates a statistical approach that allows to account for the effect of the random density fluctuations in plasma. The results of this model will be used further in the manuscript. One of the last sections of the Chapter is devoted to the generation of the fundamental radio emission of type III radio bursts in a randomly inhomogeneous plasma, necessary to revise before we proceed to the harmonic emission of type IIIs in the following Chapters.

2.2 Quasi-linear theory of wave-particle interaction in plasma

2.2.1 Initial equations and assumptions

Plasma as a medium contains a wide spectrum of collective oscillations that are known as plasma waves. Their frequency and velocity of propagation is defined by their wavenumber and various given, or basic parameters of plasma, such as density, average velocity spread, magnetic field intensity etc. Their growth rate, on

the contrary, depends on finer characteristics of plasma, such as the slope of the velocity distribution function in the phase space. A very important role is played by the particles of plasma that satisfy the resonance condition: $\omega - \boldsymbol{k} \cdot \boldsymbol{v} = 0$, where ω and $\boldsymbol{k}$ are the frequency and the wavevector of the wave and $\boldsymbol{v}$ is the velocity of the particle. These particles resonantly interact with the waves and exchange the energy, reinforcing or weakening the waves.

One of the most common approaches to describe such resonant interaction between waves and particles in plasma is the quasi-linear theory (QLT), which was initially developed in early works by Vedenov et al. (1961, 1962a); Drummond & Pines (1962). The assumption behind the QLT is that the energy of the plasma waves is sufficiently above their thermal noise level but much less than the total thermal energy of plasma particles. The quintessence of QLT approach is the division of the particle distribution function on rapidly varying (oscillating) and slowly varying parts and calculation of the influence of the mean square of the oscillating part on the slowly varying one.

In order to obtain the equations of QLT for fully ionized rarefied plasma, we start with the Vlasov equation

$$\frac{\partial f_\alpha}{\partial t} + \boldsymbol{v}\frac{\partial f_\alpha}{\partial \boldsymbol{x}} + \frac{e_\alpha}{m_\alpha}\left(\boldsymbol{E} + \frac{\boldsymbol{v}}{c} \times \boldsymbol{H}\right)\frac{\partial f_\alpha}{\partial \boldsymbol{v}} = 0, \tag{2.1}$$

where f_α is the distribution functions of particles with the charge e_α and mass m_α, and self-consistent fields $\boldsymbol{E}$ and $\boldsymbol{H}$ are defined by the distribution of all particles of plasma:

$$\frac{\partial \boldsymbol{E}}{\partial \boldsymbol{x}} = 4\pi \sum_\alpha e_\alpha \int f_\alpha d\boldsymbol{v}, \qquad \nabla \times \boldsymbol{E} = \frac{1}{c}\frac{\partial \boldsymbol{H}}{\partial t}, \tag{2.2}$$
$$\nabla \times \boldsymbol{H} = \frac{4\pi}{c} \sum_\alpha e_\alpha \int \boldsymbol{v} f_\alpha d\boldsymbol{v} + \frac{1}{c}\frac{\partial \boldsymbol{E}}{\partial t}.$$

This equation system describes correctly a plasma that is nearly ideal. This

means that in such plasma the number of particles inside the Debye sphere N_D is very large and N_D^{-1} is considered as a small parameter. Taking into account the smallness of N_D^{-1}, the exact equations of motion of all plasma particles are expanded into equation system (2.1)-(2.2) in the first approximation.

Another small parameter in this approach is, as mentioned before, the ratio between the energy of the plasma waves and total thermal energy of plasma particles, or, in terms of energy densities W/nk_BT, where n is plasma number density, k_B is a Boltzmann constant and T is plasma temperature. If the quantity W/nk_BT noticeably exceeds N_D^{-1}, it means that the effect of diffusion of the particles in the phase space due to the interaction with the waves is much more important than their diffusion due to collisions with other particles and thus the collisions may be neglected in the first approximation:

$$1 \gg W/nk_BT \gg N_D^{-1}. \tag{2.3}$$

2.2.2 Equations of quasi-linear theory

To proceed to the QL equations, the particle distribution function is considered as a sum of oscillating part f^0 and slowly varying part f^1, such that $|f^1| \ll f^0$. At the same time electric fields $\boldsymbol{E}$ will have a form of a product of quickly oscillating in space and time functions and slowly varying amplitudes. Thus for rather small f^1 and $\boldsymbol{E}$ their average values (taken over times much larger that the period of plasma oscillations) will be zero:

$$\langle f^1 \rangle = \langle \boldsymbol{E} \rangle = 0. \tag{2.4}$$

If we consider the case of Langmuir waves in plasma without external magnetic

field, and take into account

$$f = f^0 + f^1, \qquad f^1 = \sum_{\boldsymbol{k}} f^1_{\boldsymbol{k}} e^{i\boldsymbol{k}x - i\omega_{\boldsymbol{k}} t}, \tag{2.5}$$

where the oscillating component f^1 is decomposed into Fourier series, the equation system (2.1) - (2.2) will turn into

$$\frac{\partial f^0}{\partial t} = \frac{\partial}{\partial \boldsymbol{v}} D \frac{\partial f^0}{\partial \boldsymbol{v}}, \tag{2.6}$$

$$\frac{\partial W_{\boldsymbol{k}}}{\partial t} = 2\gamma_{\boldsymbol{k}} W_{\boldsymbol{k}}, \tag{2.7}$$

where

$$D(\boldsymbol{v}) = \frac{8\pi^2 e^2}{m_e^2} \sum_{\boldsymbol{k}} W_{\boldsymbol{k}} \delta(\omega_{\boldsymbol{k}} - \boldsymbol{k}\boldsymbol{v}), \tag{2.8}$$

is the diffusion coefficient of the velocity of the electrons in a phase space due to interaction with Langmuir waves, and

$$\gamma_{\boldsymbol{k}} = \frac{\pi \omega_{p_e}^3}{2} \int d\boldsymbol{v} \frac{\boldsymbol{k}}{k^2} \frac{\partial f^0}{\partial \boldsymbol{v}} \delta(\omega_{\boldsymbol{k}} - \boldsymbol{k}\boldsymbol{v}) \tag{2.9}$$

is the growth rate of Langmuir waves. Equations (2.6)-(2.7) compose a closed system of QLT equations for the averaged distribution function $f^0 = \langle f \rangle$ and for the spectral energy density of a separate harmonic $W_{\boldsymbol{k}} = |\boldsymbol{E}^2_{\boldsymbol{k}}|/8\pi$.

A very important condition that may be inferred from the system of QLT equations, is that this system describes the interaction of particles and waves that satisfy a resonance condition $\omega_{\boldsymbol{k}} = \boldsymbol{k}\boldsymbol{v}$. Another words, the phase velocity of the waves $V_{ph_{\boldsymbol{k}}} = \omega_{\boldsymbol{k}}/k$ and the velocity of the particles v should be equal in order to exchange energy. This is also known as Cherenkov resonance condition.

2.2.3 Quasi-linear equations in one-dimensional consideration

In many problems it is possible to consider the wave-particle interactions in the framework of one-dimensional (1D) approach. In this case it is assumed that all wavevectors $\boldsymbol{k}$ are quasi-parallel and QLT equations are sufficiently simplified, allowing to find analytical solutions of the system. In 1D approximation the resonance condition has a simpler form

$$v = \frac{\omega_{p_e}}{k} = V_{ph}. \tag{2.10}$$

Here we have made use of the fact that the frequency of the Langmuir wave is typically very close to the local plasma frequency: $\omega \approx \omega_{p_e}$. And the QLT equation system turns into

$$\frac{\partial f}{\partial t} = \frac{\partial}{\partial v}\left(D(v)\frac{\partial f}{\partial v}\right), \qquad D(v) = \frac{\omega_{p_e}^2}{n_e m_e v} W, \tag{2.11}$$

$$\frac{\partial W}{\partial t} = 2\gamma W, \qquad \gamma = \frac{\pi \omega_{p_e} v^2}{2}\frac{\partial f}{\partial v}, \tag{2.12}$$

here and further we simply write $f^0 = f$, remembering that it is the averaged distribution function. Equation system (2.11)-(2.12) describes the interaction of the resonant electrons (with velocity that satisfies the Eq.(2.10)) and Langmuir waves with phase velocity V_{ph} in one-dimensional consideration.

2.2.4 The role of Landau damping

The process, responsible for resonant interaction of waves and particles in plasma is known as Landau damping. In case of interaction between Langmuir waves and electrons in plasma, resonant electrons can be divided into two categories: 1) the ones that stream infinitesimally slower than the wave phase velocity, i.e., with $v_e^- \lesssim V_{ph}$, and 2) the ones that stream infinitesimally faster that the wave phase velocity,

i.e., with $v_e^+ \gtrsim V_{ph}$. If the electron belongs to the first category, it gains the kinetic energy from the waves by means of Landau damping. In the opposite case the faster electron will give part of its energy to the wave. Thus the growth of the Langmuir wave will be observed when there are more electrons with velocities v_e^+ and fewer electrons with velocities v_e^- in the resonance with the wave. Another words, the growth or the absorption of the wave occurs depending on the slope of the electron distribution function $f(v_e)$ in the vicinity of the resonance $v_e = V_{ph}$.

In the state of a thermodynamic equilibrium, i.e., when electron velocity spectrum is Maxwellian, the derivative of the distribution function is always negative $df(v_e)/dv_e \sim -v_e/v_T^2 f(v_e)$ and thus in Maxwellian plasma the Langmuir waves are always damping. However, in such plasma, if the waves have a phase velocity V_{ph} much larger than the electron thermal velocity v_T, the damping becomes rather weak due to the decreasing number of resonant particles. But if there is a deviation from equilibrium somewhere in the electron distribution, for instance, an electron beam in plasma, the waves can be amplified to a very significant level.

In general Landau damping is applied not only to the interaction of Langmuir waves and electrons, but to a variety of plasma waves interactions with electrons, protons or heavy ions.

2.2.5 Generation of Langmuir waves by electron beam

When a plasma is unstable regarding the excitation of Langmuir waves, for instance, when there is an electron beam that propagates through plasma, there are two extreme cases that may occur: (1) when the electron beam is almost mono-energetic and moves with a very large velocity with respect to plasma, then it triggers the growing oscillations in plasma that have a frequency and a growth rate that is determined by all the parameters of the system; (2) when the velocity and density of the beam are not very large and velocity dispersion is not too small, the frequency of excited oscillations is equal to plasma frequency and only the growth rate is defined

by the properties of the system - it is proportional to $\partial f/\partial v_e$ in vicinity of the point $v_e = \omega_{p_e}/k$, where f stands for total distribution function of plasma and the beam. QLT is only applicable to description of the second case, where the condition $\gamma/\omega_{p_e} \ll 1$ is satisfied. Equations of QLT describe the dynamics of beam instability in plasma, which is also known as quasi-linear (QL) relaxation of the beam.

Let us consider the QL relaxation of the electron beam in plasma in 1D approximation. The beam itself has a mean velocity v_b typically much larger than thermal velocity of electrons in plasma v_T, and a velocity dispersion $\Delta v_b \ll v_b$. The presence of a beam in plasma creates the bump on the equilibrium distribution function of electrons and thus creates an interval in the velocity space where the derivative $\partial f/\partial v_e > 0$, which means, according to Eq.(2.12) that growth rate γ is positive and Langmuir waves start to grow. At the same time, the process of the diffusion of electrons of the beam in the velocity space begins, according to Eq.(2.11), smoothing the distribution function in the same interval, and reducing the growth rate of the waves γ. This leads to a progressive diminution of the derivative of electron distribution function within given interval until it becomes zero and a plateau on the distribution function is formed. Meanwhile the energy of the waves grows until the moment when the plateau occurs. In the process of relaxation, the left border of the electron beam distribution function u, is moving towards lower velocities (see Fig.2.1b) with the rate

$$\frac{du}{dt} = -\frac{\pi}{\Lambda}\omega_{p_e}\frac{n_b}{n_0}\frac{u^2}{v_b - u}, \tag{2.13}$$

where Λ is a Coulomb logarithm and n_b is the number density of electrons in a beam. Eventually the distribution function of the beam comes to a final quasi-stationary state as completely plateaued (see Fig.2.1a):

$$f_\infty = \begin{cases} n_b/v_b, & 0 < v_e < v_b \\ 0, & v_e > v_b. \end{cases} \tag{2.14}$$

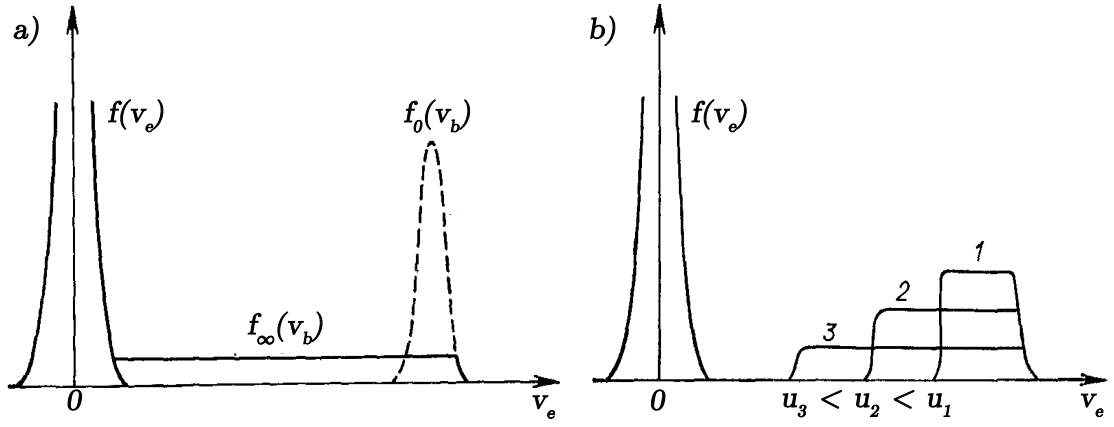

Figure 2.1: The form of the electron distribution function in a plasma with the energetic beam according to QLT. Panel a) The temporal evolution of the one-dimensional electron beam distribution function from initial state $f_0(v_b)$ to the state of full relaxation $f_\infty(v_b)$ with a formation of a plateau. $f(v_e)$ is an equilibrium (thermal) distribution function of electrons. Panel b) the relaxation of the beam for three consecutive moments of time $t_1 < t_2 < t_3$ (adopted from (Vedenov & Ryutov, 1975)).

By the end of quasi-linear relaxation, the energy of the beam comprises 1/3 of its initial energy while 2/3 of it has transformed into the energy of Langmuir waves. The energy density of such waves is

$$W_\infty = \begin{cases} \frac{n_b m_e v_b^2}{3}, & 0 < v_e < v_b \\ 0, & v_e > v_b. \end{cases} \tag{2.15}$$

When the stage of QL relaxation has come to an end, the quasi-stationary state is established. The following stage is characterised by a very slow modification of the distribution function due to the collisions between particles and as a result - a slow diffusion in velocity space that leads to establishment of Maxwellian distribution

function and damping of the waves to the level of a thermal noise.

2.3 Justification of a 1D consideration

Quasi-linear relaxation of the electron beam in plasma has many practical applications, among them - the interaction of energetic electron beams that were produced by solar eruptive events, with a solar wind plasma. Of course, in solar wind parameters vary in all three dimensions (3D). However, the theoretical analysis and description of three-dimensional dynamics is extremely difficult. For instance, contrary to 1D consideration, there were no analytical results obtained for 3D relaxation of non-relativistic electron beam and the final state of relaxation remains unknown. There have been a number of simulations performed in order to better understand QL relaxation for 2D (e.g. by Ziebell et al. (2008, 2011)) and 3D problems (e.g. by Harding et al. (2020)).

To this day, however, 1D consideration remains the most convenient way to analyze the dynamics of beam-plasma interaction. And not only it is convenient but also well justified by the arguments, presented in this section. The electron beam, generated by solar eruptive events, always propagates into outer space along the opened magnetic field line, otherwise called a Parker spiral. The presence of such rather weak magnetic field may be otherwise neglected in equations and calculations, but affects the propagation of the beam by forcing the particles of the beam to move along the field line. The angular dispersion of the electron velocity vectors and of generated Langmuir waves wavevectors plays thus the major role in an applicability of 1D approach.

2.3.1 Electron beam angular dispersion

Early *in situ* observations of energetic electron beams, plasma waves and radio emissions associated with type III radio bursts, were carried out by the *ISEE 3* (In-

ternational Sun-Earth Explorer) spacecraft. Analyzing the burst that has occurred on February 17, 1979, Lin et al. (1981) have concluded that the angular distribution of the particles in the beam depends on the value of the energy of the particle. Electron beams typically have a dispersion in velocities, i.e., faster electrons of the beam arrive before the slower ones. This is known as a *bump-on-tail* distribution. It allows to separate electrons by energy and analyze their behavior. Lin et al. (1981) have found that the electrons with energies $\lesssim 10$ keV have a beam-like quasi1D structure with rather small pitch angles, whilst the faster electrons with energies from about 20 keV to more than 100 keV have a very broad angular distribution that widens with the growth of the electron energy.

The observations performed later by *WIND* spacecraft have reported a higher ratio of high-energy events observed compared to *ISEE 3* and typical beam angular width of $\sim 15^o$ (Ergun et al., 1998).

Early theoretical investigations of the relaxation of an ultra-relativistic beam in a homogeneous plasma have yielded the one-dimensional character of relaxation (Fainberg et al., 1970; Breizman & Ryutov, 1971). The growth rate of the waves in this case has its maximum at smallest values of angular dispersion of particles in the beam (Fig.2.2). This leads to a conclusion that even if the high energy beams gain a wider angular width compared to lower energy ones, the relaxation process remains quasi 1D, and the waves are mainly excited in the angular space that is majorly aligned with the direction of the beam (and the magnetic field).

2.3.2 Langmuir waves angular dispersion

At the same time the observations of the spatial structure of Langmuir waves by *STEREO* spacecrafts has indicated that one-dimensional wave structure prevails over multi-dimensional. (Malaspina & Ergun, 2008) have analyzed ~ 2000 Langmuir waves observations between 15 December 2006 and 31 July 2007 and reported that in $\sim 75\%$ of cases the structures are aligned with the local magnetic field and thus quasi

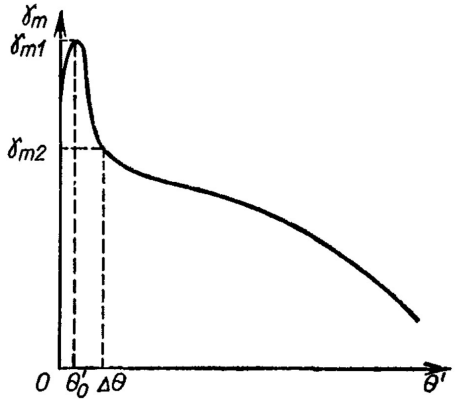

Figure 2.2: Dependence of the growth rate γ_m that was maximized by wavenumber value, on the propagation angle $\theta^{'}$ in the wavevector space. $\Delta\theta$ is the angular spread of the beam (Breizman & Ryutov, 1971; Vedenov & Ryutov, 1975).

one-dimensional (Fig.2.3). Two- and three-dimensional Langmuir wave structures comprise the minority and appear in temporal clusters on the timescales of order of hours.

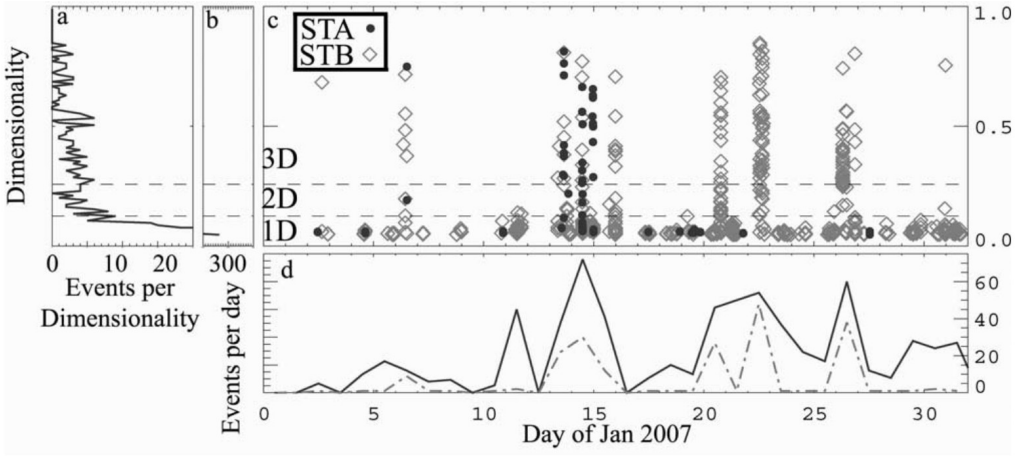

Figure 2.3: (a – b) Number of events from January 2007 with each hodogram dimensionality. (c) A scatterplot of hodogram dimensionality against time for all Langmuir events in January. (d) Total telemetered Langmuir wave observations each day of January 2007 (solid line). Number of Langmuir wave observations with 2D and 3D hodograms (dot-dash line). Dots denote events recorded by STEREO A and diamonds denote events recorded by STEREO B (Malaspina & Ergun, 2008).

Similar conclusion was made by Krasnoselskikh et al. (2011) from observations of the *WIND* spacecraft of Langmuir waves generated at the Earth's bow-shock. The associated beams were rather weak with typical energies in range from several

hundreds of eV to several keV. It was possible to measure two components of the electric field of Langmuir wave, E_x and E_y, and the investigation has shown that their wavevectors align very well with the direction of the magnetic field: a semi-major axis of polarization ellipse was rarely exceeding a 20^o angle with respect to the direction of magnetic field (Fig.2.4). Analysis of different events has revealed that the close alignment remains no matter how the magnetic field is oriented.

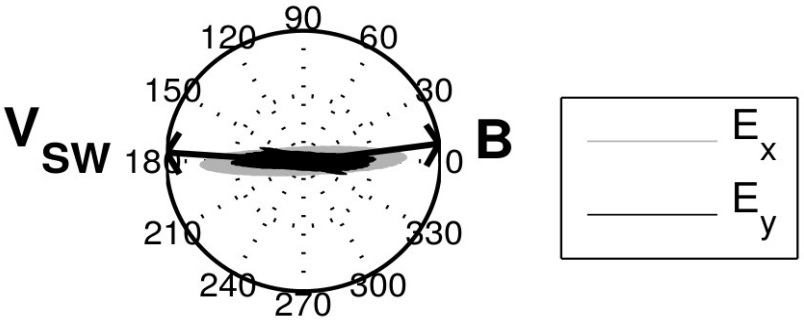

Figure 2.4: A hodogram to compare the polarisation with the orientation of the magnetic field. The direction of the solar wind velocity varies and is not necessarily aligned with the magnetic field (Krasnoselskikh et al., 2011).

All of the aforementioned observations were performed at around 1 a.u. Typically the electron beams are generated very close to the Sun and then propagate through the interplanetary space, loosing part of the energy on generation of the Langmuir waves. In the absence of scattering, the angular width of the such electron beam at 1 a.u. should be much less than 1^o (Ergun et al., 1998). Even though the propagation effects cause the angular dispersion of the beam, we may conclude that the one-dimensional consideration may be a good approximation for the beam-plasma interaction at 1 a.u. and becomes even more justified for smaller heliocentric distances. Thus we will further imply an assumption about quasi 1D character of beam relaxation in space plasmas and will use this approach in the following discussion of beam-plasma interaction.

2.4 Quasi-linear relaxation of the electron beam in a plasma with monotonically decreasing density profile

2.4.1 Persistence of the electron beam

Sturrock (1964) has applied QLT description of beam-plasma interaction in a homogeneous plasma to solar radio bursts. The analysis of the beam-plasma interaction under conditions relevant to solar corona and solar wind resulted in so-called "Sturrock paradox": the QL relaxation of the beam should have stopped after only several meters. However, Langmuir waves and associated beams had been observed around the Earth orbit. Later satellite measurements have shown that such beams are observed in the solar wind even on the distances of about 5 a.u.

Among the early ideas proposed to overcome this contradiction there was a *beam-plasma structure*, that suggests the following: electrons of the beam propagate accompanied by Langmuir waves which are permanently generated at the front of the beam (by faster electrons) and reabsorbed at the back (by slower electrons) (Zheleznyakov & Zaitsev, 1970; Zaitsev et al., 1972). For this process to proceed, it is necessary that Langmuir waves are reflected from the region of higher phase velocities to the one with lower V_{ph}. This is normally happening if there is a negative density gradient in plasma.

2.4.2 QL relaxation for monotonically decreasing density profile

The quasi-linear relaxation of the electron beam in plasma was first of all applied to a homogeneous plasma. However, later studies have explored how the presence of the inhomogeneity of density profile may affect the process of relaxation (Ryutov, 1969; Breizman & Ryutov, 1969; Vedenov & Ryutov, 1975; Nishikawa & Ryutov,

1976; Smith & Sime, 1979). For instance, the case that is directly applicable to the beam-plasma interaction within solar wind, is the plasma with monotonically decreasing density profile in the direction of injection of the beam.

In order to consider this problem it is normally assumed that the parameters of plasma and of the beam depend only on one coordinate z directed along the constant magnetic field and that characteristic wavelength of Langmuir waves that are exited by the beam is small compared to the scale of plasma inhomogeneity and characteristic scale of quasi-linear relaxation.

As the Langmuir waves, generated by electron beam, propagate through the region with decreasing density, their phase velocity decreases. In order to estimate this decrease over a distance Δz, we start with the dispersion relation for Langmuir waves:

$$\omega_l \approx \omega_{p_e}(z)\left(1+\frac{3}{2}\frac{v_T^2}{V_{ph}^2}\right). \tag{2.16}$$

The frequency of the wave that propagates in the medium with stationary parameters does not change, thus

$$\Delta\omega_l = \left(1+\frac{3}{2}\frac{v_T^2}{V_{ph}^2}\right)\frac{d\omega_{p_e}}{dz}\Delta x - 3\omega_{p_e}\frac{v_T^2}{V_{ph}^2}\frac{\Delta V_{ph}}{V_{ph}} = 0. \tag{2.17}$$

Obvious conclusion from Eq.(2.17) is that $\Delta V_{ph} < 0$ when $d\omega_{p_e}/dz < 0$. Since $V_{ph} \sim v_b \gg v_T$ and having applied estimation $d\omega_{p_e}/dz \sim \omega_{p_e}/L$, where L is the characteristic scale of inhomogeneity (basically the length of the region, occupied by plasma for the case of monotonically changing profile), we obtain

$$|\Delta V_{ph}| \sim v_b\frac{\Delta z}{L}\frac{v_b^2}{v_T^2}. \tag{2.18}$$

If the velocity spread of the electron beam is Δv_b, a Langmuir wave will be excited by this beam if it's phase velocity lies in the range $v_b - \Delta v_b < V_{ph} < v_b$. However, when the plasma density and consequently the phase velocity of the wave

decreases, V_{ph} will eventually be shifted out from the aforementioned range and the waves will stop growing. This effect will occur over a distance

$$\Delta z \sim L \frac{\Delta v_b}{v_b} \frac{v_T^2}{v_b^2}, \tag{2.19}$$

and over time

$$\tau \sim \frac{\Delta x}{V_{gr}} \sim \frac{L}{v_b} \frac{\Delta v_b}{v_b}. \tag{2.20}$$

The growth rate γ for rather small values of density of the beam $n_b \ll n$ may be estimated as

$$\gamma \sim \omega_{p_e} \frac{n_b}{n} \left(\frac{v_b^2}{\Delta v_b} \right)^2. \tag{2.21}$$

Thus the product $\gamma\tau$ which determines the efficiency of the growth of the waves is

$$\gamma\tau \sim \frac{n_b}{n} \frac{v_b}{\Delta v_b} \frac{\omega_{p_e} L}{v_b} \tag{2.22}$$

and decreases when Δv_b increases. The quasi-linear relaxation stops when $\gamma\tau \sim \Lambda$, or when beam velocity spread reaches

$$\frac{\Delta v_b}{v_b} \sim \frac{1}{\Lambda} \frac{n_b}{n} \frac{\omega_{p_e} L}{v_b}. \tag{2.23}$$

We may obtain a rough estimation of the characteristic length of relaxation by substituting Δv_b from Eq.(2.23) into Eq.(2.19):

$$l_{dn/dz<0} \sim \frac{L}{\Lambda} \frac{n_b}{n} \frac{\omega_{p_e} L}{v_b} \frac{v_T^2}{v_b^2} < L. \tag{2.24}$$

This brings up the conclusion that quasi-linear relaxation in plasma with monotonically decreasing density profile is much less efficient that the one in homogeneous

plasma. The characteristic scale of relaxation in homogeneous plasma is (Breizman & Ryutov, 1969)

$$l_{n=const} \sim \Lambda \frac{n}{n_b} \frac{v_b}{\omega_{p_e}} \frac{v_T^2}{v_b^2}. \tag{2.25}$$

In order to make a small estimation, we will take typical electron beam (associated with type III solar radio bursts) and solar wind parameters at 1 a.u. (e.g., see (Robinson, 1992)): $n_b/n \approx 10^{-5}$, $v_T \approx 1.5 \cdot 10^8$ cm/s, $v_b \approx 5 \cdot 10^9$ cm/s, $\omega_{p_e} \approx 10^4$ Hz and $\Lambda \approx 15$. We take L, the characteristic scale of inhomogeneity, equal to 1.a.u., i.e., $1.5 \cdot 10^8$ km. Thus the estimation gives

$$l_{dn/dz<0} \sim 10^7 km, \qquad l_{n=const} \sim 100 km. \tag{2.26}$$

As a result, we see that the characteristic scale of QL relaxation in a plasma with the monotonically decreasing density profile may be much larger than the one in homogeneous plasma and depends strongly on the initial parameters of the beam and plasma, especially on the value of the scale of density inhomogeneity L. However, it is supposed that in order to persist to such enormous distances as several a.u., there should be some additional effect taken into account that slows down the relaxation of the beam.

Numerical simulations of beam-plasma interaction in a plasma with monotonically decreasing density profile were performed by (Kontar, 2001; Kontar & Reid, 2009; Reid & Kontar, 2010, 2013). They have demonstrated that the electron beams ejected from the Sun lose their energy via QL relaxation much slower than it would be if plasma was homogeneous, and thus the beam can persist to the distances larger than 1 a.u. The relaxation is slowing down due to the refraction of waves towards lower phase velocities, what allows them to be absorbed by a slower particles of the beam, what is consistent with the *beam-plasma structure*. The results of simulations have been confirmed by observations of STEREO spacecrafts (Krupar et al., 2015).

Kontar & Reid (2009); Reid & Kontar (2010, 2013) have studied the energy spectrum of the electron beam at a distance around 1 a.u. They have demonstrated that the density inhomogeneity has a direct impact on the spectral characteristics of such beams. These electron beams are detected near the Earth with a double power-law energy spectrum and the simulations have allowed to reproduce it.

Thus we have seen that the presence of a negative density gradient slows down the relaxation of the beam, resulting in larger value of relaxation scale and lower values of amplitudes of excited Langmuir waves. The final state of the relaxation here is the same as in case of homogeneous plasma. In fact, various configurations of plasma density profile have been studied in the scope of QL relaxation, among them the monotonically increasing density profile, plasma with randomly distributed density cavities, plasma with random density fluctuations etc (Ryutov, 1969; Breizman & Ryutov, 1969; Vedenov & Ryutov, 1975; Nishikawa & Ryutov, 1976; Smith & Sime, 1979; Kontar, 2001; Voshchepynets & Krasnoselskikh, 2013; Voshchepynets et al., 2015; Voshchepynets & Krasnoselskikh, 2015). All of them have been demonstrated to suppress the relaxation process, however, we will consider in a more detailed manner only the latter one, as it is most relevant to the space plasma description.

2.5 Impact of the random density fluctuations in the solar wind

2.5.1 Observations of clumpy Langmuir waves

The attempts to detect *in situ* plasma electron oscillations or Langmuir waves, associated with type III solar radio bursts source regions were made back in 1970s. Combining observations from several spacecrafts (*Imp* 6 and 8, *Helios* 1 and 2, *Voyager* 1 and 2) and covering a wide range of heliocentric distances from 0.29 to 2.2 a.u., Gurnett et al. (1978) have analyzed 153 type III radio bursts that occurred

during the considered time range, and 18 among them had associated Langmuir waves. It appeared that in all these events Langmuir waves were not distributed uniformly in space but clumped into the spikes with peak amplitudes typically three orders of magnitude above the mean, in contrast to the EM radiation which was relatively smooth. The phenomenon of Langmuir clumping is important because it indicates that since the spikes of intense plasma waves occupy only $\sim 10^{-3}$ of the total radiation source volume, the radiation produced by the spikes has to be $\sim 10^3$ times as intense as the case of plasma waves distributed uniformly throughout the whole source region. Smith & Sime (1979) have performed an analysis in order to find the reason for such clumping. They have inferred that it is likely that density inhomogeneities in plasma are responsible for the observed clumpiness and gave no support for non-linear strong turbulence processes such as soliton formation or collapse. Spectral analysis of Langmuir waves time series from the *ISEE* 3 plasma wave instrument has confirmed that the clumps have the same size distribution as the ambient low-frequency density fluctuations in the solar wind Robinson et al. (1992).

2.5.2 Stochastic Growth Theory

Robinson (1992); Robinson et al. (1992); Robinson & Cairns (1993); Robinson et al. (1993); Robinson (1995); Cairns & Robinson (1997, 1999) have proposed a stochastic growth theory (SGT) in order to explain the observed clumping of Langmuir waves in source regions of type III radio bursts. QLT predicts the electron beam to reach the state of marginal stability which implies that net growth of Langmuir waves only balances net losses. SGT suggests that ubiquitous density fluctuations in plasma perturb this state by only allowing the growth of the waves in the localized *growth regions* where the density gradient is approximately parallel to the direction of the beam. In this case both the beam and the waves develop inhomogeneities on the scales comparable with the scales of density fluctuations. This leads to occurrence

of local fluctuations of the waves growth rate as the beam passes by. Thus the logarithmic energy density of the waves is undergoing a random walk, growing when the waves remain in the *growth region* and damping otherwise (Robinson et al., 1992).

SGT predicts a normal distribution of the waves growth rate around zero and thus a log-normal distribution of the Langmuir waves intensity. The assumption behind this is that waves amplitudes are rather small and are not sufficient to trigger the nonlinear processes. The analysis of several *in situ* measurements has confirmed that the distributions of waves intensity closely resembled a log-normal distribution (for example, see (Robinson et al., 1993; Robinson & Cairns, 1993; Cairns & Robinson, 1997, 1999)). However, a statistical study of the large database measured by *CLUSTER* spacecraft as well as the numerical model of wave propagation in an unstable plasma with inhomogeneities have demonstrated that deviations from the log-normal distribution of the waves amplitudes are quite significant (Krasnoselskikh et al., 2007). As the main reason of such deviations there was suggested (1) the violation of a central limit theorem implied in SGT, caused by a rather small effective number of regions where the waves grow under the typical conditions for the Earth's electron foreshock and (2) a significant change in the statistical properties of wave amplitudes due to the saturation of waves caused by wave–particle interactions. Similar conclusions were made by Musatenko et al. (2007) and Vidojević et al. (2011) based on the statistical analysis of the Langmuir waves measurements performed by *CLUSTER* and *WIND* spacecraft respectively.

2.5.3 A dynamical model

The dynamical model is a self-consistent model that describes wave-particle and wave-wave interaction in randomly inhomogeneous plasma. More specifiaclly, it is a Hamiltonian numerical model where the background plasma is described by Zakharov equations (Krafft et al., 2013; Krafft & Volokitin, 2014; Volokitin & Krafft,

2016, 2018, 2020), while the beam and its interaction with waves is modeled by a particle-in-cell code. In this model the system is periodic and is chosen to be long enough to incorporate several modes of density fluctuations.

Comparison of the waveforms of the Langmuir waves measured by *STEREO* and *WIND* satellites has shown that their characteristic features are very similar to those predicted by the dynamical model (Krafft & Volokitin, 2014). A statistical study of the amplitudes of Langmuir waves based on the results of the dynamical model have demonstrated that their PDFs belong to Pearson types I, IV and VI. This comes in a good agreement with the observations of *CLUSTER* and *WIND* spacecrafts (Krasnoselskikh et al., 2007; Musatenko et al., 2007; Vidojević et al., 2011). However, the dynamical model fails to reproduce the state of a marginal stability during the relaxation of the beam and, in addition, requires large computational resources.

2.5.4 Random density fluctuations in solar wind

The presence of the random density fluctuations in solar wind is ubiquitous. They were a subject of active studies since 1970s by means of several methods: (1) *in situ* spacecraft measurements, (2) phase scintillation or spectral broadening of signals transmitted from spacecraft to Earth and (3) interplanetary scintillation of extragalactic radio sources (see Woo & Armstrong (1979) and references therein). By means of these methods it was attempted to reconstruct the power spectral density (PSD) of the density fluctuations in solar wind in various frequency domains. Celnikier et al. (1983) have analyzed the data of *ISEE* 1 and 2 on then unprecedented frequency range and reported for the first time the presence of not singular but double power law in PSD of density fluctuations in solar wind. They found that in the low frequency range the spectral index is very close to -5/3, consistent with Kolmogorov spectrum. Later numerous investigations have confirmed and extended this finding. For instance, nowadays it is known that there are at least several power laws present in turbulent spectrum of solar wind, following the Kolmogorov spec-

trum for the frequency range of $\sim 10^{-3}$ Hz $\div 10^{-1}$ Hz, then on ~ 0.1 Hz $\div 1$ Hz it flattens slightly (spectral index varies among the authors, for instance Celnikier et al. (1987) report a value ~ -0.64), in the frequency domain ~ 1 Hz $\div 100$ Hz it demonstrates a steeper -2.7 power law index and at larger frequencies it flattens to almost a constant value (see Fig.2.5).

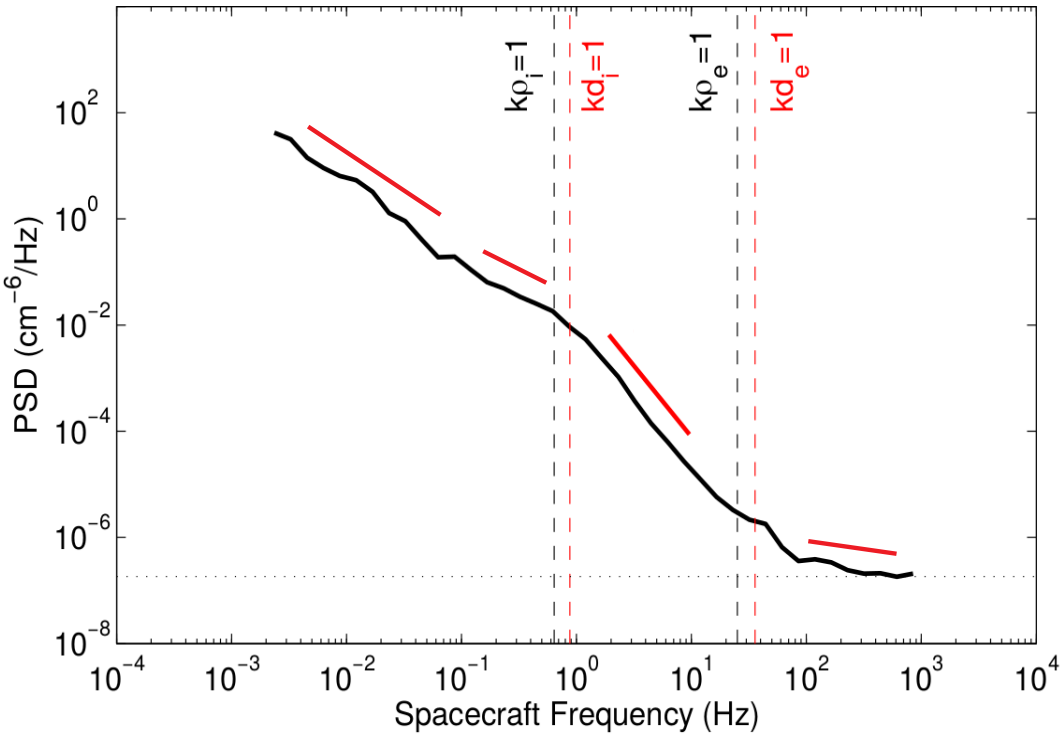

Figure 2.5: A smoothed power spectra of electron density fluctuations: Ion and electron gyroscales, ρ, and inertial lengths, d, are marked with vertical dashed lines. The empirical noise floor is marked with a horizontal dotted line (adapted from (Chen et al., 2012)).

Turbulent properties of the solar wind plasma were summed up in numerous reports (e.g., see the review by Horbury et al. (2012) and references therein). Voshchepynets et al. (2015) have estimated that the $\sim 10^{-1}$ Hz $\div \sim 10^{2}$ Hz spectrum range of density fluctuations defines the beam-plasma interaction in inhomogeneous plasma around 1 a.u. and the fluctuations outside this range have no impact on the process whatsoever.

In situ measurements of the density fluctuations spectrum on board *ISEE* 1 and 2 satellites have reported the level of density fluctuations $\sim 10^{-2}$ at around 1 a.u. on the scale range of the order of 100 km Celnikier et al. (1983). Recent observations as well as *in situ* measurements by *Parker Solar Probe* (*PSP*) spacecraft confirm, that the level of density fluctuations in the solar wind can go up to seven percent of the average background density at $\sim 36\ R_{\odot}$, and the analysis based on comparison of Monte Carlo simulations with *PSP* observations of decay times of the type III bursts predicts a growth of the level of density fluctuations towards the Sun, reaching up to twenty percent in the high corona (Krupar et al., 2020).

2.5.5 Langmuir waves in an inhomogeneous solar wind

Density fluctuations and Langmuir wave phase velocity variations

The importance of the varying density profile for the resonant interaction of an electron beam with plasma was pointed out earlier in this section. As the fluctuations of density have a direct effect on the Langmuir wave phase velocity (see Eq.(2.17)), their presence may remove the waves from the resonance with the beam and thus slow down the relaxation process. Kellogg et al. (1999) have reconstructed the time series of density fluctuations from an averaged density spectrum reported by Neugebauer (1976) and have shown that even small density variations are sufficient to remove the Langmuir waves, that have a frequency very close to local plasma frequency, from the resonance with the beams, typically observed in association with type III radio bursts near 1 a.u.

Similarly to this procedure, Voshchepynets & Krasnoselskikh (2015) have reconstructed the time series of density from the density spectrum reported by Celnikier et al. (1987) and demonstrated the variations of Langmuir wave phase velocity caused by background density fluctuations. Again, the conclusion was that even rather small variations of density trigger considerably large response of wave phase velocity (see Fig.2.7).

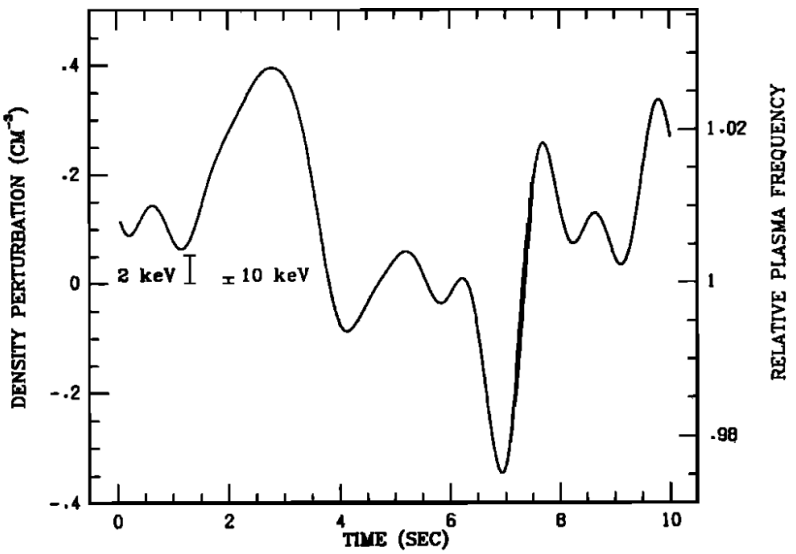

Figure 2.6: A time series of density fluctuations reconstructed from an averaged spectrum (Neugebauer, 1976). The two brackets at the left show the difference between the plasma frequency and the resonant frequency for electron beams of 2 keV and 10 keV (Kellogg et al., 1999).

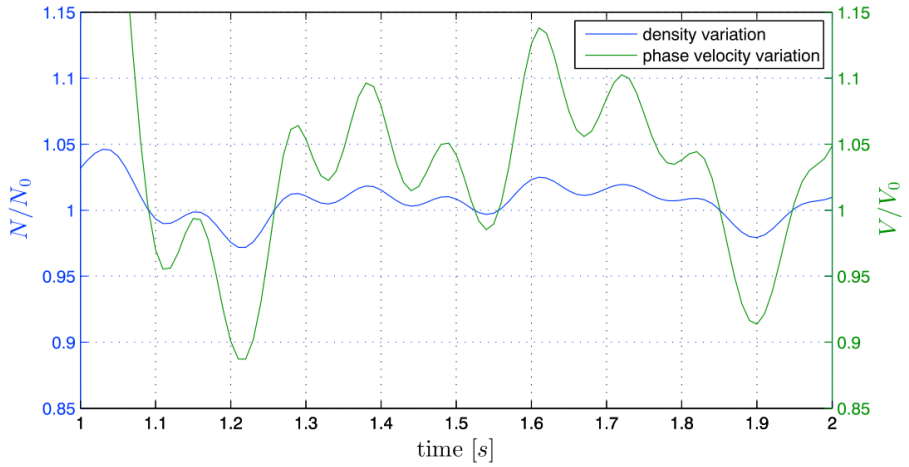

Figure 2.7: A synthetic time series of density fluctuations reconstructed from the density fluctuations spectrum Celnikier et al. (1987) (the blue curve) and a corresponding variations of the phase velocity of the Langmuir waves (the green curve) (Voshchepynets & Krasnoselskikh, 2015).

Wavevector deviations and angular diffusion

Another important effect which may affect the beam-plasma interaction is the angular diffusion of Langmuir waves caused by the wavevector deviations. Nishikawa & Ryutov (1976) have studied beam-plasma interaction in a plasma with random density inhomogeneitites. If the amplitude of the density fluctuations is small compared to Langmuir wave dispersion:

$$|\delta n/n_0| \ll 3k_l^2\lambda_D^2, \tag{2.27}$$

where δn is the deviation from the average density n_0, Langmuir wave packets cannot be trapped or reflected by these inhomogeneities, and are only scattered. This scattering appears to be elastic, i.e., it does not change the frequency and the absolute value of the wavevector. It was found that such inhomogeneities affect the development of the beam-plasma instability and it was suggested that the major effect of small amplitude density fluctuations can be taken into account in the form of effective angular diffusion of the Langmuir wave wavevector, which in turn results in the deviation of the wave phase velocity and quenching the instability. However, Voshchepynets et al. (2015) have made an estimation of the characteristic time of such angular diffusion and has shown that it is much larger than the characteristic time of the propagation of Langmuir waves on the given sub-interval. This means that the angular diffusion is too 'slow' to affect significantly the beam-plasma interaction. Besides, the arguments presented in current Chapter in favor of quasi one-dimensional spatial structure of Langmuir waves observed in space plasma, suggest that angular diffusion is indeed of minor importance.

On the contrary, when density fluctuations have rather large amplitudes

$$\delta n/n_0 \geq 3k_l^2\lambda_D^2, \tag{2.28}$$

they can cause the reflections of Langmuir waves and change the magnitude of

a wavevector in the direction of wave propagation. In this case scattering may be inelastic, i.e., part of the energy of the wave may be dissipated during the reflection (for instance, because of generation of an EM wave via linear mode conversion). Such large amplitude density fluctuations are considered further in this manuscript.

2.6 Probabilistic model of a beam-plasma interaction in randomly inhomogeneous plasma

In order to more properly describe the relaxation of an electron beam in a plasma with the density fluctuations, Voshchepynets et al. (2015) have suggested a new *probabilistic model of beam-plasma interaction*. Its main goal is to retrieve the average characteristics of wave intensities and particle distributions during and after the relaxation using the PDF of density fluctuation. In such a manner, it is possible to describe statistically the effect of random density variations on the process of relaxation.

2.6.1 The quintessence of a probabilistic model

The main approach of this 1D model is to divide a continuous spatial interval where the beam-plasma interaction takes place, into smaller equally sized intervals of the length a, such that the wave-particle interaction on each interval in considered independent from the one on previous intervals. The length of the interval a must be much larger than the wavelength of the waves that are in resonance with the beam, but much smaller that characteristic scale after which the waves escape the resonance. The latter depends on the inhomogeneity scale L (Voshchepynets et al., 2015):

$$\lambda \ll a \ll L\frac{n_0}{\delta n}\frac{\Delta v_b}{v_b}\frac{v_T^2}{v_b^2}. \tag{2.29}$$

The density profile for each interval is replaced by its linear approximation:

$$n(z) = n_0 + \delta n(z_{in}) + \frac{\delta n(z_{in} + a) - \delta n(z_{in})}{a}(z - z_{in}), \tag{2.30}$$

here $\delta n(z_{in})$ and $\delta n(z_{in}+a)$ are deviations from n_0 at the start and the end of interval correspondingly (Voshchepynets & Krasnoselskikh, 2015). These deviations of the plasma density are considered as random and independent with a predetermined statistical distribution, $P_{\delta n}(\delta n)$. It is assumed that in the center of the interval the density is random and described by a predetermined statistical distribution.

These assumptions allow to describe the action of the of the field of a wave with a known frequency and small amplitude on a particle, and calculate the effect of a wave-particle interaction on each particular interval.

As we could have seen from dispersion relation (2.16) and Fig.2.7, the fluctuations of plasma density result in a fluctuations of a phase velocity of the waves. Thus the PDF of density fluctuations $P_{\delta n}(\delta n)$ uniquely determines the PDF of waves phase velocity $P_\omega(V_{ph})$. The PDF that corresponds to the observations of density fluctuations in solar wind plasma is non-Gaussian (Celnikier et al., 1987; Kellogg & Horbury, 2005; Chen et al., 2012). However, in this model for the sake of simplicity the authors have used a Gaussian distribution as a first step approximation. Further we will make a distinction between δn as a variable with a PDF $P_{\delta n}(\delta n)$ and $\langle \Delta n \rangle$ as it's standard deviation, which we will often refer to as a 'level' or 'amplitude' of the density fluctuations.

Voshchepynets et al. (2015) have estimated the normalized PDFs of wave phase velocity for different amplitudes of density fluctuations (see Fig.2.8) and have shown that the increase of the magnitudes of density variations leads to a broadening of the wave phase velocity PDF in the velocity space and thus consequently to the blurring of the resonance with the beam particle. In the case when $\langle \Delta n \rangle / n_0 \to 0$, $P_\omega(V_{ph})$ tends towards The Dirac delta function, what corresponds to a homogeneous plasma case and determines a unique value of a phase velocity of the wave $V_{ph} = \omega/k$.

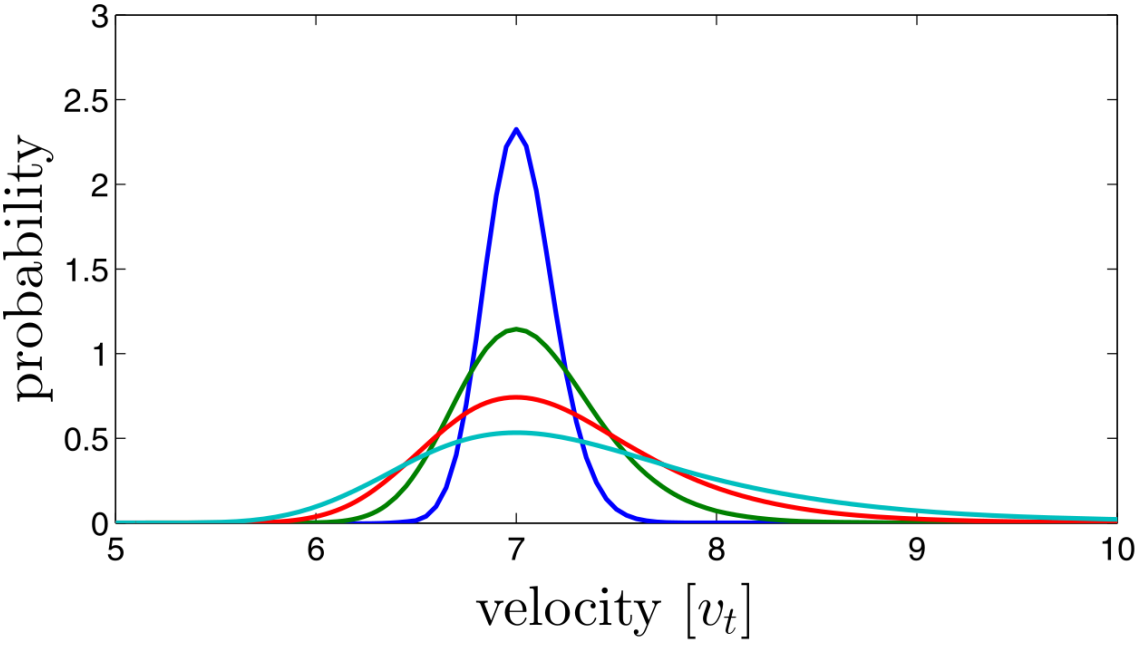

Figure 2.8: Normalized PDFs $P_\omega(V_{ph})$ for the various levels of density fluctuations. $P_\omega(V_{ph})dV_{ph}$ here is the probability that the wave with a ratio $\omega/k = 7v_T$ will have a phase velocity V_{ph} within the given interval. Colors correspond to the level of density fluctuations: $\langle\Delta n\rangle/n_0 = 0.005$ (blue), $\langle\Delta n\rangle/n_0 = 0.01$ (green), $\langle\Delta n\rangle/n_0 = 0.015$ (red), $\langle\Delta n\rangle/n_0 = 0.02$ (cyan) (Voshchepynets et al., 2015).

2.6.2 Equations of probabilistic model and main results

In order to transition from description of the mechanisms of wave-particle interactions on the discrete intervals to the global picture of full-stage relaxation in plasma, the authors have performed the statistical averaging of the expressions over a large number of intervals. The basic equations of the probabilistic model of beam-plasma interaction were obtained in (Voshchepynets et al., 2015) and describe the interaction of the beam with several monochromatic waves with energy densities W_i and frequencies ω_i :

$$\frac{\partial f}{\partial t} = \frac{\partial}{\partial v} v \sum_{i=1}^{K} W_i P_{\omega_i}(v) \frac{\partial f}{\partial v}, \tag{2.31}$$

$$\frac{dW_i}{dt} = \int_0^\infty W_i V_{ph}^2 \frac{\partial f}{\partial V_{ph}} P_{\omega_i}(V_{ph}) dV_{ph}. \tag{2.32}$$

One can see, that the equations resemble closely the equations of QLT in 1D case. Table 2.1 allows to compare the two approaches:

1D QLT equations	Probabilistic model equations
$\frac{\partial f}{\partial t} = \frac{\omega_{pe}^2}{n_e m_e} \frac{\partial}{\partial v} \left(\frac{W}{v} \frac{\partial f}{\partial v} \right) \Big\vert_{v=V_{ph}}$	$\frac{\partial f}{\partial t} = \frac{\omega_{pe}^2}{2 n_e m_e} \frac{\partial}{\partial v} v \sum_{i=1}^{K} \frac{W_i}{\omega_i} P_{\omega_i}(v) \frac{\partial f}{\partial v}$
$\frac{\partial W}{\partial t} = \pi \omega_{p_e} W v^2 \frac{\partial f}{\partial v} \Big\vert_{v=V_{ph}}$	$\frac{dW_i}{dt} = \pi \omega_{p_e} \frac{n_b}{n_0} W_i \int_0^\infty V_{ph}^2 \frac{\partial f}{\partial V_{ph}} P_{\omega_i}(V_{ph}) dV_{ph}$

Table 2.1: A comparative table of quasi-linear equations that describe the wave-particle interaction in 1D case. Left panel: homogeneous plasma (Vedenov et al., 1962b). Right panel: plasma with random density fluctuations (Voshchepynets & Krasnoselskikh, 2015)

The equation system (2.31)-(2.32) has been solved numerically for a set of 2000 waves with a median of the $P_\omega(V_{ph})$ uniformly distributed in a range between $2v_T$ and $38v_T$. The numerical solution for the level of density fluctuations of 2% is represented on Fig.2.9. According to current model, the beam relaxation results in the formation of the plateau in the range of velocities $v < v_b$, similarly to the case of the homogeneous plasma. For the opposite interval of velocity space, $v > v_b$, the number of particles increases. Thus there is an acceleration of a certain amount of particles to the velocities $v > v_b$ due to the reabsorbtion of the waves triggered by the presence of density fluctuations and blurring of the wave-particle resonance. Such reabsorbtion significantly increases the relaxation time.

Authors distinguish three cases of the level of density fluctuations with respect to the wave dispersion $k_l^2 \lambda_D^2 \approx v_T^2 / v_b^2$ that determine the character of the relaxation:

(1) $\langle \Delta n \rangle / n_0 \ll v_T^2 / v_b^2$, the relaxation process is the same as in a homogeneous plasma as the density fluctuations are too small to affect it;

(2) $\langle \Delta n \rangle / n_0 \sim v_T^2 / v_b^2$, an intermediate regime, characterized by a presence of a small percentage of accelerated particles;

(3) $\langle \Delta n \rangle / n_0 \gg v_T^2 / v_b^2$, fluctuations play a major role in the relaxation process, creating an effective energy transfer to both cold and accelerated particles, while

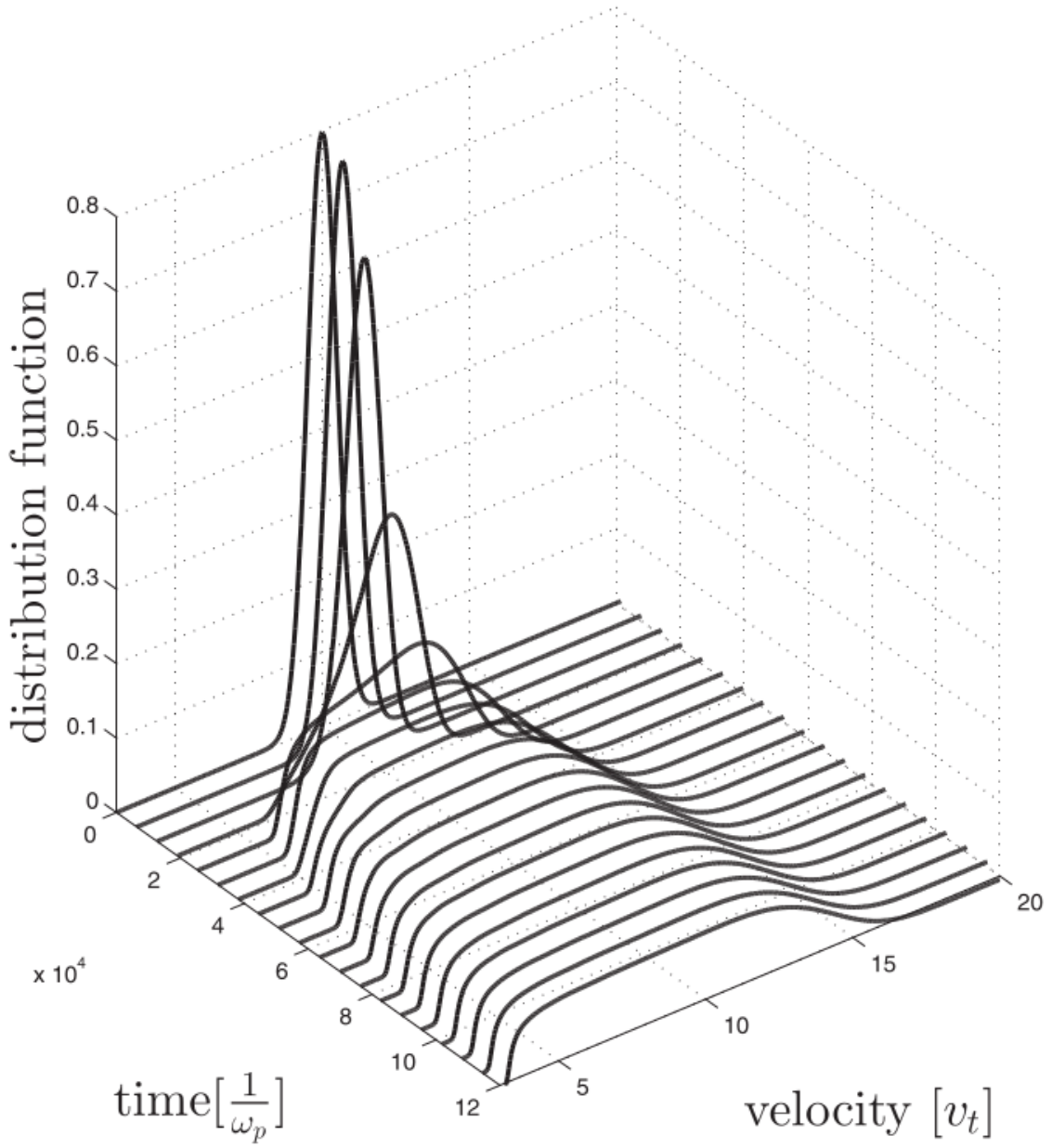

Figure 2.9: Evolution of the normalized electron distribution function according to probabilistic model. Initial conditions are: Gaussian distribution of beam electrons, $v_b = 10v_T$, $\Delta v_b = 0.5v_T$, $n_b/n_0 = 2.5 \cdot 10^{-5}$, $\langle \Delta n \rangle / n_0 = 0.02$. The core distribution (cold electrons) has not been taken into consideration (Voshchepynets et al., 2015).

the energy of the latter may reach up to 70 % of the initial beam energy.

The characteristics of the accelerated particles strongly depend on the density fluctuations level. Voshchepynets et al. (2015) have defined the accelerated particles as the ones, which have the velocities larger than $v_b + \Delta v_b$. For instance, it was found that the ratio of the number of the accelerated particles as well as their energy by the end of the relaxation is increasing with the amplitude of the density variations as $\sim \sqrt{\langle \Delta n \rangle / n_0}$. The characteristic time of the relaxation t_r varies as $\sim (\langle \Delta n \rangle / n_0)^{-2}$. The effects of different values of initial beam velocity v_b and its thermal spread Δv_b were also studied. For instance, higher initial energies of the beam resulted in higher ratio of accelerated particles, whilst higher thermal spread of the beam would result in smaller number of accelerated particles, which, however, comes naturally from the definition of the accelerated particles.

2.6.3 Two stage relaxation according to a probabilistic model

Voshchepynets & Krasnoselskikh (2015) have studied the question of the temporal evolution of the electron distribution function under different levels of density fluctuations and have distinguished two stages in the beam relaxation according to the probabilistic model. The first stage, also called the major stage, the relaxation proceeds quite quickly, triggering the intense wave growth and energy transfer from the beam to the cold and accelerated particles. After this follows the second stage when the relaxation slows down, and the instability occurs only at a marginal level causing the relaxation to proceed very slow. It was shown that with the increase of the level of density fluctuations the characteristic time of the second stage will increase significantly. Generally speaking, a small but positive slope of the distribution function may exist during the second stage for a considerably large time (see Fig.2.10). Authors have also applied two types of PDF of density fluctuations: Gaussian and Pearson type II. They found that the relaxation process slightly differs for these two types of PDFs, and the divergence is more pronounced for the larger level of density

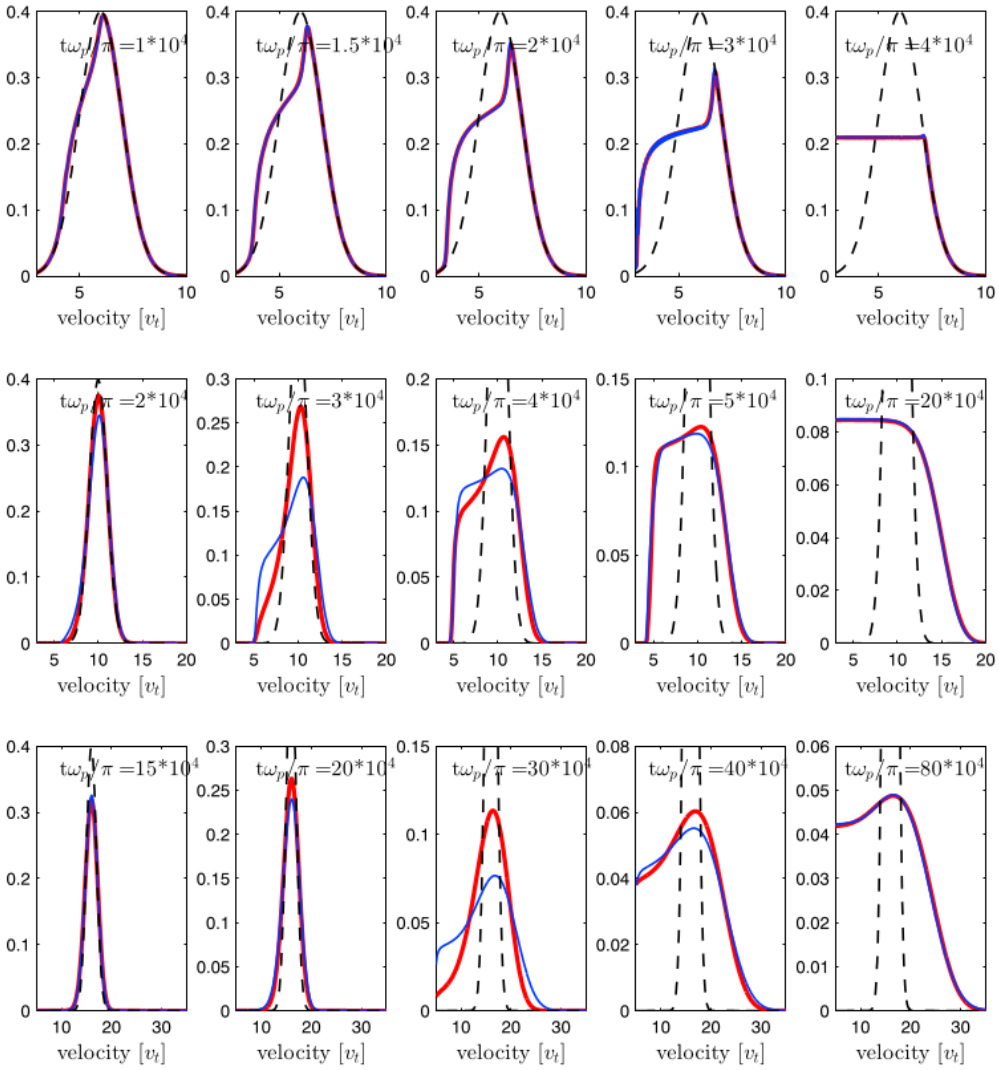

Figure 2.10: A temporal evolution of the normalized electron velocity distribution functions. The core distribution that corresponds to cold electrons of the background plasma was not considered. Each plot provides a snapshot of the electron distribution function at different moments of time. Colors that correspond to simulations with various distributions for the density fluctuations are as follows: blue, the normal distribution, and red, the Pearson type II distribution. Results were obtained for various parameters of the beam and levels of the density fluctuation. Upper panel: $\langle \Delta n \rangle / n_0 = 0.005$, $v_b = 6v_T$, $\Delta v_b = v_T$. Medium panel: $\langle \Delta n \rangle / n_0 = 0.02$, $v_b = 10v_T$, $\Delta v_b = v_T$. Lower panel: $\langle \Delta n \rangle / n_0 = 0.03$, $v_b = 16v_T$, $\Delta v_b = v_T$ (Voshchepynets & Krasnoselskikh, 2015).

fluctuations. Nevertheless, the eventual state after the relaxation is very similar for both of them. Early *in situ* measurements of the electron distribution functions solar wind at around 1 a.u. have revealed that there was no plateau-like structure of $f(v_e)$ but rather a small slope on the distribution function. Lin et al. (1981) has reported that there was a qualitative agreement between variations in the plasma wave levels and in the development of regions of positive slope in $f(v_e)$. The evolution of this distribution function, however, predicted far higher plasma wave levels than those observed. They stated that the lack of obvious plateauing of the distribution suggests that the observed waves have been removed from resonance with the beam electrons. Probabilistic model is able to give an explanation to that phenomena as it predicts the state of marginal stability when the distribution function maintains a small positive slope on a considerably large distances and also the diminution of the energy density of the waves in the process of relaxation because of the energy transfer to accelerated particles.

2.6.4 Estimation of the energy density of Langmuir waves according to the probabilistic model

Probabilistic model of beam-plasma interaction allows one to determine the temporal evolution of the energy density of associated Langmuir waves. As discussed in the previous paragraph, the relaxation demonstrates two-stage behavior, first one being the phase of the intense growth of the Langmuir waves and the second being a marginal stability phase, when the growth rate of the waves significantly decreases but remains above zero for a considerably long period of time. Fig.2.11a shows the temporal evolution of energy density of Langmuir waves, generated in randomly inhomogeneous plasma by an electron beam, according to a probabilistic model. Results are provided for typical physical parameters in source region of solar type III radio burst: beam density $n_b = 10^{-5} n_0$, beam velocity $v_b = 16 v_T$; and for six levels of density fluctuations: $\langle \Delta n \rangle / n_0 = 0.01, 0.02, 0.03, 0.04, 0.07$ and 0.1. Langmuir waves

energy density is shown as a ration of initial energy density of the beam W_{b0}. The panel b) of Fig.2.11 demonstrates the ratio χ between the maximum energy density of the Langmuir waves achieved during the relaxation and the W_{b0}. One can see that this ratio can be approximated as a power-law function of a level of density fluctuations with typical index around ~ -0.6. Panel c) of Fig.2.11 represents the time scale t_r of the growth of the Langmuir waves up until their energy density reaches a maximum. t_r is increasing with the growth of the level of density fluctuations, and the effect is more pronounced for larger values of the initial beam velocity v_b. An

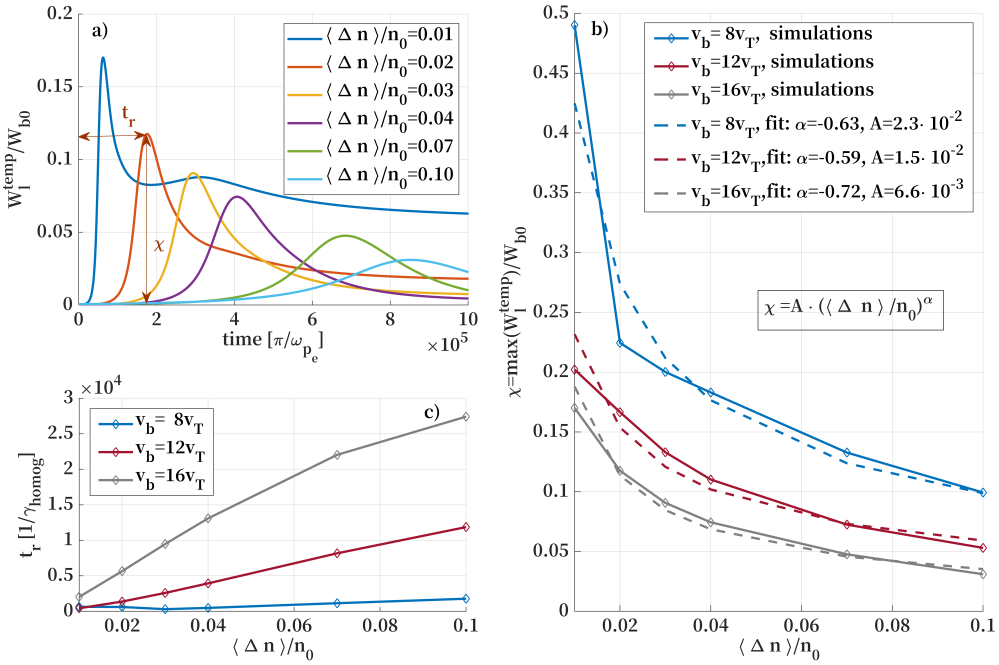

Figure 2.11: Panel a) temporal evolution of energy density of Langmuir waves W_l^{temp} in units of initial energy density of electron beam W_{b0}, obtained by means of probabilistic model (Voshchepynets et al., 2015). Numerical solutions were found under following conditions: $n_b = 10^{-5}n_0$, $v_b = 16v_T$ and for six different levels of average density fluctuations $\langle\Delta n\rangle/n_0$. Panel b) maximum values of Langmuir wave energy density (see panel a)) vs average level of density fluctuations, for three different ratios of initial beam velocity v_b and electron thermal velocity v_T. Simulation results (solid lines) are fitted by power-law (dashed lines). Panel c) time of Langmuir waves energy growth during the beam relaxation (see panel a)) in units of a growth rate for homogeneous plasma γ_{homog} vs average level of density fluctuations, for three different ratios of initial beam velocity v_b and electron thermal velocity v_T (Tkachenko et al., 2021).

important remark is that the probabilistic model describes the *temporal* evolution of Langmuir waves while for present study the problem should be treated as the *spatial* one, with the boundary condition corresponding to continuous ejection of electron beam. It is well known that solutions of these two problems are rather similar, but the quasi-equilibrium saturation state corresponds to redistribution of the energy fluxes rather than the energy itself. This implies higher level of electrostatic waves energy in spatial problem with respect to temporal. The wave energy flux is carried with the group velocity of waves, and the wave energy density may be found from the solution of the temporal problem:

$$W_l^{SBP} = \frac{V_{ph}}{V_{gr}} W_l^{temp}, \tag{2.33}$$

here W_l^{SBP} is the wave energy in framework of spatial boundary problem, while W_l^{temp} is the wave energy corresponding to quasi-saturation in the framework of the temporal problem, V_{gr} is a group velocity of Langmuir waves. Since for the waves, generated by the beam the ratio is $V_{ph}/V_{gr} = v_b^2/3v_T^2$, it implies that for beams having velocities $10 \div 15 v_T$ value of ratio may vary from 33 to 75. It also leads to intensification of the waves in relatively small region of space.

Another significant feature is the resemblance of the temporal profiles of the Langmuir wave energy density, presented on Fig.2.11a and of the typical intensity profiles of the type III radio bursts. The type IIIs exhibit the initial relatively short phase of a high intensity followed by a much longer phase of mediocre intensity which keeps decreasing until reaches a thermal noise level. Thus the observations ultimately speak in favor of a two-stage relaxation process.

Voshchepynets et al. (2017) have performed a statistical study of the amplitudes of the electric fields of Langmuir waves, obtained in a numerical simulations based on the probabilistic model and the dynamical model (Krafft et al., 2013). As a result of both simulations, the PDFs of the logarithmic amplitudes were distributed according

to Pearson type IV, I and VI distributions, which is consistent with the observations of *CLUSTER* and *WIND* spacecrafts (Krasnoselskikh et al., 2007; Musatenko et al., 2007; Vidojević et al., 2011). Moreover, both models exhibit the formation of spikes of Langmuir waves energy density with the magnitudes several times above the mean, reproducing the observed clumpy structure of Langmuir waves in solar wind. The major advantage of the probabilistic model in this case is that it requires way less computational resources compared to the dynamical model.

2.7 Radio emission on fundamental frequency in a randomly inhomogeneous plasma

Ginzburg & Zheleznyakov (1958) have suggested of a plasma emission mechanism in order to explain the type III emissions. According to their assumption, the EM emission at a fundamental frequency was associated with the elastic scattering of Langmuir waves on the thermal ions. Later it became obvious that this mechanism requires reconsideration, as the observations did not confirm the assumption about Rayleigh scattering.

The most widely accepted and recognized mechanism that came instead is the nonlinear wave-wave interaction of Langmuir, ion sound, and EM waves: $l \pm s \rightarrow t$ (e.g., see the review by Reid & Ratcliffe (2014)). The most important question concerning the efficiency of such process is the presence of ion sound waves with wavevectors $\mathbf{k}_s \approx \pm\mathbf{k}_l$ required to satisfy the resonant condition $\mathbf{k}_l \pm \mathbf{k}_s \rightarrow \mathbf{k}_t$, where $k_l = \omega_{p_e}/v_b \gg k_t = \omega_{p_e}/c$. It means that either the broad spectrum of ion sound waves should contain the required waves or they should be generated by the decay instability, otherwise there is a high probability that some other process is responsible for generation of the EM emission at the fundamental frequency (Melrose, 1987). The ion sound wave, generated by the decay instability $l \rightarrow l' + s$ in general cannot be directly involved in generation of the EM emission since the secondary Langmuir

wave has the wavevector almost opposite to the wavevector of the primary wave, the wavevector of the sound wave is typically too large $\mathbf{k}_s \approx -2\mathbf{k}_l$. We will provide a more detailed insight to the role of the ion sound waves in nonlinear wave-wave processes further in a Section 3.2. However, already now it is obvious that some other mechanism may be playing a dominant role in the generation of a fundamental EM emission of type IIIs.

And such mechanism was already suggested: the linear mode conversion (LMC) of Langmuir waves directly into EM waves in presence of an increasing density gradient. The importance of the encounters of Langmuir waves with the regions with higher density for the generation of EM waves was pointed out by a number of authors (e.g., see (Hinkel-Lipsker et al., 1992) and references therein) and extensively studied by Mjølhus (1983, 1990); Kim et al. (2007, 2008, 2009, 2013); Schleyer et al. (2013, 2014) for the case of a magnetized plasma. It was shown by Krasnoselskikh et al. (2019) that even a simple reflection of Langmuir waves on a density inhomogeneity can result in an efficient generation of fundamental EM emission.

Krasnoselskikh et al. (2019) have decided to implement a probabilistic approach in order to estimate the impact of ubiquitous density fluctuations on the generation of fundamental EM emission via LMC. Authors have used the analytical expression for the conversion coefficient derived in (Hinkel-Lipsker et al., 1992) as a function of the scale of density inhomogeneity and an angle of the Langmuir wave wavevector with respect to the direction of the density gradient. To obtain the efficiency of the conversion of Langmuir waves into EM fundamental emission, the conversion coefficient was averaged over a spectrum of scales of density fluctuations and also over the angles. The latter were assumed to be distributed uniformly over a range from 0 to π. The last but not the least, authors have also taken into account the total probability of the reflection of the Langmuir wave, as such reflection is crucial for realization of LMC. In our investigation further we will make a use of the PDF of the spatial scales of density fluctuations and a reflection coefficient used

by Krasnoselskikh et al. (2019) and inferred by Voshchepynets et al. (2015), and for this reason we will consider them in a more detail here.

2.7.1 Probability distribution of the scales of density fluctuations

The PDF of scales $P_L(L)$ was determined based on the synthetic density data calculated from a published density power spectra, following the procedure suggested by Kellogg et al. (1999). The inverse Fourier transform allows to reconstruct density profiles $n(t)$ from the power spectrum under assumption that the phases of the waves are random. After this the transformation of temporal profiles $n(t)$ to spatial ones $n(z)$ can be performed making use of a Taylor hypothesis, assuming that density fluctuations are convected with the characteristic velocity of the solar wind v_{sw}. The reconstruction was performed for the interval of frequencies between 10^{-2} Hz and 530 Hz, which has been established by Voshchepynets et al. (2015) as the range that determines the beam-plasma interaction in an inhomogeneous plasma. This corresponds to the interval of scales between 750 m and $4 \cdot 10^4$ km for the value of $v_{sw} = 400$ km/s.

The next statement made by authors is that locally the density profiles may be approximated by a linear function, and the PDF of the characteristic scales may be inferred from the PDF of density gradients: $(1/n)\nabla n = \partial \ln n(z)/\partial z = 1/L$. Knowing the $n(z)$ the authors have calculated the PDF of density gradients, $P(\partial \ln n(z)/\partial z)$ and have found that it is very close to a Gaussian distribution with a standard deviation A_{sc}. Having approximated this PDF with a Gaussian curve, they derived the analytical expression for the PDF of the scales $P_L(L) = P((\partial \ln n(z)/\partial z)^{-1})$, which has the form

$$P_L(L) = \frac{L_{sc}}{\sqrt{2\pi}L^2} \exp\left(-\frac{L_{sc}^2}{2L^2}\right), \tag{2.34}$$

where $L_{sc} = 1/A_{sc}$ is a characteristic scale of the distribution. The dependence of the characteristic scales L_{sc} on the level of density fluctuations can be approximated by a simple power-law (Tkachenko et al., 2021):

$$L_{sc} \approx 1.4 \cdot (\langle \Delta n \rangle / n_0)^{-1} [km]. \tag{2.35}$$

2.7.2 Reflection coefficient

The reflection coefficient is an important parameter as it stands for the probability of the wave reflection from the region where the plasma frequency becomes equal to the wave frequency. Such reflection may occur once or multiple times. The probability of a single reflection is

$$P_{ref}(\omega) = \int_{\omega}^{\infty} f_{\omega_{p_e}}(\omega_{p_e}) d\omega_{p_e}, \tag{2.36}$$

where $f_{\omega_{p_e}}(\omega_{p_e})$ is a distribution function of plasma frequencies on an interval that is small compared to the characteristic scale of change of electron velocity distribution function (Voshchepynets et al., 2015). Such distribution will be determined by distribution function of the density fluctuations $P_{\delta n}(\delta n)$ on this interval.

The wave will remain in it's initial direction in the case when there either no reflections or they compensate each other. If the aforementioned interval is small enough and we compute the probability of the wave keeping its initial direction over a very large number of such intervals, after multiple reflections, we will obtain

$$P_{forw}(\omega) = 1 - P_{ref}(\omega) + P_{ref}^2(\omega)(1 - P_{ref}(\omega)) + P_{ref}^4(\omega)(1 - P_{ref}(\omega)) + ... = \frac{1}{1 + P_{ref}(\omega)}. \tag{2.37}$$

And the probability of the wave moving in the opposite direction after multiple

reflections will be

$$P_{backw}(\omega) = \frac{P_{ref}(\omega)}{1 + P_{ref}(\omega)}. \tag{2.38}$$

Typically we will use the value $P_{ref} = 0.5$ throughout this manuscript.

2.7.3 Efficiency of Langmuir wave conversion into the EM fundamental emission in presence of density fluctuations

Efficiency of the conversion represents simply a ratio of the energy density of the generated EM waves to the energy density of the Langmuir waves that were involved in the process. This parameter allows to estimate how 'efficient' is the process of EM wave generation and we will also make a use of it for estimation of processes involved in a generation of a harmonic EM emission. Regarding the fundamental emission, Krasnoselskikh et al. (2019) have found that the efficiency of conversion via LMC in a turbulent plasma may reach up to $10^{-4} \div 10^{-3}$ what results in brightness temperatures even higher than observed. Authors argue that if one accounts for the absorption, angular broadening and damping along the trajectory, this may resolve the discrepancy between predicted and observed brightness temperatures. It was also found that the efficiency of conversion increases with the increasing level of density fluctuations (see Fig.2.12).

2.8 Conclusions

Wave-particle interaction has been a fulcrum of interest in plasma physics since the dawn of the discipline. It was crucial to understand the way that the waves are excited and how the particles with the non-equilibrium distribution function contribute to this. Based on quasi-linear equations, a quasi-linear theory of a beam-

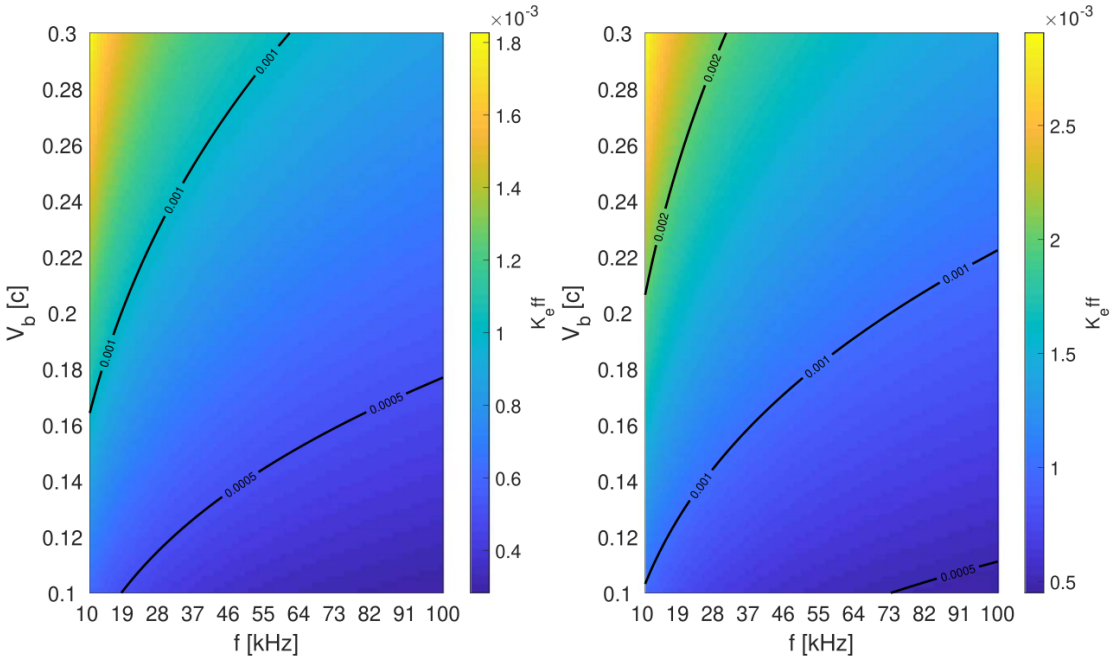

Figure 2.12: Efficiency of the conversion of the Langmuir waves into EM fundamental emission via LMC in randomly inhomogeneous plasma vs beam velocity v_b and frequency of Langmuir waves f. Left panel: $\langle \Delta n \rangle / n_0 = 0.01$. Right panel: $\langle \Delta n \rangle / n_0 = 0.04$ (Krasnoselskikh et al., 2019).

plasma interaction was proposed in 1960s. It has allowed to describe the relaxation of an electron beam in a homogeneous plasma and has yielded a simple analytical solution for one-dimensional problem. Yet, in it's initial form the results of QLT failed to reproduce the observational parameters of particle distributions and associated waves in solar wind plasma at around 1 a.u., nevertheless giving a plausible general dynamics of the relaxation. For this reason QLT was refined by many authors in order to include the effects that could modify and slow down the relaxation and correspond better to the observations.

One of the first attempts was to take into account the decreasing density profile. It was shown that indeed the relaxation is slowed down as the density gradient causes the deflection of the waves phase velocities from the resonance with beam particles. However, the studies continued as the model still couldn't explain some of the particular observational features.

Numerous investigations and measurements have unambiguously shown that so-

lar wind plasma is highly turbulent medium with ubiquitous density fluctuations that manifest their impact in various observed properties of the waves and definitely suggestive on their influence on the processes of generation of these waves. Thus various investigations have been performed aiming to describe the phenomenon of beam-plasma interaction in the framework of a plasma with random density fluctuations.

A probabilistic model of beam-plasma interaction suggests the statistical approach in order to determine the dynamics and the eventual state of the system making use of modified quasi-linear equations. It predicts lower levels of energy density of the Langmuir waves compared to QLT, what is consistent with the observations. It also suggests a two-stage relaxation with a phase of rapid growth of the waves followed by the much longer phase of slowly decreasing intensity of waves that allows the beam and associated waves to persist for a very long distances, a feature often observed in solar wind plasma at 1 a.u. The model agrees well with the QLT in a limiting case of the small insignificant density fluctuations. And for the level of fluctuations of even several percent, it gives a plausible predictions of waves intensity and its dependencies on the initial beam velocity, beam thermal spread and the level of the density fluctuations.

Further in this manuscript will make a use of the predictions of the probabilistic model in order to estimate the energy density of the Langmuir waves, generated by an electron beam with typical parameters of the one associated with type III radio bursts. As an estimate we will use the maximum of the energy, reached by Langmuir waves during the relaxation with the help of the parameter χ (see Fig.2.11b) which signifies the ratio of the maximum energy of Langmuir waves with respect to the initial energy of the electron beam. This will allow us to estimate the energy involved in a harmonic radio emission which is originating from the aforementioned Langmuir waves.

2.9 Résumé en français

L'interaction onde-particule a été un pivot d'intérêt en physique des plasmas depuis l'aube de la discipline. Il était crucial de comprendre comment les ondes sont excitées et comment les particules avec la fonction de distribution hors équilibre y contribuent. Basée sur des équations quasi-linéaires, une théorie quasi-linéaire d'une interaction faisceau-plasma a été proposée dans les années 1960. Cela a permis de décrire la relaxation d'un faisceau d'électrons dans un plasma homogène et a donné une solution analytique simple pour un problème unidimensionnel. Pourtant, dans sa forme initiale, les résultats du QLT n'ont pas réussi à reproduire les paramètres d'observation des distributions de particules et des ondes associées dans le plasma du vent solaire à environ 1 a.u., donnant néanmoins une dynamique générale plausible de la relaxation. Pour cette raison, QLT a été affiné par de nombreux auteurs afin d'inclure les effets qui pourraient modifier et ralentir la relaxation et mieux correspondre aux observations.

L'une des premières tentatives a été de prendre en compte le profil de densité décroissant. Il a été montré qu'en effet la relaxation s'est ralentie car le gradient de densité provoque la déviation des vitesses de phase des ondes par rapport à la résonance avec les particules du faisceau. Cependant, les études se sont poursuivies car le modèle ne pouvait toujours pas expliquer certaines des caractéristiques d'observation particulières.

De nombreuses enquêtes et mesures ont montré sans ambiguïté que le plasma du vent solaire est un milieu hautement turbulent avec des fluctuations de densité omniprésentes qui manifestent leur impact dans diverses propriétés observées des ondes de plasma et sont définitivement évocatrices sur leur influence sur les processus de génération de ces ondes. Ainsi, diverses investigations ont été menées visant à décrire le phénomène d'interaction faisceau-plasma dans le cadre d'un plasma à fluctuations aléatoires de densité.

Un modèle probabiliste d'interaction faisceau-plasma suggère l'approche statis-

tique afin de déterminer la dynamique et l'état éventuel du système en utilisant des équations quasi-linéaires modifiées. Il prédit des niveaux inférieurs de densité d'énergie des ondes de Langmuir par rapport au QLT, ce qui est cohérent avec les observations. Il suggère également une relaxation en deux étapes avec une phase de croissance rapide des vagues suivie de la phase beaucoup plus longue d'intensité des vagues lentement décroissante qui permet au faisceau et aux ondes associées de persister sur de très longues distances, une caractéristique souvent observée en plasma du vent solaire à 1 a.u. Le modèle s'accorde bien avec le QLT dans un cas limite des petites fluctuations de densité insignifiantes. Et pour le niveau de fluctuations même de quelques pour cent, il donne des prédictions plausibles de l'intensité des ondes et de ses dépendances sur la vitesse initiale du faisceau, la dispersion thermique du faisceau et le niveau des fluctuations de densité du fond.

Plus loin dans ce manuscrit, nous utiliserons les prédictions du modèle probabiliste afin d'estimer la densité d'énergie des ondes de Langmuir, générées par un faisceau d'électrons avec des paramètres typiques de celui associé aux sursauts radio de type III. Comme estimation nous utiliserons le maximum de l'énergie, atteint par les ondes de Langmuir lors de la relaxation, à l'aide du paramètre χ (voir Fig.2.11 b) qui signifie le rapport de l'énergie maximale des ondes de Langmuir par rapport à l'énergie initiale du faisceau d'électrons. Cela nous permettra d'estimer l'énergie impliquée dans une émission radio harmonique qui provient des ondes de Langmuir susmentionnées.

Chapter 3

Harmonic radio emission of type III solar radio bursts in a quasihomogeneous plasma (revisited)

3.1 Introduction

In the original work by Ginzburg & Zheleznyakov (1958), harmonic emission of type III solar radio bursts was attributed to the induced scattering of beam-driven Langmuir waves on thermal ions and subsequent coalescence of the forward-moving and scattered waves. A few decades later Melrose (1980a,b) has argued that ion scattering is not efficient enough to be consistent with the brightness temperatures of type IIIs, observed in corona. This has lead to the investigation of the role of ion sound waves in producing the back-scattered Langmuir waves via the electrostatic decay process $l \rightarrow l^{'} + s$ (e.g., see (Cairns, 1987) and the references therein). Based on this idea, Willes et al. (1996) have derived the analytic solutions to describe the $l + l^{'} \rightarrow t$ process for a broad class of Langmuir waves spectra, including the case of almost anti-parallel waves (a head-on approximation). The ion sound waves, playing role in such process, should be generated in a highly non-isothermal plasma with

the electron temperature T_e much larger than the ion temperature T_i ($T_e \gg T_i$) (Chen et al., 1984). If this condition is not satisfied, the ion sound waves are quickly damped by resonant interactions with ions by means of Landau damping. Observations indicate, that in solar wind typically $T_e \sim T_i$ (e.g., (Lin et al., 1986)), which leads to a conclusion that the electrostatic decay might be insufficient to account for the observed properties of harmonic type III emissions.

In this Chapter we suggest another source of back scattered Langmuir waves - the reflection of the forward moving Langmuir waves from ubiquitous density fluctuations in plasma. Such waves would meet head-on with the forward moving ones and coalescence $l + l' \rightarrow t$ would occur (Tkachenko et al., 2021).

First we provide a description of the basic properties of the ion sound waves in plasma. We discuss and provide the evidence why these waves possibly do not play a significant role in the generation of the harmonic EM emission (Section 3.1).

After we suggest the encounter of Langmuir waves with the density fluctuations as the possible mechanism that plays a major role in the production of harmonic EM emission in a solar wind plasma (Section 3.3). We describe the two main regions where the coalescence of the waves may take place: (1) first one, considered in detail in this Chapter, is far from the reflection region in a quasihomogeneous plasma and may be investigated in a manner, similar to those in (Willes et al., 1996), (2) second one is thoroughly studied in the next Chapter and it considers the coalescence of the Langmuir waves in the close vicinity of the reflection region inside the density clump, where the inhomogeneous profile of density has a significant impact on the amplitudes of the electric fields of the Langmuir waves and consequently on the harmonic emission that is produced.

In our calculations we assume that the two Langmuir waves meet head-on, what allows us to simplify some expressions as in this case the wavenumber of harmonic EM wave should be much smaller than the wavenumber of the Langmuir wave in order to satisfy the momentum conservation law. This assumption has been also

used by numerous authors and is called a 'head-on approximation'. We discuss the reasonableness of this approximation and its validity for in the framework of our problem in Section 3.4.

And the final Section 3.5 we provide all the calculations concerning the case of Langmuir waves coalescence in a quasihomogeneous plasma. We start out with the same equations as (Willes et al., 1996) for Gaussian spectra of forward moving and reflected Langmuir waves. Then we carry out the calculations and eventually come to the point where Willes et al. (1996) have made an approximation that we override and perform further calculations directly. In the end we obtain the expression for the energy density of the harmonic EM emission expressed in terms of the energy density of the parent Langmuir waves. Our estimation of the eventual energy density of the waves appears to be higher than the one obtained by Willes et al. (1996).

3.2 Ion sound waves in a solar wind plasma

Another type of electrostatic longitudinal oscillations in plasma apart from Langmuir waves are the ion sound waves or another words ion acoustic waves. In solar wind they have a rather low frequency compared to Langmuir waves ($\omega_s \sim 10^{-3}\omega_l$) and their dispersion relation is

$$\omega_s = k_s c_s, \tag{3.1}$$

where ω_s is the wave frequency, k_s is the wavenumber and c_s is the sound speed, defined as

$$c_s = \left[\frac{k_B T_e + k_B T_i}{m_i}\right]^{1/2}. \tag{3.2}$$

Ion acoustic waves in plasma may be excited by means of several mechanisms (Stix, 1992). The most important for this study is the electrostatic decay instability

$l \rightarrow l^{'} + s$. This process is considered by numerous authos (e.g., see (Melrose, 1980a; Melrose & Melrose, 1986; Cairns, 1987; Willes et al., 1995, 1996; Robinson et al., 1994; Robinson & Cairns, 1998; Melrose, 2008) etc.) as responsible for the generation of the backscattered Langmuir waves, which in turn coalesce with the forwards moving Langmuir waves and produce the EM emission on the second harmonic of the plasma frequency $l + l^{'} \rightarrow t$.

However, electrostatic decay instability, which belongs to a class of parametric instabilities, has an on-set threshold, below which it does not develop (Fig.3.1). Thus to ensure the development of the instability, the following criterion should be satisfied (Bardwell & Goldman, 1976)

$$\frac{E_l^2}{8\pi n k_B T_e} \gtrsim 4\frac{\gamma_{l'}\gamma_s}{\omega_{l'}\omega_s}, \tag{3.3}$$

where E_l is the electric field of the pump Langmuir wave, $\gamma_{l'}$ and γ_s are the damping rates of daughter Langmuir and ion sound wave and $\omega_{l'}$ is the frequency of the daughter Langmuir wave. It appears that the damping rate of the ion sound waves can be rater significant in plasma. If in the equilibrium state the distribution functions of electrons and ions are Maxwellian, the damping rate of ion sound wave is

$$\gamma_s \approx -\sqrt{\pi/8}\omega_s \left[\left(\frac{m_e}{m_i}\right)^{1/2} + \left(\frac{T_e}{T_i}\right)^{3/2} \exp\left(-\frac{T_e}{2T_i}\right)\right]. \tag{3.4}$$

Thus the excitation of weakly damped ($\gamma_s \ll \omega_s$) ion sound waves is only possible in a highly non-isothermal plasma with $T_e \gg T_i$. In solar wind, where plasma is almost collisionless, ion sound waves, as well as the Langmuir waves, are a subject of Landau damping. They can resonantly interact with ions and electrons and exchange energy with them. However, the influence of electrons is rather weak for these waves, with a damping rate of order $\sim (m_e/m_i)^{1/2}$ with respect to the wave frequency. But if we remove the ions from the resonance by implying $T_i \ll T_e$,

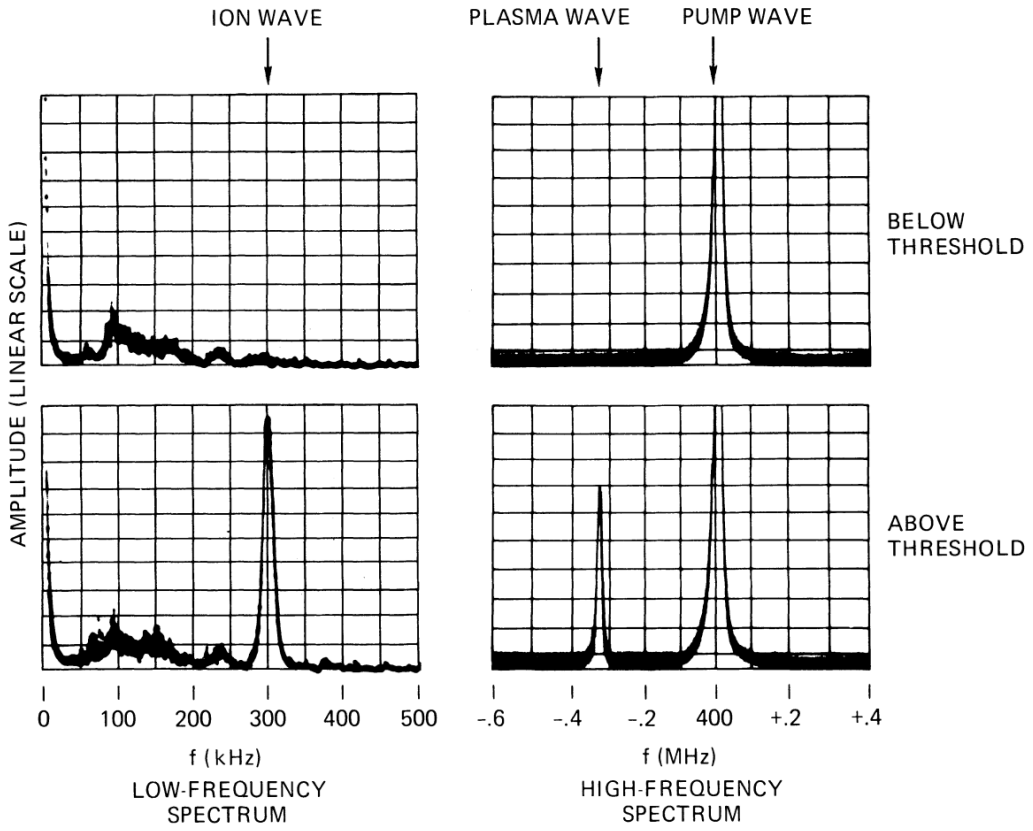

Figure 3.1: Frequency spectra showing the appearance of the electron plasma wave and the ion acoustic wave excited by the pump wave above the threshold power (Chen et al., 1984).

ion sound waves will only interact with a small number of ions on the tail of the distribution and the damping will be rather weak (Artsimovich & Sagdeev, 1979).

The *in situ* observations of Langmuir waves in solar wind plasma have shown that sometimes they may be accompanied by low-frequency oscillations that can be interpreted as ion sound waves. (Lin et al., 1986) have shown that electrostatic decay is unlikely to be responsible for excitation of ion acoustic waves observed by ISEE 3 around 1 a.u., as the threshold of such parametric decay remains too high. This same study provides the measurements of electron and ion temperatures that demonstrate a quasi-isothermal behaviour of plasma with $T_e/T_i \approx 3 \div 5$. (Kellogg et al., 1999) have observed Langmuir waves associated with type III solar radio bursts that passed by a *WIND* satellite, and have concluded that there is no evidence of a parametric decay of non-linear processes that include ion sound waves. Later Krasnoselskikh

et al. (2011) have analyzed the *in situ* observations of Langmuir wave packets at the Earth's bow shock, also made by *WIND* spacecraft. They have shown that two Langmuir waves of a close frequency (the one with the larger frequency typically has a higher amplitude) that are often interpreted as a pump and daughter wave participating in an electrostatic decay, are actually likely to be an incident and a reflected wave. The calculations of the wavelength of such waves requires the presence of a density fluctuations in order to be consistent with observations.

Extremely large number of studies that investigate the generation of the harmonic EM emission in plasma, attribute the back-scattered Langmuir waves to the electrostatic decay process $l \rightarrow l^{'} + s$ (see the review by Reid & Ratcliffe (2014) and references therein). To summarize this section we state that the electrostatic decay might be insufficient to account for the generation of the harmonic type II and type III emissions. Thus we address to the density fluctuations as the sources of a back-scattered Langmuir waves required for nonlinear process $l + l^{'} \rightarrow t$.

3.3 The role of density fluctuations

Our goal here is to study the generation of harmonic emission of type III solar radio bursts in a randomly inhomogeneous plasma. The process is supposed to be as follows: an electron beam resonantly generates a spectrum of Langmuir waves with a frequency ω_l very close to the local electron plasma frequency ω_{p_e} and with wavevectors quite highly aligned with the beam direction (see paragraph 2.3.2). As the average density of the background plasma decreases, random density fluctuations provide local density enhancements (clumps). Langmuir waves may encounter these clumps, and if the electron plasma frequency inside this structures reaches ω_l, waves will be reflected in the opposite direction, forming a spectrum of backward moving (reflected) Langmuir waves (see Fig.3.2b). The forward and backward moving Langmuir waves may then interact and produce harmonic EM emissions. We

will formally distinguish two different regions of such interaction: (1) a quasihomogeneous plasma with average local electron density n_0 distant from the localized density perturbations (see Fig.3.2c), and (2) the locally inhomogeneous plasma inside the density clumps, confined between the start of the positive density gradient and the reflection point, i.e., confined within the *conversion region* (see Fig.3.2d).

For the first case, we evaluate the process of nonlinear coupling of Langmuir waves assuming a mirror-type reflection and a Gaussian spectrum of forward moving and reflected Langmuir waves. The reflection process is taken into account by means of the coefficient P_{ref}, characterizing the part of energy carried by reflected waves. The coupling process itself is described similarly to the one in a homogeneous plasma, assuming that it is not affected by the density fluctuations. The second case, when we consider a coalescence of a single forward moving (incident) Langmuir wave with its reflected part inside the conversion region, in the close vicinity of the reflection point, will be studied in detail in the following Chapter.

3.4 The head-on approximation

The head-on approximation (HOA) considers two almost antiparallel Langmuir waves, which are coalescing into a harmonic EM wave ($l + l' \rightarrow t$). This approximation naturally comes from the comparison between the wavevectors of such Langmuir waves and the EM wave, required to satisfy the resonance conditions. Langmuir wave, generated by electron beam, has the absolute value of the wavevector $k_l \approx \omega_{p_e}/v_b$, whereas the wavevector of a second harmonic emission is $k_t \approx \sqrt{3}\omega_{p_e}/c$. Thus the ratio of wavevectors $k_t/k_l = \sqrt{3}v_b/c$. Depending on the beam velocity, it can be either quite small, or approach 1. The case $k_t/k_l \ll 1$ corresponds to HOA, as the relevant configuration of wavevectors that satisfies the resonant condition $\mathbf{k}_l + \mathbf{k}_{l'} = \mathbf{k}_t$ implies that two Langmuir waves meet head-on: $\mathbf{k}_l \approx -\mathbf{k}_{l'}$ (see Fig.3.3).

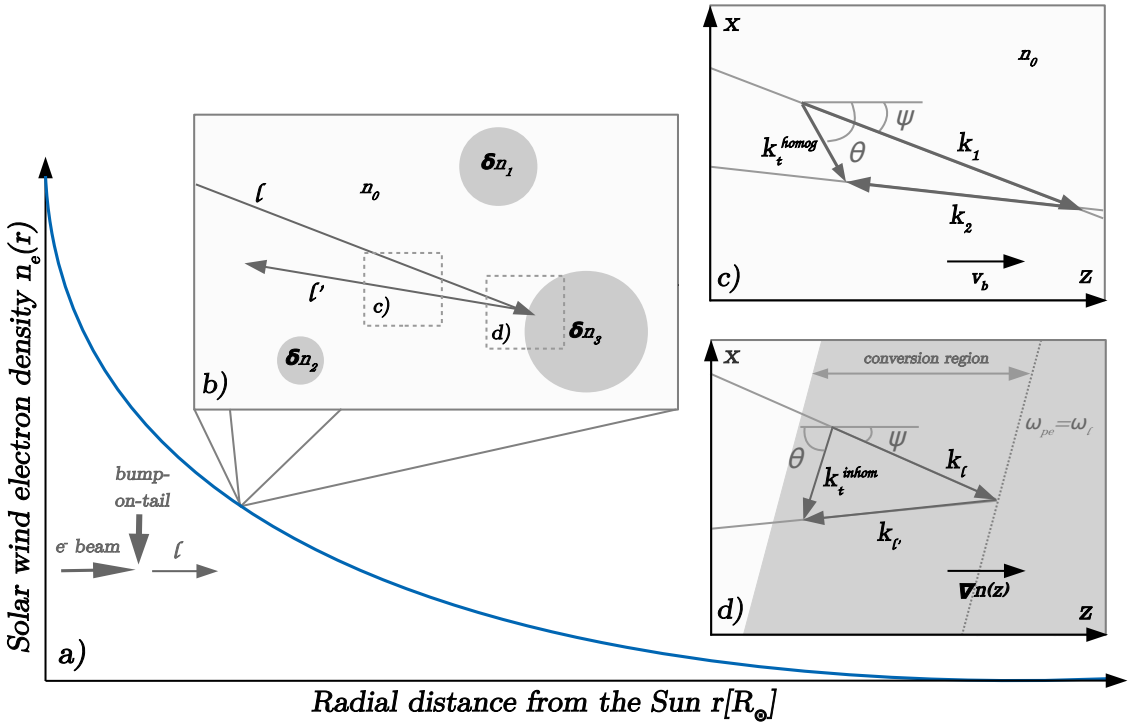

Figure 3.2: Schematic illustration of the generation of harmonic EM emission in a randomly inhomogeneous plasma. Panel a) electron beam propagates from the Sun and generates a spectrum of Langmuir waves (l) with frequency ω_l. The background electron plasma density decreases with the distance from the Sun (blue line). Panel b) Langmuir waves are reflected (l') after an encounter with density clumps. Panel c) coalescence of two oppositely directed waves $\mathbf{k}_1$ and $\mathbf{k}_2$ from the spectra of Langmuir waves in quasihomogeneous plasma, the z-axis is directed along the electron beam direction, the x-axis is an arbitrary perpendicular direction. Panel d) coalescence of the incident Langmuir wave with it's reflected part inside the conversion region, the z-axis is directed along the density gradient inside the clump, the x-axis is an arbitrary perpendicular direction. In panels c) and d) ψ is the acute angle between the wavevector of a forward moving (incident) Langmuir wave and the z-axis, and θ is the acute angle between the wavevector of harmonic EM wave and the z-axis. Generally, z-axes in these two different cases do not coincide. However, since the wavevectors of beam-generated Langmuir waves are usually highly aligned with the beam direction, and since we will consider coalescence in both regions under head-on approximation, we may assume that these axes are roughly equivalent (Tkachenko et al., 2021).

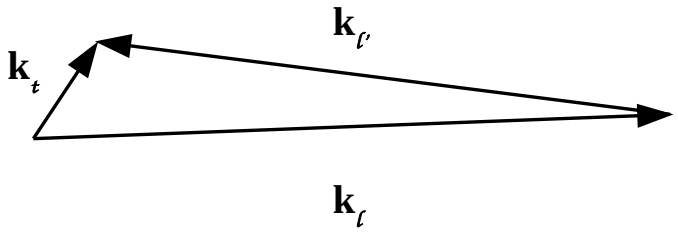

Figure 3.3: Wavevector configuration that satisfies the conservation law $\mathbf{k}_l + \mathbf{k}_{l'} = \mathbf{k}_t$ and allows the head-on approximation.

The validity of the HOA has been investigated by a number of authors. For isotropic power law Langmuir spectra Melrose & Stenhouse (1979) found that HOA may overestimate the emission rate at low wavenumbers and for narrow spectra. Willes et al. (1996) has introduced the narrow-spectrum approximation (NSA) that implies $\Delta k_l/k_l \ll 1$ and $\Delta k_{l'}/k_{l'} \ll 1$ and does not require $k_t/k_l \ll 1$. As the HOA, the NSA fails to reproduce the low wavenumber peak in emission rate due to the coalescence of two Langmuir waves propagating in the same direction.

However, in the majority of such investigations, the spectrum of backscattered Langmuir waves strongly depends on the assumption that it is produced by the electrostatic decay process $l \to l' + s$. For instance, the offset k_0 defines the wavenumbers of backscattered Langmuir waves $k_{l'} \approx k_0 - k_l$ and thus the accuracy of HOA in this case, depends on the ion sound speed. Some authors have tried to relax the HOA by introducing additional angular dependencies (e.g., (Ratcliffe, 2013)).

In present study we consider the case when the backscattered Langmuir waves are produced by reflections of forward moving Langmuir waves from the density fluctuations (or density clumps) in plasma. As it was already mentioned in Section 2.3, Langmuir waves have a very weak angular diffusion with respect to the magnetic field direction (i.e., the direction of the beam propagation). Thus together with the assumption about the mirror-type reflection of these waves and the momentum conservation law, HOA is a justified approximation for our problem.

3.5 Generation of harmonic emission in a quasihomogeneous plasma

3.5.1 Initial equations

Here we describe the process of generation of harmonic EM emission by nonlinear coupling of Langmuir waves in quasihomogeneous plasma. We consider a coalescence of two oppositely directed Langmuir waves, one of which, with a wavevector $\mathbf{k}_1$, is aligned with the beam (belongs to a spectrum of primarily generated waves), and the other, with a wavevector $\mathbf{k}_2$, is supposed to be reflected by density fluctuations (is attributed the the spectrum of reflected waves) (see Fig.3.2c). Even though density fluctuations play an important role here providing reflected waves, we examine harmonic wave generation as happening in a quasihomogeneous plasma, i.e. far from localized density perturbations. The process of EM waves generation by the coupling of Langmuir waves is described by the following set of equations (Tsytovich, 2012)

$$\frac{dN_t(\mathbf{k}_t)}{dt} = \iint \frac{d^3\mathbf{k}_1 d^3\mathbf{k}_2}{(2\pi)^6} w_{ll}^t(\mathbf{k_1}, \mathbf{k}_2, \mathbf{k}_t)[N_l(\mathbf{k}_1)N_l(\mathbf{k}_2) - N_l(\mathbf{k}_1)N_t(\mathbf{k}_t) - N_l(\mathbf{k}_2)N_t(\mathbf{k}_t)], \tag{3.5}$$

$$w_{ll}^t(\mathbf{k}_1, \mathbf{k}_2, \mathbf{k}_t) = \frac{(2\pi)^6 e^2 (k_1^2 - k_2^2)^2}{32\pi m_e^2 \omega_{p_e} k_t^2} \frac{[\mathbf{k}_1 \times \mathbf{k}_2]^2}{k_1^2 k_2^2} \delta(\omega_t - \omega_1 - \omega_2)\delta(\mathbf{k}_t - \mathbf{k}_1 - \mathbf{k}_2), \tag{3.6}$$

here $N_l(\mathbf{k}_1)$, $N_l(\mathbf{k}_2)$ and $N_t(\mathbf{k}_t)$ are the numbers of wave quanta of Langmuir and EM waves respectively, $\mathbf{k}_1, \omega_1, \mathbf{k}_2, \omega_2$ are the wavevectors and frequencies of Langmuir waves, $\mathbf{k}_t, \omega_t$ are the wavevector and frequency of EM wave. It is reasonable to suppose that the number of quanta of Langmuir waves is much larger than the

number of quanta of EM waves,

$$N_l(\mathbf{k}_1), N_l(\mathbf{k}_2) \gg N_t(\mathbf{k}_t), \tag{3.7}$$

then the second and the third terms under the integral in Eq.(3.5) may be neglected. The number of quanta is related to the energy density of waves via the following formulas:

$$W_l(\mathbf{k}_l) = \omega_l N_l, \qquad W_t(\mathbf{k}_t) = \omega_t N_t. \tag{3.8}$$

The spectrum of Langmuir waves is formed by two processes: direct excitation of Langmuir waves due to the bump-on-tail instability (thus it may be approximated as Gaussian, centered at the resonant wavevector $\mathbf{k}_b$ with the width Δk_b), and by reflection of Langmuir waves, assuming the reflection to be mirror-type (i.e. also Gaussian centered at $-\mathbf{k}_b$ having the same width in the wavevector space). Here we note that a similar approximation was used by Willes et al. (1996), where the backscattered spectrum of Langmuir waves was attributed to the electrostatic decay instability $l \rightarrow l^{'} + s$, but the results obtained here are very different, what will be discussed later. Thus, the spectrum of Langmuir waves has the form

$$\begin{aligned} N_l\left(k_\parallel, k_\perp\right) = (1 - P_{ref}) N \exp\left(-\frac{(k_\parallel - k_b)^2 + k_\perp^2}{\Delta k_b^2}\right) + \\ P_{ref} N \exp\left(-\frac{(k_\parallel + k_b)^2 + k_\perp^2}{\Delta k_b^2}\right), \end{aligned} \tag{3.9}$$

where N is normalized accordingly

$$N = \frac{1}{\pi^{3/2} \Delta k^3} \frac{W_l}{\omega_{p_e}}. \tag{3.10}$$

Here we choose the parallel direction to be the direction of the beam propagation, N is the total number of Langmuir waves quanta, P_{ref} is the reflection coefficient

that defines the redistribution of wave energy between primary (forwards moving) and reflected waves. Taking into account all previous assumptions, the Eq.(3.5) takes the form:

$$\frac{dN_t(\mathbf{k}_t)}{dt} = \frac{e^2 P_{ref}(1-P_{ref})N^2}{32\pi m_e^2 \omega_{pe}(\pi^3 \Delta k^6)} \times$$
$$\iint d^3\mathbf{k}_1 d^3\mathbf{k}_2 \frac{(k_1^2-k_2^2)^2}{k_t^2} \frac{[\mathbf{k}_1 \times \mathbf{k}_2]^2}{k_1^2 k_2^2} \delta(\omega_t - \omega_1 - \omega_2)\delta(\mathbf{k}_t - \mathbf{k}_1 - \mathbf{k}_2) \times \tag{3.11}$$
$$\exp\left[-\frac{(k_{1\parallel}-k_b)^2 + k_{1\perp}^2}{\Delta k^2}\right] \exp\left[-\frac{(k_{2\parallel}+k_b)^2 + k_{2\perp}^2}{\Delta k^2}\right].$$

3.5.2 The reference frame

We use the reference frame where the z-axis is parallel to the direction of propagation of the beam (or equally the direction of the background magnetic field) that is generating primary Langmuir waves. The x-axis is a perpendicular direction that is chosen to be along the second component of the $\mathbf{k_t}$ vector. The spatial configuration of wavevectors in the framework of this problem is shown on Fig.3.4. Three vectors $\mathbf{k}_t, \mathbf{k}_1$ and $\mathbf{k}_2$ make the triangle (see Fig.3.4) according to momentum conservation so that

$$\mathbf{k}_2 = \mathbf{k}_t - \mathbf{k}_1. \tag{3.12}$$

The natural assumption here is $|\mathbf{k}_t| \ll |\mathbf{k}_{1,2}|$, thus

$$\mathbf{k}_2^2 = \mathbf{k}_1^2 - 2k_{t\parallel}k_{1\parallel} - 2k_{1\perp}k_{t\perp}\cos\varphi \simeq \mathbf{k}_1^2 - 2k_t k_1(\cos\psi\cos\theta + \sin\psi\sin\theta\cos\varphi), \tag{3.13}$$

here ψ and θ are the angles between z-axis and vectors $\mathbf{k}_1$ and $\mathbf{k}_t$ respectively, φ is the angle between the projections of $\mathbf{k}_1$ and $\mathbf{k}_t$ to the plane perpendicular to z-axis (xy-plane). The vector $\mathbf{k}_t$ without loss of generality is chosen to be in the xz-plane.

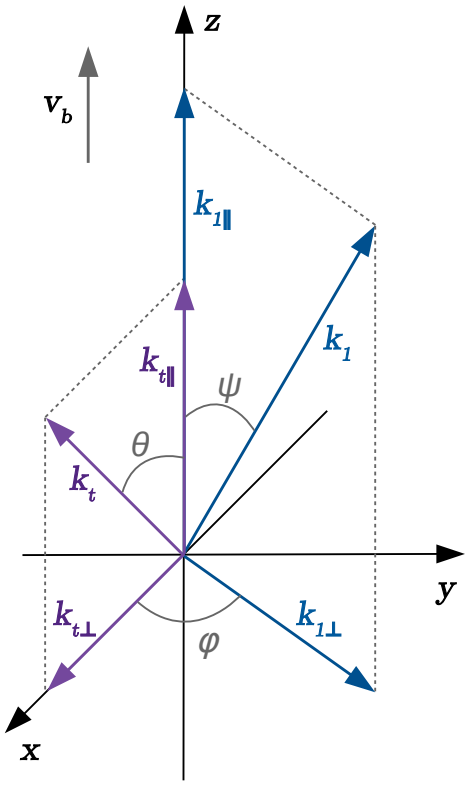

Figure 3.4: Schematic illustration of wavevectors $\mathbf{k}_1$ and $\mathbf{k}_t$ against the direction of the electron beam (z-axis) (Tkachenko et al., 2021).

Consequently the multiplier from Eq.(3.11) may be rewritten as

$$\frac{(k_1^2 - k_2^2)^2}{k_t^2} \frac{[\mathbf{k}_1 \times \mathbf{k}_2]^2}{k_1^2 k_2^2} = 4k_t^2 \times R(\psi, \theta, \varphi), \tag{3.14}$$

where the trigonometric expression $R(\psi, \theta, \varphi)$ stands for

$$\begin{aligned} R(\psi, \theta, \varphi) = \\ = (\sin^2\psi \sin^2\theta \cos^2\varphi + 2\sin\psi\cos\psi\sin\theta\cos\theta\cos\varphi + \cos^2\psi\cos^2\theta)\times \\ [-\sin^2\theta\sin^2\psi\cos^2\varphi - 2\sin\theta\cos\theta\sin\psi\cos\psi\cos\varphi + (\cos^2\psi\sin^2\theta + \sin^2\psi)]. \end{aligned} \tag{3.15}$$

3.5.3 Direct calculations

After the integration of Eq.(3.11) over $\mathbf{k}_2$ we obtain

$$\frac{dN_t(\mathbf{k}_t)}{dt} = \frac{e^2 P_{ref}(1-P_{ref})N^2\mathbf{k}_t^2}{8\pi m_e^2\omega_{pe}(\pi^3\Delta k^6)} \times G, \tag{3.16}$$

here we used a denotation

$$G = \int_{-\pi}^{\pi} d\varphi \int_{0}^{\pi} \sin\psi d\psi \int k^2 dk \delta(\omega_t - \omega_1 - \omega_2) R(\psi,\theta,\varphi) \times$$
$$\exp(-\frac{(k_{1\parallel}-k_b)^2+k_{1\perp}^2}{\Delta k^2}) \exp(-\frac{(k_{t\parallel}-k_{1\parallel}+k_b)^2+(k_{1\perp}^2+k_{t\perp}^2-2k_{1\perp}k_{t\perp}\cos\varphi)}{\Delta k^2}).$$

The first integration over $\mathbf{k}_1$ should take into account the delta function over frequencies. In the first order approximation, neglecting terms that are linear on $\mathbf{k}_t$, the argument of the delta function may be rewritten as follows

$$\omega_t - \omega_1 - \omega_2 = \omega_t - 2\omega_{p_e} - 3\omega_{p_e}\lambda_D^2 k_1^2 = -3\omega_{p_e}\lambda_D^2(k_1^2 - k_r^2), \tag{3.17}$$

where

$$k_r^2 = \frac{\omega_t - 2\omega_{p_e}}{3\omega_{p_e}\lambda_D^2}. \tag{3.18}$$

Thus the delta function has the form

$$\delta(\omega_t - \omega_1 - \omega_2) = \frac{1}{6\omega_{p_e}\lambda_D^2 k_r}\delta(k_1 - k_r), \tag{3.19}$$

and consequently

$$G = \frac{k_r}{6\omega_{p_e}\lambda_D^2} \int_{-\pi}^{\pi} d\varphi \int_{0}^{\pi} \sin\psi d\psi R(\psi,\theta,\varphi) \exp(-\frac{2(k_r^2 - 2k_r k_b\cos\psi + k_b^2)}{\Delta k^2}). \tag{3.20}$$

The expression $R(\psi, \theta, \varphi)$ stands for

$$\begin{aligned} R(\theta,\psi,\varphi) = &-\frac{1}{8}\cos 4\varphi \sin^4\theta \sin^4\psi - \\ &-\cos 3\varphi \sin^3\theta\cos\theta\sin^3\psi\cos\psi + \\ &+\frac{1}{2}\cos 2\varphi[-\sin^4\theta\sin^4\psi + \sin^4\theta\sin^2\psi\cos^2\psi + \\ &+\sin^4\psi\sin^2\theta - 5\sin^2\theta\cos^2\theta\sin^2\psi\cos^2\psi] + \\ &+\cos\varphi[-3\sin^3\theta\cos\theta\sin^3\psi\cos\psi - 2\sin\theta\cos^3\theta\sin\psi\cos^3\psi + \\ &+2\sin^3\theta\cos\theta\sin\psi\cos^3\psi + 2\sin\theta\cos\theta\sin^3\psi\cos\psi] + \\ &-\frac{3}{8}\sin^4\theta\sin^4\psi + (\cos^2\psi\sin^2\theta + \sin^2\psi)\cos^2\psi\cos^2\theta + \\ &+\frac{1}{2}[\sin^4\theta\sin^2\psi\cos^2\psi + \sin^4\psi\sin^2\theta - 5\sin^2\theta\cos^2\theta\sin^2\psi\cos^2\psi]. \end{aligned} \tag{3.21}$$

Next step consists in integration over $d\varphi$, taking into account the following relation

$$\int_0^{2\pi} d\varphi \cos n\varphi \exp(Z\cos\varphi) = I_n(Z), \tag{3.22}$$

here $I_n(Z)$ is a modified Bessel function of the n-th order.We should point out a very important difference of our calculation with the one by Willes et al. (1996). The assumption made by Willes et al. (1996) consists in inequality

$$\frac{2k_r k_t \sin\psi\sin\theta}{\Delta k^2} \gg 1, \tag{3.23}$$

and their approximate estimation is strongly dependent on this assumption. We carried out exact calculations without such assumption and the result obtained shows that the major input comes from the region in wavevector space where this inequality is not satisfied. It is worth noting here that there is quite simple interpretation of this disagreement. The condition above corresponds to neglecting currents parallel to the direction of propagation of Langmuir waves. On the other hand the multiplier $\sin^2\psi\cos^2\psi$ indicates that the major directions of the emission comprise

angles $\pi/4$ and $3\pi/4$ with the electron beam direction, that unambiguously shows the quadrupolar character of the emission and that the major input comes exactly from these parallel electric currents. The inequality

$$\frac{2k_r k_t}{\Delta k^2} \gg 1 \tag{3.24}$$

may be satisfied since $\Delta k \ll k_r$ (the spectrum of generated waves may be considered to be rather narrow), but the multiplier $\sin\psi \sin\theta$ may be quite small as we use a head-on approximation that naturally comes from our problem statement. Integration over $d\varphi$ results in

$$\begin{aligned} G = \frac{k_r}{6\omega_{p_e}\lambda_D^2} \int\limits_0^\pi \sin\psi d\psi \exp(-\frac{2(k_r^2 - 2k_r k_b \cos\psi + k_b^2)}{\Delta k^2}) \times \\ \exp(-\frac{2k_t \cos\theta (k_b - k_r \cos\psi)}{\Delta k^2}) \times \\ \{-\frac{1}{8}\sin^4\theta \sin^4\psi I_4(\Xi) - \sin^3\theta \cos\theta \sin^3\psi \cos\psi I_3(\Xi) + \\ + \frac{1}{2}[-\sin^4\theta \sin^4\psi + \sin^4\theta \sin^2\psi \cos^2\psi + \\ + \sin^4\psi \sin^2\theta - 5\sin^2\theta \cos^2\theta \sin^2\psi \cos^2\psi] I_2(\Xi) + \\ + [-3\sin^3\theta \cos\theta \sin^3\psi \cos\psi - 2\sin\theta \cos^3\theta \sin\psi \cos^3\psi + \\ + 2\sin^3\theta \cos\theta \sin\psi \cos^3\psi + 2\sin\theta \cos\theta \sin^3\psi \cos\psi] I_1(\Xi) + \\ [-\frac{3}{8}\sin^4\theta \sin^4\psi + (\cos^2\psi \sin^2\theta + \sin^2\psi)\cos^2\psi \cos^2\theta + \\ + \frac{1}{2}[\sin^4\theta \sin^2\psi \cos^2\psi + \sin^4\psi \sin^2\theta - 5\sin^2\theta \cos^2\theta \sin^2\psi \cos^2\psi] I_0(\Xi)\}, \end{aligned} \tag{3.25}$$

where $\Xi = \frac{2k_r k_t \sin\psi \sin\theta}{\Delta k^2}$. The last step in our calculation consists in calculation of the following integral

$$\int\limits_{-1}^{1} d(\cos\psi) \exp(\frac{4k_r k_b \cos\psi}{\Delta k^2}) g(\cos\psi), \tag{3.26}$$

where the factor $4k_r k_b/\Delta k^2$ is very large. The standard asymptotic estimation of

such integral, when the function has the maximum on the given interval and when the parameter $Y \gg 1$ is, according to Wasow (2018)

$$\int_{-1}^{1} dt \exp(Yt) g(t) dt = \frac{1}{Y} \exp(Y) g(1) + O(Y^{-2}). \tag{3.27}$$

Accordingly the Eq.(3.25) reduces to

$$G = \frac{\Delta k^2}{6\omega_{p_e} \lambda_D^2 k_b} \sin^2\theta \cos^2\theta \exp[-\frac{2(k_r - k_b)^2}{\Delta k^2} - \frac{2k_t \cos\theta (k_b - k_r)}{\Delta k^2}]. \tag{3.28}$$

Taking into account that the maximum of this expression corresponds to $k_r = k_b$, we will estimate the result as

$$\frac{dN_t(\mathbf{k}_t)}{dt} = \frac{P_{ref}(1 - P_{ref})\omega_{p_e}^2}{768\pi^5} \left(\frac{k_b}{\Delta k}\right)^4 \frac{\mathbf{k}_t^2}{k_b^5} \frac{N_l^2}{n_0 m_e v_T^2} \sin^2\theta \cos^2\theta, \tag{3.29}$$

or

$$\frac{dW_t^{homog}(\mathbf{k}_t)}{dt} = \frac{P_{ref}(1 - P_{ref})\omega_{p_e}}{768\pi^5} \left(\frac{k_b}{\Delta k}\right)^4 \frac{\mathbf{k}_t^2}{k_b^5} \frac{W_l}{n_0 k_B T_e} W_l \sin^2\theta \cos^2\theta, \tag{3.30}$$

where a superscript $'homog'$ indicates that we perform an estimation for a quasihomogeneous plasma. In order to evaluate the characteristic energy of EM wave, we integrate over $d^3\mathbf{k}_t$

$$\frac{dW_t^{homog}}{dt} = \frac{P_{ref}(1 - P_{ref})\omega_{p_e}}{7200\pi^4} \left(\frac{k_b}{\Delta k}\right)^4 \frac{\mathbf{k}_t^5}{k_b^5} \frac{W_l}{n_0 k_B T_e} W_l. \tag{3.31}$$

Observations show that the dynamics of the burst on its initial stage is quite similar to the exponential growth from some noise level till the maximum amplitude. Thus the Langmuir waves dynamics may be presented in the form

$$W_l = W_{noise} \exp(\gamma t). \tag{3.32}$$

The characteristic growth factor till the instability saturation is supposed to be of the order of $(\gamma t_s) = \Lambda = \ln(n\lambda_D^3)$, thus

$$\frac{W_l}{W_{noise}} = \exp\Lambda, \tag{3.33}$$

and the saturation occurs at time $t_s = \Lambda/\gamma$. Consequently the equation for W_t^{homog} may be solved to

$$W_t^{homog}(t) = \frac{P_{ref}(1-P_{ref})\omega_{p_e}}{7200\pi^4\gamma}\left(\frac{k_b}{\Delta k_b}\right)^4 \frac{\mathbf{k}_t^5}{k_b^5}\frac{W_l^2}{n_0 k_B T_e}. \tag{3.34}$$

here γ may be evaluated as γ_{lin}/Λ, where γ_{lin} is the linear increment of the bump-on-tale instability in inhomogeneous plasma with random fluctuations. We will evaluate the parameters W_l and γ_{lin} according to the probabilistic model of beam-plasma interaction in randomly inhomogeneous plasma (see paragraph 2.6.4), and will quantitatively estimate the energy density of harmonic EM emission in a quasi-homogeneous plasma as well as the efficiency of generation of such emission in Chapter 6. There we will also provide a comparison between the mechanism that operates in a quasi-homogeneous plasma and the one that occurs in a localized density inhomogeneity and is considered in detail in the next Chapter.

3.6 Conclusions

In order to investigate the generation of a harmonic emission of type III solar radio bursts we have come through the majority of the mechanisms that were suggested prior to this study. Essentially, all of them require the presence of the forwards (l) and backwards $(l^{'})$ moving spectra of Langmuir waves, in order to provide the possibility of the coalescence $l + l^{'} \rightarrow t$ and satisfy the momentum conservation. A forwards moving spectrum of Langmuir waves (primary waves) is generated by the electron beam via beam-plasma interaction mechanism, whereas a production

of a backwards moving waves in classical studies could be categorised as due to (1) scattering of the Langmuir waves by ions, and due to (2) three wave interaction of two Langmuir wave with the ion acoustic wave $l \pm s \rightarrow l^{'}$. The first mechanism was refuted decades ago, whereas the second has found a large recognition in the context of the problem of Langmuir wave conversion into an EM emission (at a fundamental frequency and at its harmonic). Numerous *in situ* measurements have reported the presence of the ion acoustic waves in solar wind plasma and yet, the theoretical constraints of a parametric decay have led many authors to a conclusion that they may not contribute to the efficient generation of a backwards directed Langmuir waves. Moreover, it was inferred from the recent observations at around 1 a.u. (Krasnoselskikh et al., 2011) that the latter ones are likely to be produced by a simple reflection of a portion of a forwards moving Langmuir waves. This is where the plasma density fluctuations, notably the ones with the increased density with respect to the background (clumps), capable of reflecting the Langmuir waves, naturally come into picture.

We suggest a new mechanism in order to describe the formation of the harmonic emission via Langmuir waves coalescence. We assume that reflections from the density clumps are responsible for the back-scattering of Langmuir waves. We divide a problem into two parts: (1) the coalescence of the waves far from the reflection point in a quasi-homogeneous plasma, and (2) the coalescence of the waves in the vicinity of the reflection point inside the clump. The first part of the problem is considered in the current Chapter, and the second - in the following.

A coalescence of forwards and backwards moving Langmuir waves in a homogeneous plasma was already studied by a number of authors. Many of them have made use of an assumption that a pair of coalescing waves should be almost antiparallel. This is known as a head-on approximation. We have also used this assumption in our calculations and have provided the arguments and constraints for its application. We have given a credit to previous studies by utilizing the same approach to the

calculations as was suggested by (Willes et al., 1996), describing the nonlinear wave-wave interactions in terms of number of quanta. Similarly to the aforementioned study, the spectra of forwards and backwards moving Langmuir waves was assumed to be Gaussian. We perform the calculations following the same path until the point where another assumption is made. It consists in neglecting the waves (both l and t) that are closely aligned with the direction of the electron beam. However, after having performed direct calculations and withdrawing this assumption, we have figured out that in fact these closely aligned waves make the largest contribution into the energy density of the resulting harmonic emission in case of a homogeneous plasma. For this reason our estimation of the resulting energy density of the EM harmonic emission is higher than the one obtained by Willes et al. (1996).

So, as the main result of this Chapter, we obtain the analytical expression for the energy density of EM harmonic emission in a quasi-homogeneous plasma in terms of the energy density of the primary Langmuir waves, under the following assumptions:

(1) the harmonic emission is generated by means of the coalescence of forwards and backwards moving Langmuir waves $l+l^{'} \rightarrow t$, and the backwards directed waves were generated by the reflections from the density clumps in plasma,

(2) the spectra of both populations of Langmuir waves is Gaussian,

(3) the waves were meeting head-on.

3.7 Résumé en français

Afin d'étudier la génération d'une émission harmonique de sursauts radio solaires de type III, nous avons passé en revue la majorité des mécanismes suggérés avant cette étude. Essentiellement, tous nécessitent la présence des spectres en mouvement vers l'avant (l) et vers l'arrière ($l^{'}$) des ondes de Langmuir, afin de fournir la possibilité de la coalescence $l + l^{'} \rightarrow t$ et satisfait la conservation de l'élan. Un spectre en mouvement vers l'avant d'ondes de Langmuir (ondes primaires) est généré par le

faisceau d'électrons via un mécanisme d'interaction faisceau-plasma, alors qu'une production d'ondes en mouvement vers l'arrière dans les études classiques pourrait être classée comme due à (1) la diffusion des ondes de Langmuir par ions, et en raison de (2) l'interaction à trois ondes de deux ondes de Langmuir avec l'onde acoustique ionique $l \pm s \rightarrow l'$. Le premier mécanisme a été réfuté il y a des décennies, tandis que le second a trouvé une large reconnaissance dans le contexte du problème de la conversion de l'onde de Langmuir en une émission EM (à une fréquence fondamentale et à son harmonique). De nombreuses mesures *in situ* ont rapporté la présence des ondes acoustiques ioniques dans le plasma du vent solaire et pourtant, les contraintes théoriques d'une désintégration paramétrique ont conduit de nombreux auteurs à conclure qu'ils ne peuvent pas contribuer à une génération efficace d'un dirigé les vagues de Langmuir. De plus, il a été déduit des observations récentes près de 1 a.u. (Krasnoselskikh et al., 2011) que ces derniers sont susceptibles d'être produits par une simple réflexion d'une portion d'ondes de Langmuir se déplaçant vers l'avant. C'est là que les fluctuations de densité du plasma, notamment celles avec une densité accrue par rapport au fond (touffes), capables de réfléchir les ondes de Langmuir, entrent naturellement en scène.

Nous suggérons un nouveau mécanisme pour décrire la formation de l'émission harmonique par coalescence des ondes de Langmuir. Nous supposons que les réflexions des amas de densité sont responsables de la rétrodiffusion des ondes de Langmuir. Nous divisons un problème en deux parties: (1) la coalescence des ondes loin du point de réflexion dans un plasma quasi-homogène, et (2) la coalescence des ondes au voisinage du point de réflexion à l'intérieur de l'amas. La première partie du problème est examinée dans un chapitre actuel, et la seconde - dans le suivant.

Une coalescence d'ondes de Langmuir se déplaçant vers l'avant et vers l'arrière dans un plasma homogène a déjà été étudiée par un certain nombre d'auteurs. Beaucoup d'entre eux ont fait usage de l'hypothèse qu'une paire d'ondes coalescentes devrait être presque antiparallèle. Ceci est connu comme une approximation frontale.

Nous avons également utilisé cette hypothèse dans nos calculs et avons fourni les arguments et les contraintes pour son application. Nous avons donné un crédit aux études précédentes en utilisant la même approche de calculs que celle suggérée par (Willes et al., 1996), décrivant les interactions onde-onde non linéaires en termes de nombre de quanta. De manière similaire à l'étude susmentionnée, les spectres des ondes de Langmuir se déplaçant vers l'avant et vers l'arrière ont été supposés être gaussiens. Nous effectuons les calculs en suivant le même chemin jusqu'au point où une autre hypothèse est faite. Elle consiste à négliger les ondes (à la fois l et t) étroitement alignées avec la direction du faisceau d'électrons. Cependant, après avoir effectué des calculs directs et avoir retiré cette hypothèse, nous avons compris qu'en fait ces ondes étroitement alignées apportent la plus grande contribution à la densité d'énergie de l'émission harmonique résultante dans le cas d'un plasma homogène. Pour cette raison, notre estimation de la densité d'énergie résultante de l'émission harmonique EM est supérieure à celle obtenue par Willes et al. (1996).

Ainsi, comme résultat principal de ce chapitre, nous obtenons l'expression analytique de la densité d'énergie d'émission harmonique EM dans un plasma quasi homogène en termes de densité d'énergie des ondes primaires de Langmuir, sous les hypothèses suivantes:

(1) l'émission harmonique est générée au moyen de la coalescence des ondes de Langmuir se déplaçant vers l'avant et vers l'arrière $l + l' \rightarrow t$, et les ondes dirigées vers l'arrière ont été générées par les réflexions des amas de densité dans le plasma,

(2) le spectre des deux populations d'ondes de Langmuir est Gaussien,

(3) les ondes se rencontrent de front.

Chapter 4

Harmonic radio emission of type III solar radio bursts from close vicinity of reflection regions

4.1 Inroduction

The presence of the inhomogeneity in plasma and its effect on the generation of the harmonic EM emission was somewhat overlooked by the scientific community, and yet, there were several studies that attempted to give a credit to the role of density variations within the framework of this problem directly or by implication. For instance, (Galeev & Krasnoselskikh, 1976; Brejzman & Pekker, 1978; Papadopoulos & Freund, 1978; Goldman et al., 1980; Ergun et al., 2008; Malaspina et al., 2012) have suggested to explain harmonic emissions in plasma by means of the radiation by the localized bunches of Langmuir waves, and considered the generation of the emission by the nonlinear currents at twice the plasma frequency (antenna-type radiation). Some of these works imply the existence of a strong turbulence. However, in presence of strong density fluctuations, this approach becomes invalid. Ergun et al. (2008) have suggested another mechanism, based on the idea that a significant fraction

of the Langmuir waves are localized as eigenmodes inside the solar wind density cavities. To enable this mechanism, density irregularities should have the form of density holes to capture Langmuir waves inside them. This approach requires the presence of localized density depressions. However, the more common topological features that may affect the emission (naturally suggested by observations of clumpy Langmuir wave packets, wave reflections evidence etc.), are the density clumps with a varying steepness of their density gradient. The theory of the harmonic emission in inhomogeneous plasma inside the region of inhomogeneity has already been partially considered, for example by Erokhin et al. (1974) in one-dimensional case.

In this Chapter we introduce a model that describes a three-dimensional generation of harmonic EM emission inside the density clumps (Tkachenko et al., 2021). First, we will consider a single incident Langmuir wave that enters the density clump, reaches the reflection point, and reflects backwards. We will provide the analytical calculations of the electric fields of the incident and the reflected Langmuir waves in the vicinity of the reflection point. We will apply the assumption about the linear density gradient inside the clump, and estimate the amplitudes of the waves after having entered the clump in terms of their amplitudes in the homogeneous plasma. The presence of these Langmuir waves in a localized region causes the local perturbations of plasma density and electron velocity, that leads to the excitation of a non-linear current. We will provide relevant analytical expressions for the current density (Section 4.3).

In Section 4.4 we will calculate the EM field that is excited by the non-linear current. We specify the geometry of the source of this emission, as well as some constraints on the angle of incidence of the Langmuir wave which need to be satisfied in order to result in efficient generation of the harmonic EM emission. And afterwards we obtain the analytical expression for the energy density of the harmonic emission from a single act of a Langmuir wave reflection inside the density clump.

And finally in Section 4.5 we will generalize our result by accounting multiple

possible acts of Langmuir wave reflection inside various density clumps. This is achieved by averaging the expression for the energy density over the PDFs of angles of incidence, amplitudes of density fluctuations and scales of density gradients inside the clump. The energy density of such harmonic EM emission is expressed in terms of the energy density of the primary Langmuir waves.

4.2 Problem statement

As an additional source of the generation of the harmonic EM emission, that may only be present in the ihnomogeneous plasma, we consider the localized regions where the reflection of the Langmuir waves occurs (see Fig.3.2d). In these regions the field amplitudes and corresponding currents are strongly affected by the inhomogeneity, and in this Chapter we present the model that intends to describe them precisely. We consider a Langmuir wave of frequency ω_l that encounters a density clump, formed as a result of random density fluctuations, inside which the density linearly increases towards the center. Assumption about linear density gradient inside the clump is made for the sake of simplicity. As the wave enters the clump, its wavevector in the direction of the density gradient decreases and in the point where the local plasma frequency reaches the frequency of a Langmuir wave, this wave will undergo a mirror-type reflection. After reflection, two waves, the incident (l) and the reflected (l') will perturb electron trajectories, creating variations of the velocity and particle density that will produce currents with frequency close to $2\omega_{p_e}$ in the vicinity of the reflection point. These localized currents are the source that can generate an EM wave t with a frequency around $2\omega_{p_e}$. Here we shall consider this process in more detail. We choose the density gradient inside the clump to be directed along z-axis, while we assume, that along other two directions, x and y, density variations are negligible, that allows us to reduce the number of dimensions and consider our problem only in xz-plane for some time. Generation of the

harmonic EM wave in this model is only possible for certain values of the angle of incidence ψ as momentum conservation implies constrains on its value and it is determined by the ratio of the beam velocity and speed of light: $|\psi_{\max}| \approx \sqrt{3}v_b/2c$ (see more details further).

We evaluate the electric fields of these Langmuir waves assuming a linear density gradient. This allows us to obtain the perturbations of the density and velocity of electrons, caused by the presence of Langmuir waves, and consequently we may evaluate the excited nonlinear currents at a frequency around $2\omega_{p_e}$. Next, we evaluate the energy density of the EM emission produced by the aforementioned nonlinear currents, for such a single event of Langmuir wave reflection within a single density clump. In order to obtain the value of the energy density of EM emissions that corresponds to a full spectrum of Langmuir waves and to multiple reflections from density clumps with different amplitudes of density fluctuations and different characteristic scales of density gradient, we average our result over the relevant parameters.

4.3 Description of the fields and currents in the vicinity of reflection regions

4.3.1 Electrostatic potential

We begin our calculations with the system of equations for plasma oscillations (Zakharov, 1972):

$$\Delta\Phi_l^{inhom}(\boldsymbol{r},t) = 4\pi e\delta n_l, \tag{4.1}$$

$$\frac{\partial}{\partial t}\delta n_l + \nabla((n_0+\delta n)\boldsymbol{v_e}) = 0, \tag{4.2}$$

$$\frac{\partial \boldsymbol{v_e}}{\partial t} = \frac{e}{m_e}\nabla\Phi_l^{inhom}(\boldsymbol{r},t) - 3v_T^2\nabla\frac{\delta n_l}{n_0}, \tag{4.3}$$

where it was implied that the total electron number density consists of several terms:

$$n_e = n_0 + \delta n + \delta n_l.$$

Here δn is given low-frequency plasma inhomogeneity, δn_l is a high frequency density variation caused by Langmuir oscillations, $\Phi_l^{inhom}(\boldsymbol{r}, t)$ is the corresponding high-frequency part of electrostatic potential. Here and further a superscript $'inhom'$ refers to an inhomogeneous plasma inside a density clump.

Applying a method of small perturbations to our system and performing simple transformations, we obtain

$$\begin{aligned}\frac{\partial^2}{\partial t^2}\frac{\Delta\Phi_l^{inhom}(\boldsymbol{r},t)}{4\pi e} + n_0 \cdot \left(\frac{e}{m}\Delta\Phi_l^{inhom}(\boldsymbol{r},t) - \frac{3v_T^2}{4\pi e n_0}\Delta(\Delta\Phi_l^{inhom}(\boldsymbol{r},t))\right) + \\ +\nabla\left(\delta n\left(\frac{e}{m_e}\nabla\Phi_l^{inhom}(\boldsymbol{r},t) - \frac{3v_T^2}{4\pi e n_0}\nabla(\Delta\Phi_l^{inhom}(\boldsymbol{r},t))\right)\right) = 0.\end{aligned} \tag{4.4}$$

Bearing in mind that each quantity in Eq.(4.4), except $\Phi_l^{inhom}(\boldsymbol{r}, t)$ is assumed to be independent on spatial coordinates or to be a very slowly varying function of those comparatively to $\Phi_l^{inhom}(\boldsymbol{r}, t)$, we rewrite the Eq.(4.4):

$$\Delta\left(-\frac{\omega_l^2}{4\pi e} + \frac{en_0}{m} - \frac{3v_T^2}{4\pi e}\Delta + \frac{e\delta n}{m} - \frac{3v_T^2\delta n}{4\pi e n_0}\Delta\right)\Phi_l^{inhom}(\boldsymbol{r},t) = 0. \tag{4.5}$$

or, after a few transformations,

$$\left(\omega_l^2 - \omega_{p_e}^2\left(1 + \frac{\delta n}{n_0}\right) + 3v_T^2\Delta\right)\Phi_l^{inhom}(\boldsymbol{r},t) = 0. \tag{4.6}$$

We assume that in quasihomogeneous plasma outside the clump, high-frequency part of electrostatic potential has a form of a plane wave: $\Phi_l^{homog}(\boldsymbol{r}, t) = \Phi_0^{homog}\exp(-i(\omega_{p_e}t + \eta) + ik_{l_x}x + ik_{l_{z0}}z)$, where Φ_0^{homog} is the amplitude and η is the phase difference between the wave in homogeneous plasma and in density clump. As we assume that all the parameters vary only along z-axis, the solution for $\Phi_l^{inhom}(\boldsymbol{r}, t)$ can be written

in form $\Phi_l^{inhom}(\boldsymbol{r},t) = \Phi_0^{inhom}\phi(z)\exp(-i\omega_{p_e}t + ik_{l_x}x)$, where $\phi(z)$ is an unknown function of z.

Without loss of generality one can assume that the density gradient within the clump is linear, thus the density inhomogeneity profile has the form (density starts to increase at $z = 0$):

$$\frac{\delta n}{n_0} = \theta(z)\frac{z}{L},$$

where $\theta(z)$ is the Heaviside step function, L is a term, which can be interpreted as a characteristic scale of a density gradient (equivalent to the one introduced in Chapter 2).

Now, since there is no change of parameters along x-axis, and since we choose the solution to have the form $\Phi_l^{inhom}(\boldsymbol{r},t) = \Phi_0^{inhom}\phi(z)\exp(-i\omega_{p_e}t + ik_{l_x}x)$, it is justified that

$$\Delta \to \frac{d^2}{dz^2} - k_{l_x}^2,$$

and taking into account that in a homogeneous plasma

$$\omega_l^2 = \omega_{p_e}^2(1 + 3k_{l_x}^2\lambda_D^2 + 3k_{l_{z0}}^2\lambda_D^2),$$

where $k_{l_{z0}} = k_l\cos\psi$, we obtain

$$(3k_l^2\lambda_D^2\cos^2\psi - \theta(z)\frac{z}{L} + 3\lambda_D^2\frac{d^2}{dz^2})\phi(z) = 0, \tag{4.7}$$

then, considering only the region of positive values of z hereafter, that denotes the region with increasing density, we have

$$(\frac{d^2}{dz^2} + k_l^2\cos^2\psi - \frac{1}{3\lambda_D^2}\frac{z}{L})\phi(z) = 0. \tag{4.8}$$

By introducing a new dimensionless variable

$$\tilde{z} = \left(\frac{k_l^2 L^2}{3k_l^2\lambda_D^2}\right)^{1/3}\left(\frac{z}{L} - 3k_l^2\lambda_D^2\cos^2\psi\right), \tag{4.9}$$

or, if we introduce a new parameter

$$\alpha = 3k_l^2\lambda_D^2 k_l L, \tag{4.10}$$

we may rewrite previous expression:

$$\tilde{z} = \alpha^{-1/3}k_l z - \alpha^{2/3}\cos^2\psi. \tag{4.11}$$

One can find from Eq.(4.8) a well-known Airy equation for the electrostatic potential:

$$\frac{d^2}{d\tilde{z}^2}\phi(\tilde{z}) - \tilde{z}\phi(\tilde{z}) = 0. \tag{4.12}$$

It is convenient to write down the solution in form of Hankel functions $H_\nu^{(n)}$ $(n = 1, 2)$ in order to easily separate the incident and reflected wave. Within the density clump we have to regions: the conversion region, $\tilde{z}_0 < \tilde{z} < 0$, where $\tilde{z}_0 = -\alpha^{2/3}\cos^2\psi$ $(z = 0)$ corresponds to a point where density starts to increase, and the region behind the reflection point $\tilde{z} > 0$. Inside the conversion region the solution is

$$\begin{aligned}\phi(\tilde{z}_0 < \tilde{z} < 0) = \phi_i + \phi_r = \\ \frac{1}{2}\sqrt{\frac{(-\tilde{z})}{3}}\left(e^{-i\pi/6}H_{1/3}^{(2)}\left(\frac{2}{3}(-\tilde{z})^{3/2}\right) + e^{i\pi/6}H_{1/3}^{(1)}\left(\frac{2}{3}(-\tilde{z})^{3/2}\right)\right).\end{aligned} \tag{4.13}$$

in our case the Hankel function of second kind corresponds to incident (i) wave and of first kind - to reflected (r). After the conversion region, the wave simply damps

according to solution

$$\phi(\tilde{z} > 0) = \frac{1}{\pi}\sqrt{\frac{\tilde{z}}{3}} K_{1/3}\left(\frac{2}{3}\tilde{z}^{3/2}\right). \tag{4.14}$$

In order to evaluate the amplitude Φ_0^{inhom} of electrostatic potential, we will use a WKB-approximation to solve Eq.(4.12). First we assume that the solution of Eq.(4.12) has a form

$$\phi(\tilde{z})_{WKB} = \phi_0(\tilde{z}) e^{-ik_l \Psi(\tilde{z})}, \tag{4.15}$$

where amplitude $\phi_0(\tilde{z})$ and phase $\Psi(\tilde{z})$ vary slowly with $\tilde{z}$. We substitute this solution into Eq.(4.12) and obtain ($'$ denotes $\frac{d}{d\tilde{z}}$):

$$\phi_0^{''} - 2ik_l\Psi^{'}\phi_0^{'} - ik_l\Psi^{''}\phi_0 - k_l^2(\Psi^{'})^2\phi_0 - \tilde{z}\phi_0 = 0. \tag{4.16}$$

After, we divide the whole equation by $k_l^2 = 4\pi^2/\lambda_l^2$ and note, that according to our assumption, ϕ_0 and Ψ change noticeably only on scales $l \gg \lambda_l$. For this reason we can make an estimation: $\phi_0^{''} \sim \phi_0/l^2$, $\phi_0^{'} \sim \phi_0/l$, $\Psi^{''} \sim \Psi^{'}/l$. Eq.(4.16) will take a form:

$$\frac{\lambda_l^2}{4\pi^2}\frac{\phi_0}{l^2} - 2i\frac{\lambda_l}{2\pi}\frac{\phi_0}{l}\Psi^{'} - i\frac{\lambda_l}{2\pi}\frac{\Psi^{'}}{l}\phi_0 - (\Psi^{'})^2\phi_0 - \frac{\lambda_l^2}{4\pi^2}\tilde{z}\phi_0 = 0. \tag{4.17}$$

We may find an approximate solution by assigning terms of different order of λ_l/l equal to zero:

$$((\Psi^{'})^2 + \frac{\lambda_l^2}{4\pi^2}\tilde{z})\phi_0 = 0, \tag{4.18}$$

$$\phi_0^{'} + \frac{\Psi^{''}}{2\Psi^{'}}\phi_0 = 0. \tag{4.19}$$

From Eq.(4.18) we obtain ($\phi_0 \neq 0$):

$$\Psi' = \pm\sqrt{-\frac{\lambda_l^2}{4\pi^2}\tilde{z}}, \tag{4.20}$$

$$\Psi = \pm\sqrt{\frac{\lambda_l^2}{4\pi^2}}\int_{\tilde{z}_0}^{\tilde{z}}\sqrt{-\tilde{z}}d\tilde{z} = \mp\frac{\lambda_l}{2\pi}\left(\frac{2}{3}(-\tilde{z}_0)^{3/2} - \frac{2}{3}(-\tilde{z})^{3/2}\right). \tag{4.21}$$

After we proceed to the solution of Eq.(4.19):

$$\phi_0 = \frac{C}{\sqrt{\Psi'}}, \tag{4.22}$$

where C is an integration constant. Coming back to solution (4.15) and substituting (4.20) into (4.22) we obtain:

$$\phi(\tilde{z})_{WKB} = \frac{C\sqrt{k_l}}{(-\tilde{z})^{1/4}}e^{\pm i\left(\frac{2}{3}(-\tilde{z}_0)^{3/2} - \frac{2}{3}(-\tilde{z})^{3/2}\right)}. \tag{4.23}$$

The sewing will be performed at the point $\tilde{z} = \tilde{z}_0$ ($z = 0$), thus we will rewrite previous expression:

$$\phi(\tilde{z} = \tilde{z}_0)_{WKB} = \frac{C\sqrt{k_l}}{(-\tilde{z}_0)^{1/4}}. \tag{4.24}$$

The complete solution for electrostatic potential in WKB-approximation will be:

$$\Phi_l^{inhom}(\tilde{z})_{WKB} = \Phi_0^{inhom}\frac{C\sqrt{k_l}}{(-\tilde{z})^{1/4}}e^{\pm i\left(\frac{2}{3}(-\tilde{z}_0)^{3/2} - \frac{2}{3}(-\tilde{z})^{3/2}\right) - i\omega_{pe}t + i\zeta + ik_l\sin\psi x}, \tag{4.25}$$

where ζ is the phase difference between exact solution and solution under WKB-approximation for $\Phi_l^{inhom}(\tilde{z})$. Now we may proceed to sewing the incident waves from homogeneous plasma with our approximate WKB - solution (we omit $e^{-i\omega_{pe}t + ik_l\sin\psi x}$

terms, common for both waves):

$$\Phi_{incid}^{homog}(\tilde{z}_0) = \Phi_0^{homog} e^{i\eta}, \tag{4.26}$$

$$\Phi_{incid}^{inhom}(\tilde{z}_0)_{WKB} = \Phi_0^{inhom} \frac{C\sqrt{k_l}}{(-\tilde{z}_0)^{1/4}} e^{i\zeta}, \tag{4.27}$$

and putting the equal

$$\Phi_0^{homog} e^{i\eta} = \Phi_0^{inhom} \frac{C\sqrt{k_l}}{(-\tilde{z}_0)^{1/4}} e^{i\zeta}, \tag{4.28}$$

we obtain $\zeta = \eta$ and

$$C = \frac{\Phi_0^{homog}}{\Phi_0^{inhom}} \frac{(-\tilde{z}_0)^{1/4}}{\sqrt{k_l}}. \tag{4.29}$$

Thus a solution for incident wave in WKB-approximation has a form:

$$\Phi_{incid}^{inhom}(\tilde{z})_{WKB} = \Phi_0^{homog} \frac{(-\tilde{z}_0)^{1/4}}{(-\tilde{z})^{1/4}} e^{-i\left(\frac{2}{3}(-\tilde{z}_0)^{3/2} - \frac{2}{3}(-\tilde{z})^{3/2}\right) - i\omega t + ik_l \sin\psi x + i\eta}. \tag{4.30}$$

Now we need to figure out the phase η. In order to do this, we will use an asymptotic expansion of the exact solution for incident wave (see Eq.(4.13)) for large value of argument:

$$\Phi_{incid}^{inhom}(\tilde{z}) = \Phi_0^{inhom} \frac{(-\tilde{z})^{-1/4}}{2\sqrt{\pi}} e^{-i(\frac{2}{3}(-\tilde{z})^{3/2} - \frac{1}{4}\pi)}, \tag{4.31}$$

We set expressions for $\Phi_{incid}^{inhom}(\tilde{z})$ and $\Phi_{incid}^{inhom}(\tilde{z})_{WKB}$ equal at the point $\tilde{z} = \tilde{z}_0 = -\alpha^{2/3}\cos^2\psi$ and obtain:

$$\Phi_0^{homog} \cos^{1/2}\psi e^{i\frac{2}{3}\alpha\cos^3\psi + i\eta} = \Phi_0^{inhom} \frac{1}{2\sqrt{\pi}\alpha^{1/6}} e^{i\frac{\pi}{4}}. \tag{4.32}$$

From this equation system we obtain:

$$\eta = \frac{\pi}{4} - \frac{2}{3}\alpha\cos^3\psi, \qquad \Phi_0^{inhom} = 2\sqrt{\pi}\alpha^{1/6}\cos^{1/2}\psi\Phi_0^{homog}. \tag{4.33}$$

And the final expression for the electrostatic potential inside a density clump is

$$\begin{aligned}\Phi_l^{inhom}(\tilde{z}_0 < \tilde{z} < 0) = \Phi_0^{homog}\sqrt{\pi}\alpha^{1/6}\cos^{1/2}\psi\sqrt{\frac{(-\tilde{z})}{3}}e^{-i\omega t+ik_l\sin\psi x}\times \\ \left(e^{-i\pi/6}H_{1/3}^{(2)}\left(\frac{2}{3}(-\tilde{z})^{3/2}\right) + e^{i\pi/6}H_{1/3}^{(1)}\left(\frac{2}{3}(-\tilde{z})^{3/2}\right)\right)\end{aligned} \tag{4.34}$$

This solution was obtained under the assumption $(-\tilde{z}_0) \gg 1$, as the WKB-approximation can be only applied in the wave zone, far from the reflection point. The criterion $(-\tilde{z}_0) \gg 1$ may be rewritten as $\alpha^{2/3}\cos^2\psi \gg 1$, or $\alpha \gg 1$. A specific limitations on the angle of incidence ψ will be discussed a bit further.

4.3.2 Electric field components

Corresponding electric field components can be calculated from the equation

$$\boldsymbol{E}^{inhom} = -\nabla\Phi_l^{inhom}(\boldsymbol{r}, t), \tag{4.35}$$

and are

$$\begin{aligned}E_{l_x}^{inhom} = -\frac{d}{dx}\Phi_l^{inhom}(\boldsymbol{r}, t) = -ik_{l_x}\Phi_l^{inhom}(\boldsymbol{r}, t) = \\ = -i\sin\psi\sqrt{\pi}\alpha^{1/6}\cos^{1/2}\psi E_0 e^{-i\omega_{pe}t+ik_l\sin\psi x}\times \\ \sqrt{\frac{(-\tilde{z})}{3}}\left(e^{-i\pi/6}H_{1/3}^{(2)}\left(\frac{2}{3}(-\tilde{z})^{3/2}\right) + e^{i\pi/6}H_{1/3}^{(1)}\left(\frac{2}{3}(-\tilde{z})^{3/2}\right)\right) = \\ = E_{l_{x_i}}^{inhom} + E_{l_{x_r}}^{inhom},\end{aligned} \tag{4.36}$$

$$
\begin{aligned}
E_{l_z}^{inhom} = -\frac{d}{dz}\Phi_l^{inhom}(\boldsymbol{r},t) = -\alpha^{-1/3}k_l\frac{d}{d\tilde{z}}\Phi_l^{inhom}(\boldsymbol{r},t) = \\
= -\sqrt{\pi}\alpha^{-1/6}\cos^{1/2}\psi E_0 e^{-i\omega_{pe}t+ik_{l_x}x} \\
\frac{(-\tilde{z})}{\sqrt{3}}\left(e^{i\pi/6}H_{2/3}^{(2)}\left(\frac{2}{3}|\tilde{z}|^{3/2}\right)+e^{-i\pi/6}H_{2/3}^{(1)}\left(\frac{2}{3}|\tilde{z}|^{3/2}\right)\right) = \\
= E_{l_{z_i}} + E_{l_{x_i}},
\end{aligned}
\tag{4.37}
$$

where we took into account $\Phi_0^{homog} = E_0^{homog}k_l^{-1}$, where $E_0^{homog} \equiv E_0$ is the amplitude of the electric field in a homogeneous plasma (Fig.4.1).

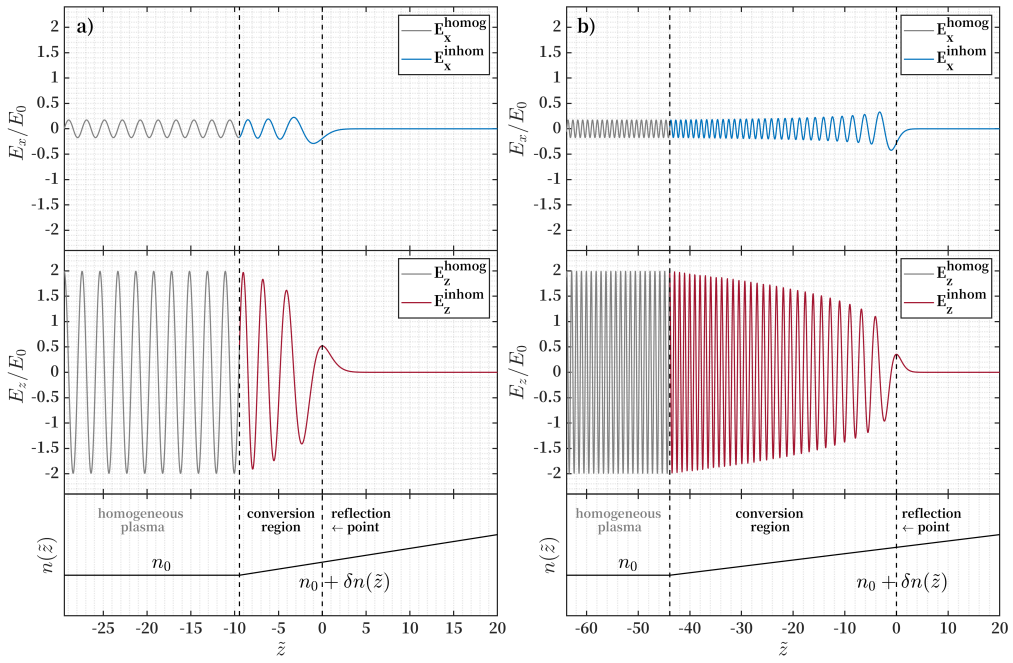

Figure 4.1: Absolute value of total electric field of incident and reflected Langmuir waves, normalized to the amplitude of electric field in homogeneous plasma E_0 plotted versus schematic illustration of corresponding electron density profile. Parameters are: $T_e = 100$ eV, $v_b/c = 0.1$, $\psi = 5^o$. Panel a) $k_l L = 5 \cdot 10^2$. Panel b) $k_l L = 5 \cdot 10^3$ (Tkachenko et al., 2021).

4.3.3 Currents at $2\omega_{p_e}$

Having obtained the expressions for two separate components of electric field, attributed to the incident and the reflected Langmuir wave, one can derive electron density and velocity perturbations excited in plasma by each wave, using simple linear relations. Thus the nonlinear current that will be the result of superposition of these perturbations, should be written in the following form:

The current that is excited by electron density and velocity perturbations caused by incident and reflected Langmuir wave should be written in the following form

$$\boldsymbol{J}_{2\omega_{p_e}}(\boldsymbol{r}) = -e(\delta n_{l_i}(\boldsymbol{r})\boldsymbol{\delta v}_r(\boldsymbol{r}) + \delta n_{l_r}(\boldsymbol{r})\boldsymbol{\delta v}_i(\boldsymbol{r})), \tag{4.38}$$

where δn_l and $\boldsymbol{\delta v}$ can be expressed from simplest linear relations:

$$-i\omega_{p_e}\boldsymbol{\delta v}_a = -e\boldsymbol{E}_a/m_e, \tag{4.39}$$

here subscript $a = i, r$, which stands for incident and reflected wave,

$$-i\omega_{p_e}\delta n_{l_a} + div(n_0\boldsymbol{\delta v}) = 0 = -i\omega_{p_e}\delta n_{l_a} + ik_{l_x}n_0\delta v_{x_a} + n_0\frac{d\delta v_{z_a}}{dz}, \tag{4.40}$$

$$\boldsymbol{\delta v}_a = -ie\frac{\boldsymbol{E}_a}{\omega_{p_e}m_e}, \tag{4.41}$$

$$\delta n_{l_a} = -\frac{ien_0k_{l_x}}{\omega_{p_e}^2m_e}E_{l_{x_a}} - \frac{en_0}{\omega_{p_e}^2m_e}\frac{dE_{l_{z_a}}}{dz}, \tag{4.42}$$

The analytical expression for J_x is

$$J_x^{inhom} = i\frac{e^3 n_0}{\omega_l^3 m_e^2}\left((-ik_l \sin\psi E_{x_i} - \frac{\partial E_{z_i}}{\partial z})E_{x_r} + (-ik_l \sin\psi E_{x_r} - \frac{\partial E_{z_r}}{\partial z})E_{x_i}\right) = \\ = -\frac{1}{6}\frac{e}{m_e c}\frac{c}{v_b}\cos\psi \sin\psi \alpha^{1/3}(-\tilde{z})\left(\sin^2\psi + \alpha^{-2/3}(-\tilde{z})\right) E_0^2 e^{-2i\omega_{p_e}t+2ik_{l_x}x}\times \\ H_{1/3}^{(2)}\left(\frac{2}{3}(-\tilde{z})^{3/2}\right) H_{1/3}^{(1)}\left(\frac{2}{3}(-\tilde{z})^{3/2}\right), \tag{4.43}$$

where we have used the fact that Langmuir waves are generated at local plasma frequency ($\omega_l \approx \omega_{p_e}$) by the electron beam under resonance condition $k_l \approx \omega_{p_e}/v_b$.

Analytical expression for J_z is

$$J_z^{inhom} = i\frac{e^3 n_0}{\omega_{p_e}^3 m_e^2}\left((-ik_l \sin\psi E_{x_i} - \frac{\partial E_{z_i}}{\partial z})E_{z_r} + (-ik_l \sin\psi E_{x_r} - \frac{\partial E_{z_r}}{\partial z})E_{z_i}\right) = \\ = i\frac{1}{12}\frac{e}{m_e c}\frac{c}{v_b}\cos\psi(-\tilde{z})^{3/2}\left(\sin^2\psi + \alpha^{-2/3}(-\tilde{z})\right) E_0^2 e^{-2i\omega_{p_e}t+2ik_{l_x}x}\times \\ \left(H_{-1/3}^{(2)}\left(\frac{2}{3}(-\tilde{z})^{3/2}\right) H_{2/3}^{(1)}\left(\frac{2}{3}(-\tilde{z})^{3/2}\right) + H_{-1/3}^{(1)}\left(\frac{2}{3}(-\tilde{z})^{3/2}\right) H_{2/3}^{(2)}\left(\frac{2}{3}(-\tilde{z})^{3/2}\right)\right). \tag{4.44}$$

This nonlinear current represents a localized source of generation of EM emission at around $2\omega_{p_e}$ (see Fig.4.2).

4.4 Emission from localized density perturbations

As the harmonic EM emission, generated in corona or interplanetary medium is mainly observed at distances, much larger that its source size and wavelength, we will consider EM field of this emission as such on a large distance from the source,

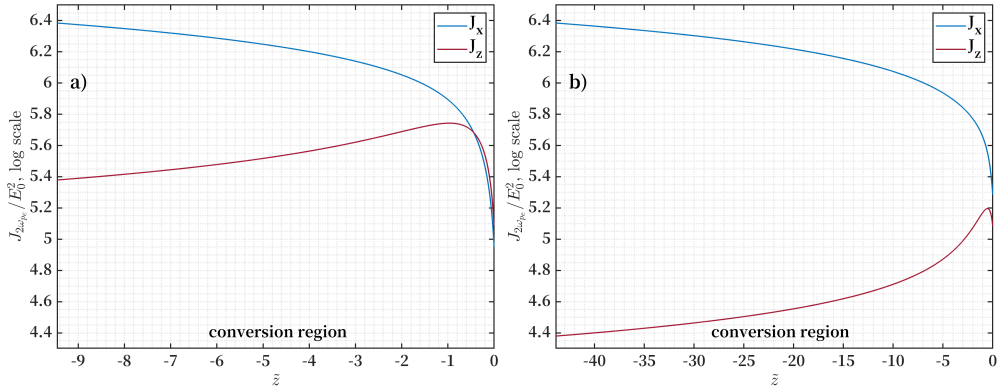

Figure 4.2: Absolute value of harmonic current density, normalized to the square of the amplitude of electric field in homogeneous plasma E_0, inside the conversion region ($\tilde{z}_0 < \tilde{z} < 0$). Parameters are: $T_e = 100$ eV, $v_b/c = 0.1$, $\psi = 5^o$. Panel a) $k_l L = 5 \cdot 10^2$. Panel b) $k_l L = 5 \cdot 10^3$ (Tkachenko et al., 2021).

which implies a decomposition (Landau & Lifshitz, 2013):

$$\begin{aligned} \boldsymbol{J}_{2\omega_{pe}}(\boldsymbol{r}, t - \frac{|\boldsymbol{R} - \boldsymbol{r}|}{c}) \approx \boldsymbol{J}_{2\omega_{pe}}(\boldsymbol{r}, t - \frac{R}{c} + \frac{\boldsymbol{rn}}{c}) = \\ = \boldsymbol{J}_{2\omega_{pe}}(z) e^{-2i\omega_{pe}t + 2i\omega_{pe}R/c - 2i\omega_{pe}\boldsymbol{rn}/c + 2ik_{l_x}x}. \end{aligned} \tag{4.45}$$

where $2\omega_{p_e}\boldsymbol{rn}/c$ stands for ratio of the source size and the wavelength of an EM wave, with a factor of $4\pi/\sqrt{3}$. We rewrite $\boldsymbol{rn} = x\sin\theta + z\cos\theta$, and θ is the angle between wavevector of the EM emission and the z-axis. There are specific constrains for the value of ψ, for which the generation of the harmonic emission is possible. As along the x-axis, physical parameters are not changing according to our assumption, x-components of wave vectors of incident and reflected Langmuir waves should be equal $k_{l_x} = k_{l'_x}$ and the momentum conservation of three wave interaction should be applied along this axis:

$$k_{t_x} = k_{l_x} + k_{l'_x}, \qquad k_{t_x} = \frac{\sqrt{3}\omega_{p_e}}{c}\sin\theta, \qquad k_{l_x} = k_{l'_x} = \frac{\omega_{p_e}}{v_b}\sin\psi. \tag{4.46}$$

This way we obtain the relation between the angles ψ and θ and a limitation for the angle ψ:

$$\sin\psi = \frac{\sqrt{3}}{2}\frac{v_b}{c}\sin\theta, \qquad |\psi_{\max}| \approx \frac{\sqrt{3}}{2}\frac{v_b}{c}. \tag{4.47}$$

Thus we may rewrite the term proportional to a source size by taking into account $k_t \sin\theta = 2k_l \sin\psi$:

$$2i\omega_{p_e}\boldsymbol{rn}/c = 2i\frac{\omega_{p_e}}{c}(x\sin\theta + z\cos\theta) = \frac{4i}{\sqrt{3}}\frac{v_b}{c}k_l x\sin\psi + 2i\frac{\omega_{p_e}}{c}z\cos\theta, \tag{4.48}$$

and the current will have the form

$$\boldsymbol{J}_{2\omega_{p_e}}(z)e^{-2i\omega_{p_e}t+2i\omega_{p_e}R/c-2i\omega_{p_e}\boldsymbol{rn}/c+2ik_{l_x}x} \approx \boldsymbol{J}_{2\omega_{p_e}}(z)e^{-2i\omega_{p_e}t+2i\omega_{p_e}R/c-2i\frac{\omega_{p_e}}{c}z\cos\theta+2ik_{l_x}x}. \tag{4.49}$$

The Liénard-Wiechert potential for a given current is:

$$\boldsymbol{A}_{2\omega_{p_e}}(\boldsymbol{r})e^{-2i\omega_{p_e}t} = \frac{\sqrt{\epsilon}}{c}\int \frac{\boldsymbol{J}_{2\omega_{p_e}}(\boldsymbol{r}, t-\frac{|\boldsymbol{R}-\boldsymbol{r}|}{c})}{|\boldsymbol{R}-\boldsymbol{r}|}d^3r. \tag{4.50}$$

It is well known that the dipole emission is linearly proportional to the amplitude of oscillations of the center of mass of charged particles. For the system that consists of only electrons (we neglect motions of ions in Langmuir waves) the center of mass may not undergo any displacement, thus the dipole emission is absent (Landau & Lifshitz, 2013). So, we imply that the quadruple component of emission is dominant. For the very same reason, the magnetic dipole radiation is also absent. Thus we will use the decomposition

$$\frac{1}{|\boldsymbol{R}-\boldsymbol{r}|} \approx 4\pi\sum_{l=0}^{\infty}\sum_{m=-l}^{l}\frac{1}{2l+1}\frac{r^l}{R^{l+1}}Y_l^{m^*}(\theta_r,\phi_r)Y_l^m(\theta_R,\phi_R), \tag{4.51}$$

and keep only the terms corresponding to $l = 2$ that account for quadrupolar emis-

sion.

$$\boldsymbol{A}_{2\omega_{pe}}(\boldsymbol{r})e^{-2i\omega_{pe}t} = \frac{4\pi\sqrt{\epsilon}}{5c}\frac{1}{R^3}e^{-2i\omega_{pe}t+2i\omega_{pe}R/c}\sum_{m=-2}^{2}Y_2^m(\theta_R,\phi_R)\times \int \boldsymbol{J}_{2\omega_{pe}}(z)e^{-2i\frac{\omega_{pe}}{c}z\cos\theta+2ik_{l_x}x}Y_2^{m^*}(\theta_r,\phi_r)r^2d^3r. \tag{4.52}$$

It is going to be convenient for us to perform integration (DLMF, 2019), (Prudnikov et al., 1986) in a cylindrical coordinate system roughly over a cylindrical volume (see Fig.4.3)

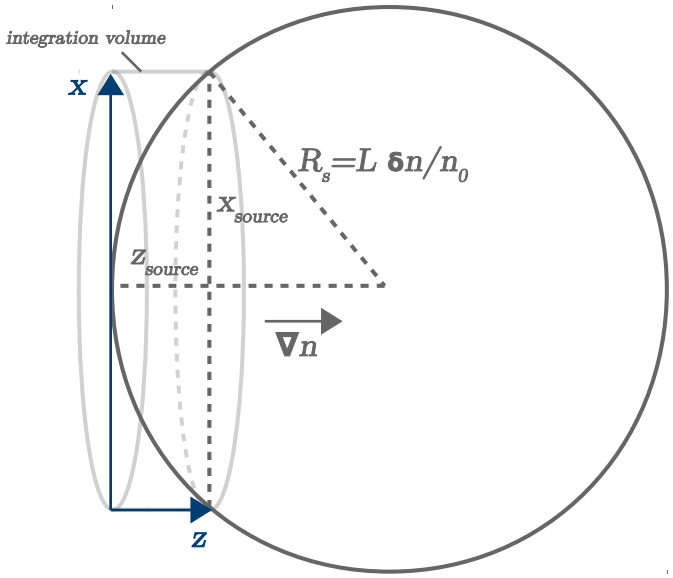

Figure 4.3: Schematic illustration of an integration volume in the vicinity of the reflection point, where the Langmuir waves coalescence into harmonic EM emission takes place. The density clump is approximately represented as a sphere with characteristic radius $R_s = L\delta n/n_0$, while the integration volume may be roughly described as a cylinder with radius x_{source} and height z_{source}, which are transverse and longitudinal characteristic sizes of conversion region, i.e., the region where nonlinear currents $J_{2\omega_{pe}}(\boldsymbol{r},t)$ are excited (Tkachenko et al., 2021).

$$\boldsymbol{A}_{2\omega_p}(\boldsymbol{r}) = \frac{4\pi\sqrt{\epsilon}}{5c}\frac{e^{2i\frac{\omega_{pe}}{c}R}}{R^3}\sum_{m=-2}^{2} Y_2^m(\theta_R,\phi_R)\times$$
$$\int_0^{z_{source}} \boldsymbol{J}_{2\omega_{p_e}}(z)e^{-2i\frac{\omega_{pe}}{c}z\cos\theta}dz\int_0^{x_{source}}\rho(\rho^2+z^2)d\rho\times \tag{4.53}$$
$$\int_0^{2\pi} e^{2ik_x\rho\cos\phi}Y_2^{m^*}(\tan^{-1}(\rho/z),\phi)d\phi,$$

where z_{source} is the distance from the start of the density gradient to the reflection point, i.e., the width of the conversion region, and it should be equal to $3k_l^2\lambda_D^2 L\cos^2\psi$ (see Section 4.3.1). As we suppose that the characteristic radius of a spherical density clump is $R_s = L\delta n/n_0$, we may obtain that under condition $z_{source} \ll R_s$, which is equivalent to $3k_l^2\lambda_D^2 \ll \delta n/n_0$, that the transverse size of the source region is $x_{source} = \sqrt{6k_l^2\lambda_D^2/(\delta n/n_0)}L\delta n/n_0$.

In order to calculate the magnetic field component of the harmonic emission, we will use the following expression

$$\boldsymbol{H}_{t_{2\omega_{p_e}}} = 2i[\boldsymbol{k}_t\boldsymbol{A}_{2\omega_{p_e}}], \tag{4.54}$$

which can be rewritten as

$$|H_{t_{2\omega_{p_e}}}| = H_y = 2i(-k_{t_x}A_{z_{2\omega_{p_e}}} + k_{t_z}A_{x_{2\omega_{p_e}}}). \tag{4.55}$$

We note that the term, proportional to $A_{x_{2\omega_{p_e}}}$ with be the most contributing as the current $J_{x_{2\omega_{p_e}}}$ prevails over $J_{z_{2\omega_{p_e}}}$ for larger angles (see Fig.4.2), and for very small angles the product $k_{t_x}A_{z_{2\omega_{p_e}}} \sim \sin\psi A_{z_{2\omega_{p_e}}}$ vanishes. Thus we calculate all the

integrals for $A_{x_{2\omega_{pe}}}$ component and obtain:

$$A_{x_{2\omega_{pe}}} = -i\frac{\sqrt{\pi\epsilon}}{8}\frac{e^{2iR\omega_{pe}/c-2i\alpha\cos\theta\cos^2\psi v_b/c+2i\alpha\cos\theta v_b/c}}{R^3}\times \\ \frac{e}{m_e c^2}\frac{c^2}{v_b^2}\frac{1}{\cos\theta}\frac{1}{k_l^5}\left(k_l x_{source}\right)^3 E_0^2\times$$

$$\left[2Y_2^0(\theta_R,\phi_R)J_1\left(2k_l x_{source}\sin\psi\right)+\sqrt{6}(Y_2^{-2}(\theta_R,\phi_R)+Y_2^2(\theta_R,\phi_R))J_3\left(2k_l x_{source}\sin\psi\right)\right]. \tag{4.56}$$

And finally we can calculate the radiation energy density

$$W_t^{inhom} = \frac{|H_{t_{2\omega_{pe}}}|^2}{8\pi}, \tag{4.57}$$

and integrate it by angles θ_R and ϕ_R using the orthonormality of spherical harmonics

$$\int_0^{\pi}\int_0^{2\pi} Y_l^m Y_{l'}^{m'^*} d\Omega = \delta_{l,l'}\delta_{m,m'}. \tag{4.58}$$

The result has the form

$$W_t^{inhom} = \frac{1}{8\pi}\frac{3\pi\epsilon}{80}\frac{1}{R^6}\frac{e^2}{m_e^2c^4}\frac{c^2}{v_b^2}\frac{1}{k_l^8}\left(\sqrt{\frac{6k_l^2\lambda_D^2}{\frac{\delta n}{n_0}}}\frac{\delta n}{n_0}k_l L\right)^6\times \\ \left(4\ J_1\left(2\sqrt{\frac{6k_l^2\lambda_D^2}{\frac{\delta n}{n_0}}}\frac{\delta n}{n_0}k_l L\sin\psi\right)+12\ J_3\left(2\sqrt{\frac{6k_l^2\lambda_D^2}{\frac{\delta n}{n_0}}}\frac{\delta n}{n_0}k_l L\sin\psi\right)\right)E_0^4. \tag{4.59}$$

We want to simplify it slightly by using limiting forms of the Bessel functions for a small value of their argument (DLMF, 2019) (this approximation is always correct for rather small values of the angle ψ):

$$4J_1^2\left(2\sqrt{\frac{6k_l^2\lambda_D^2}{\frac{\delta n}{n_0}}}\frac{\delta n}{n_0}k_l L\sin\psi\right)+12J_3^2\left(2\sqrt{\frac{6k_l^2\lambda_D^2}{\frac{\delta n}{n_0}}}\frac{\delta n}{n_0}k_l L\sin\psi\right)\approx 24\frac{\delta n}{n_0}k_l^2L^2k_l^2\lambda_D^2\sin^2\psi. \tag{4.60}$$

We will put the observation point R at the border of a density clump to estimate the emission that is detected when it leaves the source region. Since we have implied $z_{source} \ll R_s$, this approximation used for decompositions in Eqs.(4.45) and (4.51)

is valid and we may set $R \approx R_s = L\delta n/n_0$. Taking into account the approximate expression for Bessel functions and $k_l^2\lambda_D^2 \approx v_T^2/v_b^2$ for beam-generated Langmuir waves, after few simple transformations we will obtain an expression for energy density of harmonic emission for a single density clump

$$W_t^{inhom} = 4 \cdot 10^2 \pi\epsilon \frac{v_T^6}{v_b^6} \left(\frac{k_l^2\lambda_D^2}{\delta n/n_0}\right)^2 \frac{\omega_{p_e^2} L^2}{c^2} \sin^2\psi \frac{W_l}{n_0 k_B T_e} W_l. \tag{4.61}$$

where $W_l = E_0^2/8\pi$ is the energy density of Langmuir waves. This expression was derived under approximation $\delta n/n_0 \gg 3k_l^2\lambda_D^2$ and $\sin\psi \ll 1$.

4.5 Statistically averaged emission

On its way through the inhomogeneous solar wind Langmuir waves can encounter density clumps of different size and magnitude. As it was shown earlier, both of these parameters can strongly affect the harmonic emission from inside the density clump. For instance, Fig.4.1 demonstrates that with growth of L (and decrease of the amplitude of density fluctuation $\langle\Delta n\rangle/n_0 \sim L^{-1}$) the conversion region increases what allows the perpendicular current $J_{x_{2\omega_{pe}}}$ grow significantly larger than $J_{z_{2\omega_{pe}}}$ for the major part of angles ψ. In order to take this into account one can estimate statistically averaged value of W_t^{inhom}. The size of the source region of type III bursts is typically much larger that the characteristic scale of the density fluctuations within solar wind (Reid & Ratcliffe, 2014), and thus the number of encounters is large enough to justify averaging:

$$\langle W_t^{inhom}\rangle_{\psi,\delta n,L} = P_{ref} \int P(\psi)P(\delta n)P(L)W_t^{inhom}(\psi,\delta n,L)\; d\psi\; d\delta n\; dL, \tag{4.62}$$

here $P(\psi)$, $P(\delta n)$ and $P(L)$ are PDFs of the angle of incidence, amplitudes of the density fluctuations within the clumps and of the scales of gradients inside clumps, respectively.

We assume a uniform distribution over angles of incidence, $P(\psi) = \pi^{-1}$. In order to perform the integration we will remind that the value of ψ is limited by $\psi_{\max} \approx \sqrt{3}v_b/2c \ll 1$:

$$\langle W_t^{inhom} \rangle_\psi = ...\frac{1}{\pi}\int\limits_0^{\psi_{\max}} \sin^2\psi d\psi \approx ...\frac{1}{\pi}\int\limits_0^{\psi_{\max}} \psi^2 d\psi = ...\frac{1}{3\pi}\psi_{\max}^3 \approx \frac{\sqrt{3}}{8\pi}\frac{v_b^3}{c^3}. \quad (4.63)$$

We shall also assume that fluctuations follow a normal distribution with zero mean value and standard deviation $\langle \Delta n \rangle$:

$$P_{\delta n}(\delta n) = \frac{1}{\sqrt{2\pi}\langle \Delta n \rangle} \exp\left[-\frac{\delta n^2}{2\langle \Delta n \rangle^2}\right]. \quad (4.64)$$

Then, averaging over amplitudes of density fluctuations can be performed as follows:

$$\langle W_t^{inhom} \rangle_{\delta n} = ...\frac{n_0^2}{\sqrt{2\pi}\langle \Delta n \rangle}\int\limits_0^{\infty} \delta n^{-2} \exp\left[-\frac{\delta n^2}{2\langle \Delta n \rangle^2}\right] d\delta n = ...(-\sqrt{2})\left(\frac{\langle \Delta n \rangle}{n_0}\right)^{-2}. \quad (4.65)$$

Let us assume that all fluctuation have the same size P_{ref}. In this case, the probability to find a fluctuation with density variation δn should be equal to the probability of finding a fluctuation with gradient L:

$$P_{\delta n}(\delta n)\, d\delta n = P_L(L)\, dL. \quad (4.66)$$

Since $\delta n/n_0 = P/L$, we may write

$$\frac{\partial \delta n}{\partial L} = -\frac{n_0 P}{L^2}, \quad (4.67)$$

and

$$P_L(L)\, dL = P_{\delta n}(\delta n(L))\left|\frac{\partial \delta n}{\partial L}\right| dL = \frac{1}{\sqrt{2\pi}}\frac{n_0}{\langle \Delta n \rangle}\frac{P}{L^2}\exp\left[-\frac{P^2 n_0^2}{2\langle \Delta n \rangle^2 L^2}\right] dL, \quad (4.68)$$

or after substitution of $P/(\langle \Delta n \rangle / n_0) = L_{sc}$:

$$P_L(L)\, dL = \frac{1}{\sqrt{2\pi}} \frac{L_{sc}}{L^2} \exp\left[-\frac{L_{sc}^2}{2L^2}\right] dL. \tag{4.69}$$

It can be approximated as a function of the level of density fluctuations (see paragraph 2.7.1):

$$L_{sc} \approx 1.4 \cdot \left(\frac{\langle \Delta n \rangle}{n_0}\right)^{-1}, \ [km]. \tag{4.70}$$

As we have mentioned earlier, it was shown by Voshchepynets et al. (2015), random density fluctuations, described this way in terms of $P(\delta n)$ and $P(L)$, reproduce the interval of density fluctuations spectrum from 10^{-2} Hz to 530 Hz, measured within the solar wind. Again, the reason to choose this part of the spectrum is that the density fluctuations that may affect the beam-plasma interaction have the characteristic scales that fall exactly into this interval: on the one hand they are much larger than the wavelength of the Langmuir waves, and, on the other hand they are significantly smaller than the scale of the electron beam relaxation.

Now we can perform averaging over L

$$\langle W_t^{inhom} \rangle_L = ... \frac{L_{sc}}{\sqrt{2\pi}} \int_0^\infty \exp\left[-\frac{L_{sc}^2}{2L^2}\right] dL = ... \frac{L_{sc}^2}{2}. \tag{4.71}$$

Putting everything together, we obtain

$$\langle W_t^{inhom} \rangle_{\psi,\delta n,L} = 25\sqrt{6}\epsilon P_{ref} \frac{v_T^3}{c^3} \frac{v_T^3}{v_b^3} \left(\frac{k_l^2 \lambda_D^2}{\langle \Delta n \rangle / n_0}\right)^2 \frac{\omega_{p_e^2} L_{sc}^2}{c^2} \frac{W_l}{n_0 k_B T_e} W_l. \tag{4.72}$$

To perform a quantitative evaluation of this final expression, and also to estimate the efficiency of the emission mechanism, presented in the current Chapter, we will use the results of the probabilistic model of the beam-plasma interaction, described in Chapter 2. Alongside with these estimations, we will provide similar evaluations for the harmonic emission in a quasi-homogeneous plasma, which was described in

detail in a previous Chapter. All the estimations, as well as a comparison of two mechanisms of generation of harmonic emission will be provided in Chapter 6.

4.6 Conclusions

In the current Chapter we have highlighted a recent model, proposed by Tkachenko et al. (2021), that describes the generation of the harmonic EM emission in a randomly inhomogeneous plasma inside the localized regions with a positive density gradient, i.e., density clumps. This model is based on the fact that inside the density clumps, if the amplitude of the density fluctuations is high enough, the Langmuir wave that enters the clump, may be reflected backwards, and the incident wave may interact with the reflected wave so that the harmonic EM wave will be produced: $l+l' \rightarrow t$. For the sake of simplicity, the density gradient inside the clump is assumed to be linear, and the longitudinal direction in the problem was chosen to be along the density gradient. According to our assumption, there is no change of density along the directions transverse to the density gradient, and thus we have managed to reduce a three-dimensional problem to a two-dimensional, by considering only one of the transverse components of the Langmuir waves field.

We have provided the analytical expressions for the electric fields of the incident and reflected Langmuir waves in the case of a single act of wave reflection. The estimations of their amplitudes have shown that inside the clump the longitudinal component of the electric field of such waves decreases towards the reflection point, whereas the transverse component, on the contrary, increases. The larger is the conversion region (the distance that the wave crosses since entering the clump up to the reflection point), the more pronounced are these effects. At the same time the evaluation of non-linear currents, excited by the waves, shows that for the same set of parameters as in the case of the electric field, the transverse component of the current is dominant, which is contrary to the case of the currents in the quasi-

homogeneous plasma. Here we note that even though the longitudinal directions in these two problems are not identical (in case of a quasi-homogeneous plasma it was the direction of the electron beam, and in this case it is the direction of the density gradient), they are almost equivalent (see the arguments provided in paragraph 6.4.2).

After this we have calculated the EM field, generated by such current, recovering the third dimension of the problem. We have chosen the geometry of the source of the emission in a form of a cylinder with the height corresponding to the length of the conversion region and the radius that is slightly less than the radius of a quasi-spherical density clump. The conservation of the momentum limits the range of values of the Langmuir waves incidence angle, allowing the three-wave interaction only for relatively small angles: $\psi \lesssim 5^o \div 10^o$. This is consistent with the head-on approximation that we were using in the problem of quasi-homogeneous plasma. As well as the harmonic emission in the quasi-homogeneous plasma, the harmonic emission from inside the density clump is quadrupolar and we have evaluated the its energy density.

In order to obtain a general result for multiple encounters of multiple Langmuir waves with a number of various density clumps, we have performed a statistical averaging of the previously obtained analytical expression for the energy density over:

(1) the angles of incidence (to account for the angular dispersion of Langmuir waves),

(2) the level of density fluctuations (to cover different amplitudes of density fluctuations in different clumps)

(3) and the scales of density gradient (to account for different steepness of gradients possible in the clumps).

The PDF of the angles was chosen to be uniform in the range of the allowed angles. The PDF of the density fluctuations was chosen to be Gaussian and the PDF of

the scales was inferred from the assumption that all the clumps have approximately the same size. The final expression yields the energy density of the harmonic EM emission in terms of the energy density of the primary Langmuir waves, which, as in case of a quasi-homogeneous plasma, will be evaluated from the probabilistic model of the beam-plasma interaction.

4.7 Résumé en français

Dans le Chapitre actuel, nous avons mis en évidence un modèle récent, proposé par Tkachenko et al. (2021), qui décrit la génération de l'émission électromagnétique harmonique dans un plasma aléatoirement inhomogène à l'intérieur des régions localisées avec un gradient de densité positif, c'est-à-dire des touffes de densité. Ce modèle est basé sur le fait qu'à l'intérieur des touffes de densité, si l'amplitude des fluctuations de densité est suffisamment élevée, l'onde de Langmuir qui pénètre dans la touffe peut être réfléchie vers l'arrière, et l'onde incidente peut interagir avec l'onde réfléchie de sorte qu'une onde électromagnétique harmonique sera produite: $l + l' \rightarrow t$. Dans un souci de simplicité, le gradient de densité à l'intérieur de la touffe est supposé être linéaire et la direction longitudinale du problème a été choisie le long du gradient de densité. Selon notre hypothèse, il n'y a pas de changement de densité selon les directions transversales au gradient de densité, et ainsi nous avons réussi à réduire un problème tridimensionnel à un problème bidimensionnel, en ne considérant qu'une seule des composantes transversales des ondes de Langmuir domaine.

Nous avons fourni les expressions analytiques des champs électriques des ondes de Langmuir incidentes et réfléchies dans le cas d'un seul acte de réflexion d'onde. Les estimations de leurs amplitudes ont montré qu'à l'intérieur de la touffe, la composante longitudinale du champ électrique de telles ondes décroît vers le point de réflexion, tandis que la composante transversale, au contraire, augmente. Plus la

région de conversion est grande (la distance que l'onde traverse depuis son entrée dans le bloc jusqu'au point de réflexion), plus ces effets sont prononcés. Dans le même temps l'évaluation des courants non linéaires, excités par les ondes, montre que pour le même jeu de paramètres que dans le cas du champ électrique, la composante transversale du courant est dominante, ce qui est contraire au cas de les courants dans le plasma quasi homogène. On note ici que même si les directions longitudinales dans ces deux problèmes ne sont pas identiques (dans le cas d'un plasma quasi homogène c'était la direction du faisceau d'électrons, et dans ce cas c'est la direction du gradient de densité), elles sont presque équivalentes (voir les arguments fournis dans le paragraphe 6.4.2).

Après cela, nous avons calculé le champ électromagnétique, généré par un tel courant, récupérant la troisième dimension du problème. Nous avons choisi la géométrie de la source d'émission sous la forme d'un cylindre dont la hauteur correspond à la longueur de la zone de conversion et le rayon légèrement inférieur au rayon d'une touffe de densité quasi-sphérique. La conservation de l'impulsion limite la plage de valeurs de l'angle d'incidence des ondes de Langmuir, permettant l'interaction à trois ondes uniquement pour des angles relativement petits: $\psi \lesssim 5^o \div 10^o$. Ceci est cohérent avec l'approximation frontale que nous utilisions dans le problème du plasma quasi homogène. En plus de l'émission harmonique dans le plasma quasi homogène, l'émission harmonique de l'intérieur du bloc de densité est quadrupolaire et nous avons évalué sa densité d'énergie.

Afin d'obtenir un résultat général pour des rencontres multiples de plusieurs ondes de Langmuir avec certain nombre de diverses touffes de densité, nous avons effectué un moyennage statistique de l'expression analytique précédemment obtenue pour la densité d'énergie sur:

(1) les angles d'incidence (pour tenir compte de la dispersion angulaire des ondes de Langmuir),

(2) le niveau des fluctuations de densité (pour couvrir différentes amplitudes de

fluctuations de densité dans différents amas)

(3) et les échelles de gradient de densité (pour tenir compte des différentes pentes des gradients possibles dans les amas).

La distribution de probabilité des angles a été choisie pour être uniforme dans la plage des angles autorisés. La distribution de probabilité des fluctuations de densité a été choisie pour être gaussienne et la distribution de probabilité des échelles a été déduite de l'hypothèse que tous les touffes ont approximativement la même taille. L'expression finale donne la densité d'énergie de l'émission électromagnétique harmonique en termes de densité d'énergie des ondes primaires de Langmuir, qui, comme dans le cas d'un plasma quasi homogène, sera évaluée à partir du modèle probabiliste de l'interaction faisceau-plasma.

Chapter 5

Solar wind density fluctuations measured by Parker Solar Probe

5.1 Introduction

Regarding all the results listed in three previous Chapters, there is no doubt that the *in situ* measurements of plasma density fluctuations close to the Sun are important in order to verify the theoretical predictions concerning the dynamics of the type III solar radio bursts. And most importantly, it is interesting to perform such measurements directly in the source region where type IIIs are generated. In the current Chapter we perform a preliminary analysis of the density variations measured by *Parker Solar Probe* during 12 hours in the Encounter 5 phase. We infer the most important statistical properties of the electron density fluctuations over that period and establish future goals for the investigation.

5.2 Parker Solar Probe mission

Parker Solar Probe (*PSP*) is a NASA robotic spacecraft launched on 12 August 2018. It's scientific goals date back six decades to the 1958's Simpson Committee Report, when the necessity of a close encounter with the Sun was affirmed. During

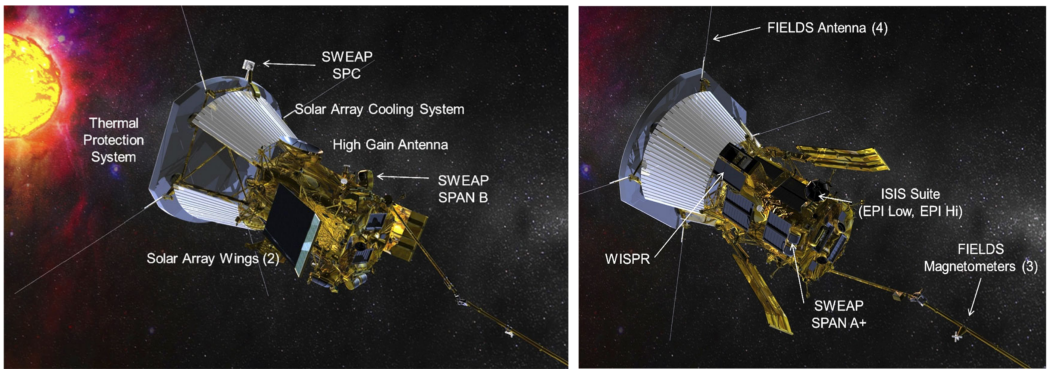

Figure 5.1: Caption

a planned seven-year mission, *PSP* will mainly remain in the ecliptic plane and will use seven Venus gravity assists in order to lower its perihelion from 35 solar radii ($R_\odot$) for the first orbit to less than 10 $R_\odot$ for final three orbits and will be the first spacecraft to fly into the low solar corona. Initially the mission was planned to use Jupiter gravity assist to enter the polar orbit with the perihelion of 4 $R_\odot$, but the trajectory was reconsidered in order to achieve a much larger number of passes and much greater data sampling during the encounters (24 orbits instead of 2 orbits and over 2100 hours instead of 160 hours inside of 30 $R_\odot$). Thus *PSP* performs unprecedented long duration *in situ* measurements of solar wind parameters.

The main scientific goals of the mission are (Fox et al., 2016):

(1) tracing the flow of energy that heats the solar corona and accelerates the solar wind,

(2) determining the structure and dynamics of the plasma and magnetic fields at the sources of the solar wind, and

(3) exploring mechanisms that accelerate and transport energetic particles.

To achieve these goals, *PSP* carries the following instruments: Fields Experiment (FIELDS), Integrated Science Investigation of the Sun (IS⊙IS), Wide-field Imager for Solar PRobe (WISPR) and Solar Wind Electrons Alphas and Protons (SWEAP) Investigation.

Orbit details

Solar pass #	Year	Date (perihelion)	Perihelion (a.u.)	Perihelion ($R_\odot$)	Encounter phase
1	2018	6 Nov (03:27 UTC)	0.163	35.66	31 Oct – 11 Nov
2	2019	4 Apr (22:40 UTC)	0.163	35.66	30 Mar – 10 Apr
3	2019	1 Sep (17:50 UTC)	0.163	35.66	16 Aug – 20 Sep [1]
4	2020	29 Jan (09:37 UTC)	0.128	27.85	23 Jan – 29 Feb
5	2020	7 Jun (08:23 UTC)	0.128	27.85	9 May – 28 Jun
6	2020	27 Sep	0.092	20.35	21 Sep - 2 Oct
7	2021	17 Jan	0.092	20.35	
8-9	2021	29 Apr, 9 Aug	0.072	15.98	
10-16	2021-2023	21 Nov, 25 Feb, 1 Jun, 6 Sep 11 Dec, 17 Mar, 22 Jun	0.06	13.28	
17-21	2023-2024	27 Sep, 29Dec, 30 Mar 30 Jun, 30Sep	0.052	11.42	
22-24	2024-2025	24 Dec, 22 Mar, 29 Jun	0.044	9.86	

Table 5.1: Orbit details for *PSP*. Colors define the orbits with common perihelia (adapted from (Fox et al., 2016), http://parkersolarprobe.jhuapl.edu/)

5.3 Data from 27th of May 2020

The measurements performed by *PSP* on the 27th of May 2020 are of a particular interest for studying. This date was quite close to the perihelion of *PSP* orbit within the Encounter 5 phase. There were several quite intense subsequent type III radio bursts detected and, most importantly *PSP* managed to detect the associated beam-generated waves (Langmuir or z-mode), which indicates that the spacecraft intersected the trajectory of the electron beam, and, consequently has measured the parameters *in situ* in the *source region* of type III radio burst. This may allow us to perform a statistical analysis of the density fluctuations directly in the localized area where type IIIs were generated, but firstly we will assess the general statistical characteristics of density variations during that day (see Fig.5.2).

We will zoom in the interval when the most intense part of the type IIIs was observed (Fig.5.3). As one may notice, at around 18:05 an intense burst has been

[1]NASA announced a substantial extension of the third solar encounter phase from 11 days to about 35 days (*PSP* was able to download much more data than NASA had expected).

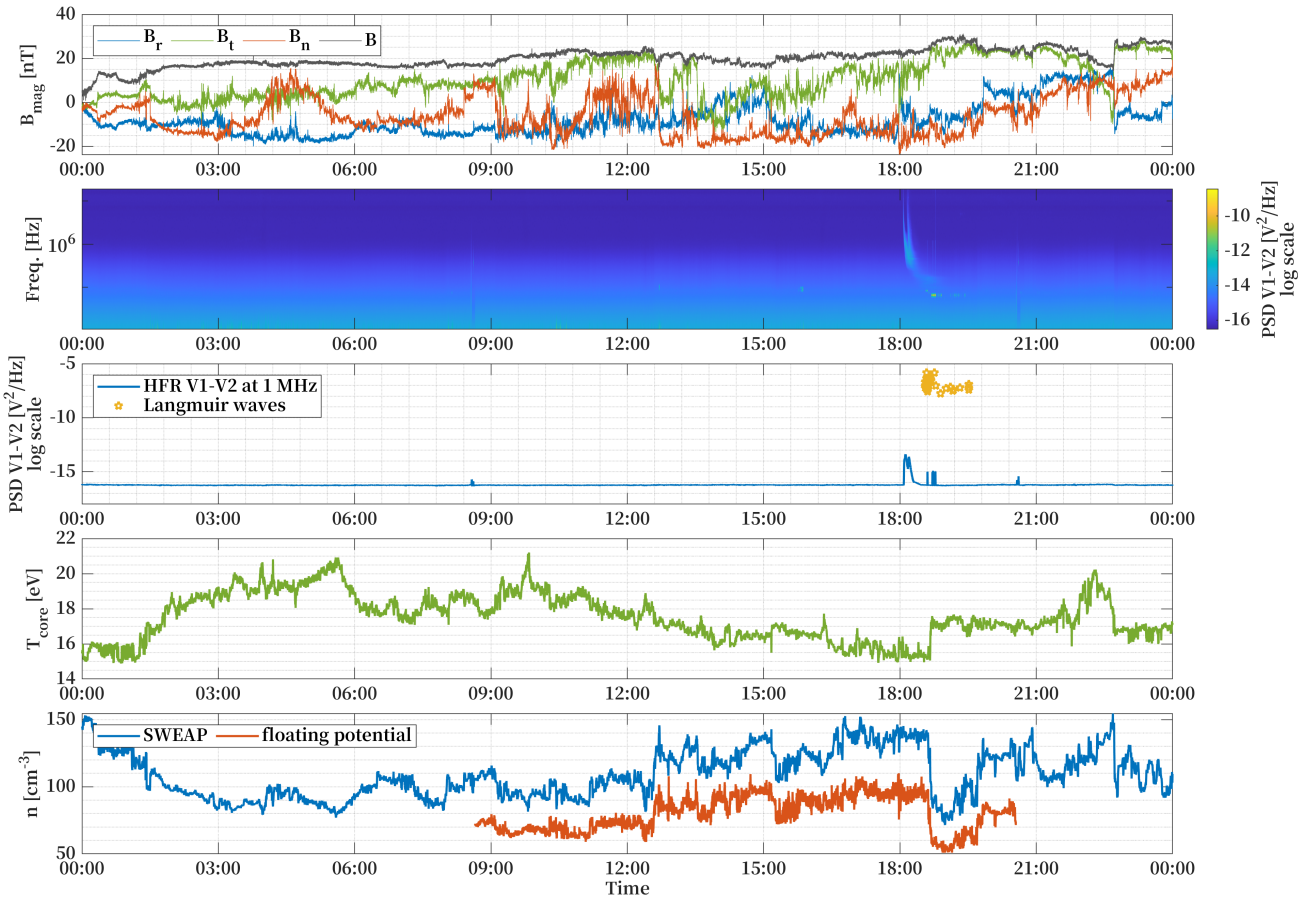

Figure 5.2: Data, measured by *Parker Solar Probe* on 27th of May 2020. From top to bottom: Magnetic field components ins RTN reference frame, radial (blue), tangential (green), normal (orange) components and module of magnetic field (black), measured by FIELDS/MAG; Power spectral density data (PSD) from FIELDS/RFS measurements; PSD in the 1 MHz frequency band (related to radio burst) and of beam-generated waves signatures; Core electron temperature measure by SWEAP; Number density of core electrons measured by SWEAP (blue line) and number density calculated from the measurements of a spacecraft potential orange line).

triggered, followed by series of quasi-simultaneous lower intensity bursts, which have started at around 18:10. A little later during about 1 hour *PSP* was registering intense signals which can be interpreted as Langmuir waves or slow extraordinary z-mode (data on exact frequencies and PSD peak values related to Langmuir waves was kindly provided by A.Larosa). Such a wast time spread of waves measurements may be interpreted as a direct evidence of a *beam-plasma structure*, when faster particles of the beam have arrived earlier than slower ones, both exciting the plasma waves.

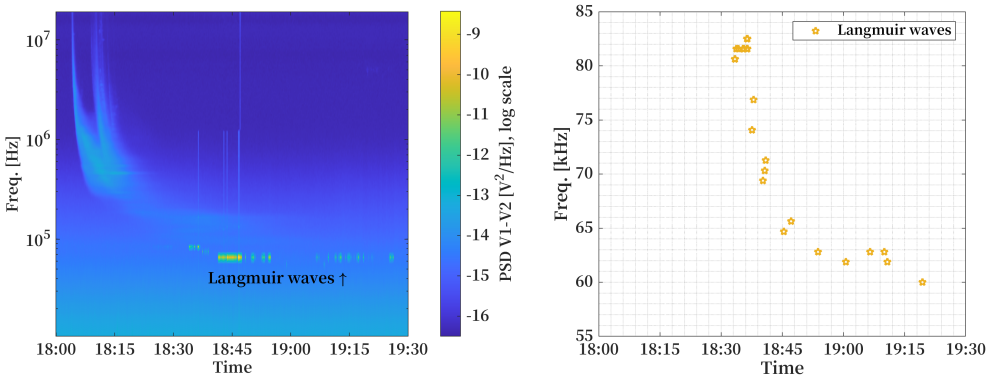

Figure 5.3: Left panel: Type III radio bursts observed on 27th of May 2020 with associated beam-generated waves (FIELDS/RFS observations). Right panel: Frequency expand of the beam-generated waves (FIELDS/TDS observations).

5.3.1 Langmuir waves and z-mode

It is important to mention that even a weak magnetic field changes the characteristics of the wave mode generated by the electron beam. Prior to this moment we have considered a beam-plasma interaction under the approximation of the unmagnetized plasma. However, in a weakly magnetized plasma of solar wind, the beam might generate a z-mode (slow extraordinary branch) with a transverse component rather that a purely longitudinal Langmuir wave. At large wavenumbers, z-mode waves are virtually identical to Langmuir waves (Bale et al., 1998).

The dispersion relation of a slow extraordinary z-mode is

$$\omega \approx \omega_{p_e} \left(1 + 3k_{\parallel}^2\lambda_D^2 + \frac{\Omega_e^2}{2\omega_{p_e}^2}\sin^2\psi\left(1 - \omega_{p_e}^2/k^2c^2\right)\right), \tag{5.1}$$

where $k_{\parallel}$ is the component of the wavevector parallel to the magnetic field, Ω_e is the electron cyclotron frequency and $\sin\psi = (k^2 - k_{\parallel}^2)/k^2$. The ratio $\Omega_e^2/\omega_{p_e}^2$ is very small in solar wind, typically of order of $10^{-3} \div 10^{-4}$. In the electrostatic limit, when $k^2c^2/\omega_{p_e}^2 \gg 1$, the dispersion relation (5.1) turns into a dispersion relation for the oblique Langmuir wave. The electrostatic limit condition may be rewritten in terms of the refractive index:

$$N^2 = \frac{c^2}{V_{ph}^2} = \frac{k^2c^2}{\omega^2} \gg 1. \tag{5.2}$$

For the waves generated by typical solar electron beams the refraction index is quite high, as $N \approx c/v_b$, and for a 10 keV beam N will be of order of 10. Given that the magnetic field magnitude is small, the dispersion relation (5.1) will be closest to the electrostatic one when $N \sim 1$. Nevertheless, the waves generated by the beam have the wavevectors mostly aligned with the magnetic field, and the most contributing dispersion term is related to the thermal dispersion

$$k_{\parallel}^2\lambda_D^2 \approx k_B T_e/(m_e v_b^2/2), \tag{5.3}$$

and for T_e around 50 eV is of order of 10^{-2}. Thus the thermal dispersion is typically order(s) of magnitude larger than the term related to the magnetic field. Moreover, for the presence of the weak transverse component in the beam-generated waves does not have an impact on the wave conversion into the EM fundamental or harmonic emission (it does not change the calculation of non-linear currents) and thus does not modify our conclusions stated in the previous Chapters. However, it is still important to note that observations indicate the presence of rather EM beam-generated mode than purely electrostatic.

According to the *in situ* measurements in solar wind plasma, the electromagnetic nature of beam-generated waves is manifested in the deviations of the electric field from electrostatic, in particular in the presence of a rotational component of the electric field along the direction of propagation in the inhomogeneous plasma. The rotation of the electric field vector was registered by electric field instrument on board the *WIND* spacecraft and reported by Bale et al. (1998) and Kellogg et al. (1999). Additionally, the magnetic field component of the field associated with slow extraordinary wave mode was recently registered by *PSP* (Dudok de Wit T., private communication). Interestingly, the density fluctuations in plasma have a huge impact on the refractive index of these waves. This results in additional motivation to study the statistical characteristics of the density fluctuations during type III solar radio-bursts.

5.4 Data processing

We have used a high-resolution electron density data that was inferred from spacecraft potential measurements [2] (courtesy of Chris Chen) on the time interval between 08:23:05 and 20:32:58. The average cadence of the data is 0.0137 s. High resolution of density data is necessary in order to analyze the characteristic scales of the density fluctuations, as the smallest scale that we are able to resolve is directly connected to the time interval between two subsequent measurements. For instance, the average time resolution for the ion density measurements performed by SWEAP instrument is ~ 0.6 s for Encounter 1 and ~ 0.2 s for Encounter 2. However, with $\Delta t = 0.0137$ s, the smallest scale that we are able to resolve is $v_{SW}\Delta t \approx 5.5$ km ($v_{SW} \approx 400$ km/s is the velocity of the solar wind), which is around ten times smaller than from SWEAP data. To begin with, we have plotted the density data against time to see its variations on the given interval (Fig.5.4).

[2]The description of similar procedure of calculation of density from spacecraft potential performed for *Solar Orbiter* measurements may be found in (Khotyaintsev et al., 2021).

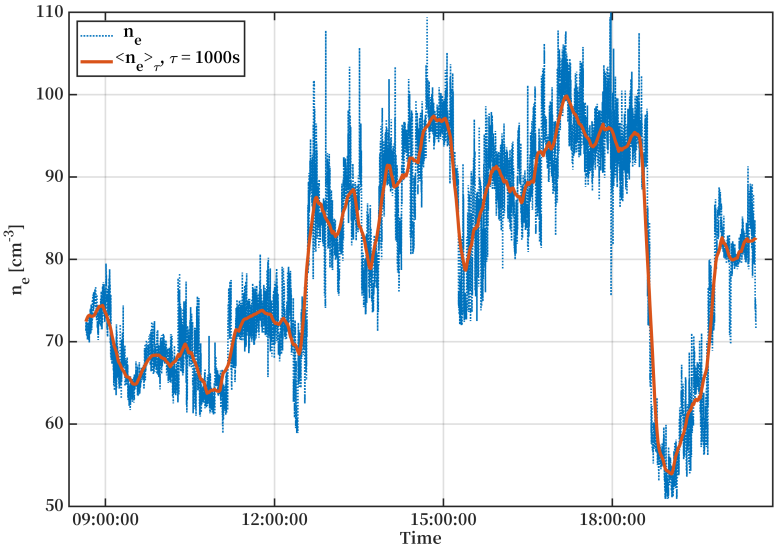

Figure 5.4: Electron density variations during 27 May from 08:23:05 to 20:32:58 (inferred from spacecraft potential measurements, courtesy of C.Chen) and a moving mean taken over the time window of 1000s.

In order to evaluate the density fluctuations on the given $\sim$ 12 hour interval, we will use the technique that is typically applied in this case (e.g., see (Huddleston et al., 1995; Krupar et al., 2020)). We estimate the moving mean of the density $\langle n_e \rangle_\tau$ for different values of a time scale: $\tau = 1$ s, $\tau = 10$ s, $\tau = 100$ s and $\tau = 1000$ s. The limit ourselves with the maximum value of 1000 s what corresponds to $\sim$ 20 mins, as increasing value of the timescale will lead to over-averaging of the statistical properties of the fluctuations mainly because the background, or moving mean density is subject to variations itself. However, this limit is not strict and was chosen for convenience. Thus, the density variations may be estimated as

$$\delta n = n_e - \langle n_e \rangle_\tau, \tag{5.4}$$

yielding different results for each value of a timescale τ. Fig.5.5 demonstrates the PDFs of the density variations for four values of τ.

Using the measurements of the Langmuir waves excited by the electron beams in the solar wind and at the Earth electron foreshock, performed by *CLUSTER*

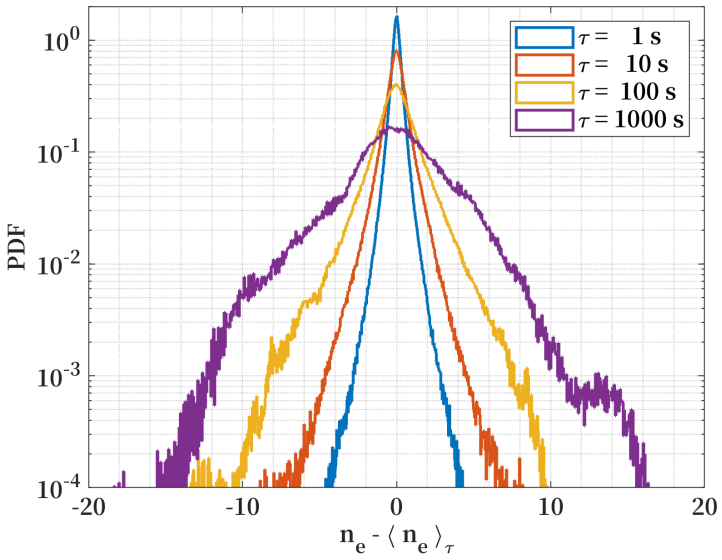

Figure 5.5: Probability density functions of density variations for four different characteristic time scales.

spacecraft, Musatenko et al. (2007) have come to a conclusion that PDFs of logarithmic energy density of the waves belongs rather to a Pearson type IV (for 5 out of 7 analyzed events) or Person type I (2 out of 7) distributions than to log-normal distribution predicted by SGT. Krasnoselskikh et al. (2007) have also analyzed *CLUSTER* data, and compared it with the results of the numerical model of wave propagation in plasma with density inhomogeneties. Both experimental data and modeling have yielded the PDFs of the logarithmic energy density of the waves that were attributed to a Pearson type IV. A statistical analysis of the Langmuir waves associated with type III solar radio bursts, measured by *WIND* spacecraft (Vidojević et al., 2011) has also manifested that the PDFs of power spectral density of such Langmuir waves belong to Pearson type I (28 out of 36 events) or Pearson type IV (7 out of 36). All of these investigations bring up an important question: whether and to which extend do the PDFs of density fluctuations determine the observed properties of Langmuir waves? In order to answer this question we will start with the classification of the PDFs of density variations according to a Pearson distribution system, which is described in detail in the next Section.

5.5 Pearson distribution system

The Pearson distributions are a family of continuous probability distributions, first published by Karl Pearson in 1895. The technique proposed by Pearson allows in the majority of cases to classify a given distribution and choose uniquely to which type it belongs. This technique must be applied only to the single-maximum distributions. Pearson distributions are defined by the differential equation

$$\frac{dp(x)}{dx} = \frac{x-a}{b_0 + b_1 x + b_2 x} p(x), \tag{5.5}$$

where a, b_0, b_1 and b_2 are the constant parameters of the distribution. Depending on their values, there are 12 different types of distributions according to Pearson classification system, and they include many well-known distributions, such a s Beta distribution (Pearson type I), Chi-squared distribution (type III), Cauchy distribution (type IV), Student's t-distribution (type VII), normal distribution (limit of type I, III, IV, V, or VI) etc.

In order to classify a probability distribution with the help of Pearson diagram (see Fig.5.6), one needs to determine its central moments, and after calculate the skewness and the kurtosis. When parameters

$$\beta_1 = skewness^2, \qquad \beta_2 = kurtosis \tag{5.6}$$

are calculated for the specific distribution, one can classify it as one of Pearson types (Elderton, 1906; Tikhonov, 1966). A more recent detailed review of the Pearson classification technique can be found in (Podladchikova et al., 2003).

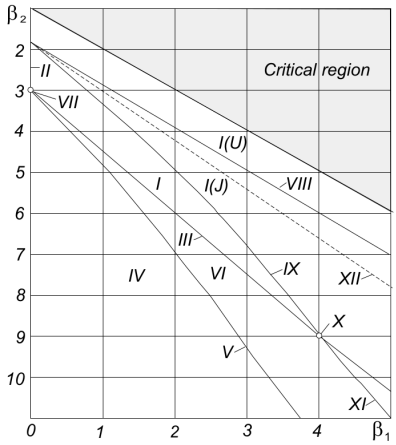

Figure 5.6: The diagram of different distributions of Pearson curves family. The shaded area is forbidden (Podladchikova et al., 2003).

5.6 Probability density functions of electron density variations

The statistical characteristics of the PDFs of density variations are provided in Table 5.2. One may notice that the standard deviation of the PDFs increases with the growth of τ, however, the PDFs are rather self-similar and highly non-Gaussian, belonging to type IV Pearson distribution.

Time scale / $P(n_e - \langle n_e \rangle_\tau)$	τ = 1s	τ = 10s	τ = 100s	τ = 1000s
$\langle n_e \rangle$, $[cm^{-3}]$	80.0151			
$\sigma_{n_e}(\tau)$, $[cm^{-3}]$	0.4429	0.8600	1.6970	3.3733
$\sigma_{n_e}(\tau)/\langle n_e \rangle$	0.0055	0.0107	0.0212	0.0422
β_1	0.0074	0.0041	0.0260	0.0220
β_2	17.7733	11.9901	7.9892	4.5814
Pearson type	IV	IV	IV	IV

Table 5.2: Statistical characteristics of the PDFs of density variations for four different characteristic time scales.

Various authors often estimate the level of the density fluctuations as the ratio between the standard deviation of density variations and the average density $\sigma_{n_e}/\langle n_e \rangle$, which corresponds to our notation $\langle \Delta n \rangle / n_0$ used in previous Chapters. It is important to specify, which timescale genuinely reflects the level of density fluctu-

ations. To find the answer we may address to the estimation, made by Krupar et al. (2020) for the characteristic timescales. They have retrieved the effective spatial scales l_{eff} from Monte Carlo simulations for the values of local plasma frequency 137 kHz and 86 kHz, using empirically derived model of the inner and outer scales of the electron density fluctuations, and have compared these spatial scales with median values of plasma bulk velocities in order to obtain the effective temporal scales of the density turbulence t_{eff}. The value of t_{eff} for both local plasma frequencies was around 300 s. In our case the local plasma frequency may be estimated from the average electron density and is around 80 kHz. Thus we may accept the timescale evaluated by Krupar et al. (2020), as our local plasma frequency is quite close to theirs and the value of the timescale does not vary dramatically with frequency. Fig.5.7 demonstrates the PDF of the density variations on a timescale τ = 300 s, and its fit with the Pearson type IV distribution, and, for comparison, with normal distribution.

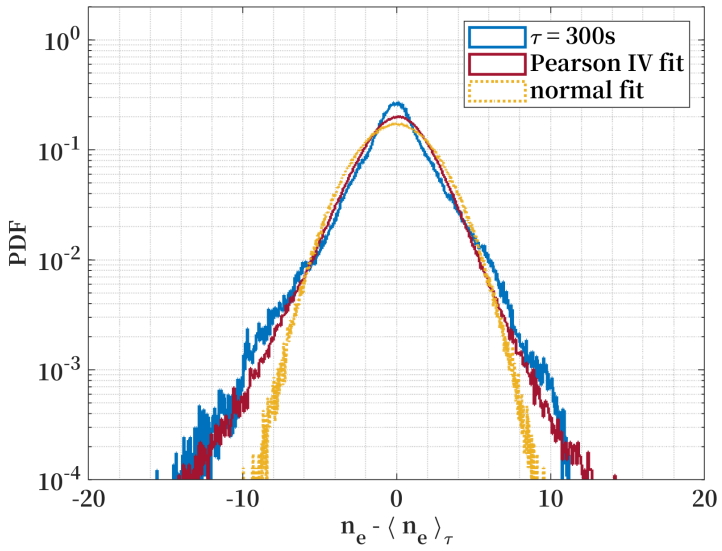

Figure 5.7: Probability density function of the density variations on the characteristic time scale τ = 300 s (blue line), its fit with Pearson type IV distribution (red line) and with normal distribution (yellow line).

In this case $\sigma_{n_e} = 2.3422\ cm^{-3}$, and correspondingly the level of density fluctuations is $\sigma_{n_e}/\langle n_e \rangle = 0.0293$, or around 3%. The distribution unambiguously belongs

to the Pearson type IV with parameters $\beta_1 = 0.0282$ and $\beta_2 = 5.9036$. The result concerning the level of the density fluctuations of 3% at a local plasma frequency of 80 kHz is in a good agreement with the results obtained by Krupar et al. (2020) for the Encounter 1 (7% at 137 kHz) and Encounter 2 (6% for 86 kHz).

One may notice that the distribution of the scales as well as it's median value for the given level of density fluctuations of 3% somewhat differ from the $P(L)$ and L_{sc} used in a previous Chapter and obtained in (Krasnoselskikh et al., 2019). For instance, for the same level of density fluctuations $L_{sc} \approx 50$ km. We are planning to investigate this discrepancy in a more detail.

5.7 Conclusions

We have performed a preliminary analysis of the electron density fluctuations measured *in situ* by *Parker Solar Probe* spacecraft during 12 hours within the Encounter 5 phase at a heliocentric distance ~ 0.2 a.u. Additionally, within this time interval Parker has managed to register a number of events interpreted as Langmuir waves, that were associated with the sequence of type III radio bursts observed on that day. A particular study of the statistical features of density variations simultaneous to the observations of Langmuir waves is one of the future objectives of a current investigation.

General study over the whole 12 hour time interval has revealed that density variations are highly non-Gaussian and belong rather to a Pearson type IV distribution. This is consistent with the PDFs of the logarithmic energy density of Langmuir waves observed by *CLUSTER* and *WIND* spacecraft, and is planned to be complemented with the similar measurements by *PSP*. The level of the density fluctuations is about 3% at the effective turbulence scale length (estimated approximately).

As a next step we want to perform a more detailed analysis of the density fluctuations and their spatial scales, possibly by splitting the 12 hour interval into several

smaller ones in order to exclude the dramatic variations of the moving average of the density, and see the fluctuations more 'locally'. And, of course, we intend to analyze the density variations inside the *source region* of the type III radio bursts.

5.8 Résumé en français

Nous avons effectué une analyse préliminaire des fluctuations de densité électronique mesurées *in situ* par le vaisseau spatial *Parker Solar Probe* pendant 12 heures au cours de la phase Encounter 5 à une distance héliocentrique de $\sim$ 0.2 u.a. De plus, dans cet intervalle de temps, Parker a réussi à enregistrer un certain nombre d'événements interprétés comme des ondes de Langmuir, qui étaient associés à la séquence de sursauts radio de type III observés ce jour-là. Une étude particulière des caractéristiques statistiques des variations de densité simultanées aux observations des ondes de Langmuir est l'un des objectifs futurs d'une enquête en cours.

Une étude générale sur l'ensemble de l'intervalle de temps de 12 heures a révélé que les variations de densité sont très non gaussiennes et appartiennent plutôt à une distribution de Pearson de type IV. Ceci est cohérent avec les PDF de la densité d'énergie logarithmique des ondes de Langmuir observées par les sondes spatiales *CLUSTER* et *WIND*, et devrait être complété par des mesures similaires par *PSP*. Le niveau des fluctuations de densité est d'environ 3% à la longueur effective de l'échelle de turbulence, qui a été estimée approximativement. Comme étape suivante, nous voulons effectuer une analyse plus détaillée des fluctuations de densité et de leurs échelles spatiales, éventuellement en divisant l'intervalle de 12 heures en plusieurs plus petits afin d'exclure les variations dramatiques de la moyenne mobile de la densité, et voir le fluctuations plus «localement».

Chapter 6

Discussion and Conclusions

6.1 Introduction

In the current Chapter we will draw a line under all that we have considered in this manuscript and highlight some important conclusions. The goal of this work was to emphasize the important role of the random density fluctuations in all the stages of the generation of type III radio bursts - from electron beam relaxation in plasma to the formation of a second harmonic radio emission. An important remark that was made all the way throughout this manuscript, is that the density fluctuations that have an influence on the physical processes, related to type III radio bursts, have an amplitude that exceeds the Langmuir wave dispersion:

$$\delta n/n_0 \gg 3k^2\lambda_D^2. \tag{6.1}$$

In the opposite case the processes resemble closely the ones in a homogeneous plasma, and the predictions of the theory in such case is far from agreement with the observations. However, numerous *in situ* measurements indicate that the condition (6.1) is satisfied in solar wind plasma at around 1 a.u. and at smaller heliocentric distances.

6.2 Beam-plasma interaction in a randomly inhomogeneous plasma

Having followed the development of the theory of the beam-plasma interaction, we have shown that consideration of plasma as a homogeneous medium has led to a contradiction between the predictions of the theory and the empirical evidence. After multiple direct and indirect observations of the density fluctuations in the solar wind, it was natural to take them into consideration when describing the relaxation of the electron beam in plasma, as it was done within the framework of a probabilistic model of beam-plasma interaction. This model yields plausible predictions not only of the asymptotic state of the system, but also allows to follow the dynamics of the physical processes that occur during the beam relaxation.

According to the probabilistic model, the maximum of energy density of Langmuir waves reached during the relaxation is

$$W_{l_{\max}} = (v_b^2/v_T^2)\chi(\langle\Delta n\rangle/n_0)n_b m_e v_b^2/6, \tag{6.2}$$

where we have rewritten the initial energy density of the beam as $W_{b_0} = n_b m_e v_b^2/2$. The linear increment of growth of such Langmuir waves may be estimated as

$$\gamma_{lin} = \xi(\langle\Delta n\rangle/n_0)\omega_{p_e}(n_b/n_0)(v_b^2/\Delta v_b^2), \tag{6.3}$$

here $\chi(\langle\Delta n\rangle/n_0)$ is the coefficient characterizing the ratio of the maximum energy density of Langmuir waves in inhomogeneous plasma with respect to initial electron beam energy (see Fig.2.11b) and $\xi(\langle\Delta n\rangle/n_0)$ is the ratio of the increment of the instability in inhomogeneous case with respect to the increment in homogeneous case. In order to estimate it in computer simulations of the beam-plasma interaction, we have made direct evaluation of the time of instability development, raising time t_r for different beam velocities and levels of the density fluctuations as shown on the

Fig.2.11. Values of the $\chi(\langle\Delta n\rangle/n_0)/\xi(\langle\Delta n\rangle/n_0)$ typically vary from 10 to 70. We will use this results in order to estimate the efficiency of conversion of the Langmuir waves into a harmonic radio emission of type III radio bursts.

6.3 Fundamental electromagnetic emission in a randomly inhomogeneous plasma

Having considered various mechanisms that attempted to explain the generation of an EM emission of type III radio bursts at a fundamental frequency and we have come to a conclusion that one of the most important roles may be played by a linear mode conversion in a presence of density fluctuations.

According to an analytical expression derived by Krasnoselskikh et al. (2019), the efficiency of Langmuir waves conversion at a fundamental frequency depends on the plasma density as:

$$K_{\omega_{pe}} \sim \omega_{pe}^{-1/3} \sim n_0^{-1/6}. \tag{6.4}$$

At the same time it depends on the level of density fluctuations as

$$K_{\omega_{pe}} \sim L_{sc}^{-1/3} \sim (\langle\Delta n\rangle/n_0)^{1/3}. \tag{6.5}$$

The *in situ* observations confirm that the amplitude of density fluctuations in solar wind plasma slowly increases towards the smaller heliocentric distances. One can notice that the implicit dependencies on the heliocentric distance are quite weak and the efficiency should be of order of $10^{-3} \div 10^{-4}$ on a considerable interval of heliocentric distances (see Fig.2.12).

6.4 Harmonic electromagnetic emission in a randomly inhomogeneous plasma

We have suggested that a harmonic emission in inhomogeneous plasma may be formally considered as originating from two different sources: quasi-homogeneous plasma and density clumps. However, in both cases a presence of a density clump is required in order to create a population of the reflected waves. For the first case we have made the following assumptions: (1) coalescence takes place in homogeneous plasma, (2) the spectrum of forward moving and reflected Langmuir waves is Gaussian, (3) the population of reflected waves is the result of the reflection of a part of forward moving population from density irregularities, reflection process is taken into account by means of a coefficient P_{ref}, (4) two coalescing Langmuir waves meet head-on (HOA). For the second case, we used the system of equations proposed by Zakharov (1972). The assumptions that we have made when deriving the solution were: (1) linear dispersion is less significant compared to the effect of density fluctuations, i.e. the condition 6.1 is satisfied (2) $k_l L_{sc} \gg 1$, i.e. characteristic scales of density gradients inside density clumps are significantly larger than the wavelength of Langmuir wave, (3) $\psi \ll 1$, i.e. incident Langmuir wave should be closely aligned with the direction of a density gradient and, consequently, almost anti-parallel with the reflected wave (HOA), (4) clumps are approximately spherical with the electron density increasing linearly towards their center, (5) radio emission is formed within the conversion region, (6) quadruple component of harmonic emission is dominant. In both cases plasma is unmagnetized and we consider only the conversion of Langmuir waves into *harmonic* emission. This way we have obtained analytical expressions for energy density of harmonic radio emission for both cases.

6.4.1 Efficiency of the waves conversion

Now we are interested in a comparison between the two mechanisms suggested for the generation of the harmonic emission. In both cases, the energy density of EM harmonic emissions is expressed in terms of energy density of Langmuir waves. To obtain a quantitative evaluation and deduce scaling laws for the dependencies of EM wave intensity, we use the results of probabilistic model of beam-plasma interaction. The assumptions used for the evaluation of harmonic emission from a quasihomogeneous plasma also allow to apply the obtained results to type II solar radio bursts. The efficiency of conversion of Langmuir waves into harmonic emission by definition is

$$K_{2\omega_{pe}} = \frac{W_{t_{\max}}}{W_{l_{\max}}}, \tag{6.6}$$

and in a quasihomogeneous plasma it takes a following form:

$$K_{2\omega_{pe}}^{homog} = \frac{\chi(\langle\Delta n\rangle/n_0)}{\xi(\langle\Delta n\rangle/n_0)}\Lambda\frac{m_e\Delta v_b^2}{k_BT_e}\frac{P_{ref}(1-P_{ref})}{2400\pi^4}\left(\frac{v_b}{v_T}\right)^2\left(\frac{k_b}{\Delta k_b}\right)^4\frac{\mathbf{k}_t^5}{k_b^5}. \tag{6.7}$$

Taking into account that $k_t = \sqrt{3}\omega_{p_e}/2c$, $k_b = \omega_{p_e}/v_b$ and $\Delta k_b/k_b \simeq \Delta v_b/v_b$, we obtain

$$K_{2\omega_{pe}}^{homog} = \frac{\sqrt{3}}{38400\pi^4}\Lambda P_{ref}(1-P_{ref})\frac{\chi(\langle\Delta n\rangle/n_0)}{\xi(\langle\Delta n\rangle/n_0)}\left(\frac{v_b}{c}\right)^9\left(\frac{v_b}{\Delta v_b}\right)^2\left(\frac{m_ec^2}{k_BT_e}\right)^2. \tag{6.8}$$

As a next step, we estimate the efficiency of conversion of a Langmuir wave into harmonic EM emission in the vicinity of reflection points. In this case the maximum energy density of harmonic emission $W_{t_{\max}}$ from Eq.(6.6) can be estimated as $\langle W_t^{inhom}\rangle_{\psi,\delta n,L}$ and consequently we obtain

$$K_{2\omega_{pe}}^{inhom} = \frac{25\sqrt{6}}{3}\epsilon\chi(\langle\Delta n\rangle/n_0)P_{ref}\frac{n_b}{n_0}\frac{v_b}{c}\left(\frac{v_T}{c}\right)^2\left(\frac{k_l^2\lambda_D^2}{\langle\Delta n\rangle/n_0}\right)^2\frac{\omega_{p_e}^2L_{sc}^2}{c^2}. \tag{6.9}$$

The dependence of the efficiency coefficients $K_{2\omega_{pe}}^{homog}$ and $K_{2\omega_{pe}}^{inhom}$ on the plasma temperature and electron plasma frequency respectively vs electron beam velocity is presented on Figure 6.1.

6.4.2 Directivity of harmonic emission

Directivity of harmonic emission of type III radio bursts in homogeneous plasma has been extensively discussed shortly after the suggestion of plasma emission mechanism. Ever since the harmonic emission was always described as quadrupolar, with the petals of a radiation pattern aligned with the direction of the background magnetic field. Angular range of visibility of such harmonic emission was established to be dependant on the value of beam velocity, and was found to be typically larger for smaller values of beam velocity (see, for example (Zheleznyakov & Zaitsev, 1970)).

The harmonic emission from density inhomogeneity, studied by Tkachenko et al. (2021) is also quadrupolar. But, unlike the aforementioned, it produces EM emission in the parallel and perpendicular directions with respect to the electron beam direction (see Fig.6.2). In this context, we have roughly implied the equivalence of the direction of density gradient inside density clump and the direction of electron beam, mentioning the following conditions: (1) angular range of directivity of Langmuir waves, generated by electron beam, is typically quite narrow (see Section 2.3.2), (2) harmonic emission inside the clumps can be generated only for an incident Langmuir wave that is highly aligned with density gradient direction, as the angle of incidence ψ, that allows successful production of harmonic, is strictly determined by beam velocity: $\psi \approx \sqrt{3}v_b/2c$, and is small ($\lesssim 10^o$).

We can schematically compare two aforementioned radiation patterns by positioning them against the direction of electron beam (Fig.6.2). Here we do not precisely represent magnitudes of relevant intensity or angular range of radiation, but rather to give a formal comparison of major emission directions, given by these two mechanisms combined. Disregarding that propagation effects, such as refrac-

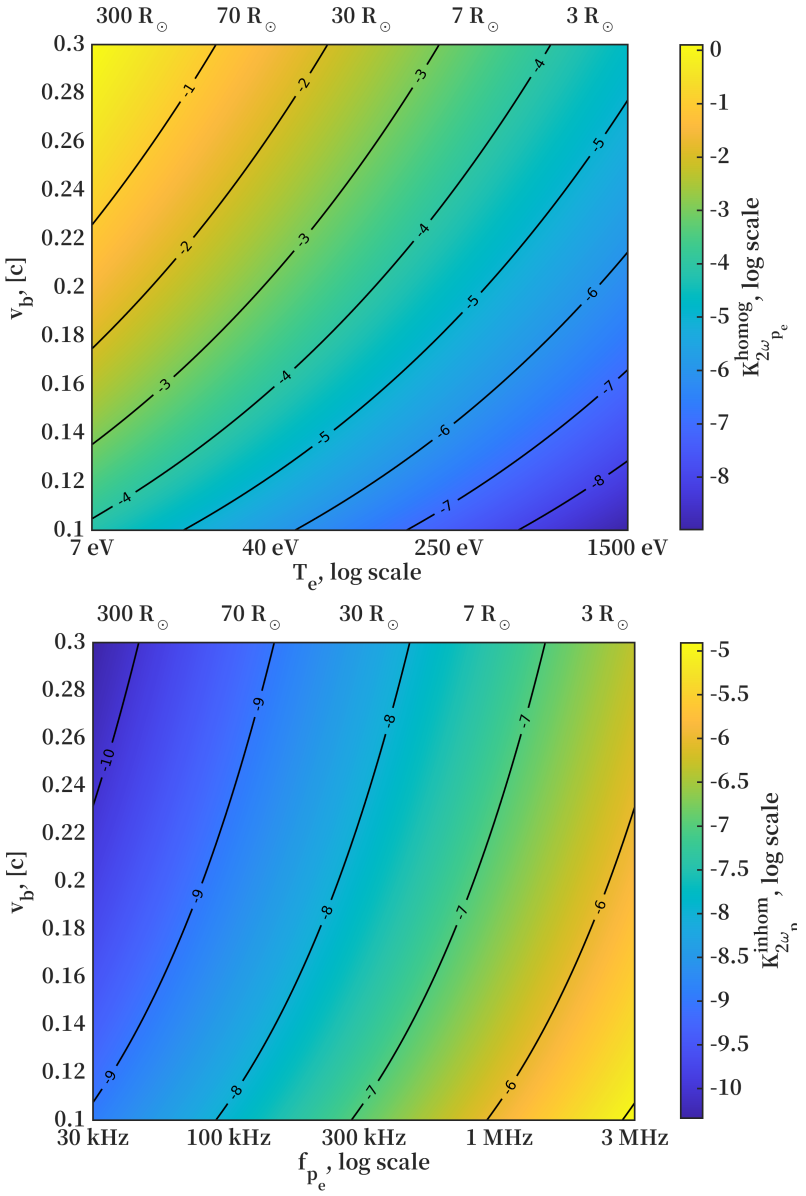

Figure 6.1: Efficiency of conversion of beam-generated Langmuir waves to harmonic EM emission in homogeneous (left panel) and inhomogeneous (right panel) plasma. Radial distance from the Sun in solar radii was inferred from temperature and ion density scaling for slow solar wind by Meyer-Vernet & Issautier (1998). Upper panel: $K^{homog}_{2\omega_{pe}}$ vs electron beam velocity v_b and electron temperature T_e. Parameters are: $\chi/\xi = 1$, $\Lambda = 10$, $P_{ref} = 0.5$, $\Delta v_b/v_b = 1/3$. Lower panel: $K^{inhom}_{2\omega_{pe}}$ vs electron beam velocity v_b and electron plasma frequency f_{p_e}. Parameters are: $\epsilon = 0.75$, $P_{ref} = 0.5$, $n_b = 2.5 \cdot 10^{-5} n_0$, $T_e = 100$ eV, $\langle \Delta n \rangle / n_0 = 0.1$ (corresponding $\chi \approx 0.1$, $L_{sc} \approx 1.4 \cdot 10^6$ cm) (Tkachenko et al., 2021).

tion, absorption and reflection (of backward-emitted emission) cause the widening of angular range, where harmonic emission from homogeneous plasma is visible, they are insufficient to explain a widespread visibility of harmonic emission of type III radio bursts (Thejappa et al., 2007). As such, the mechanism of generation of radio emission inside density clumps adds parallel and perpendicular-directed radiation to conventional harmonic radiation pattern and contributes to general visibility of harmonic emission of type IIIs.

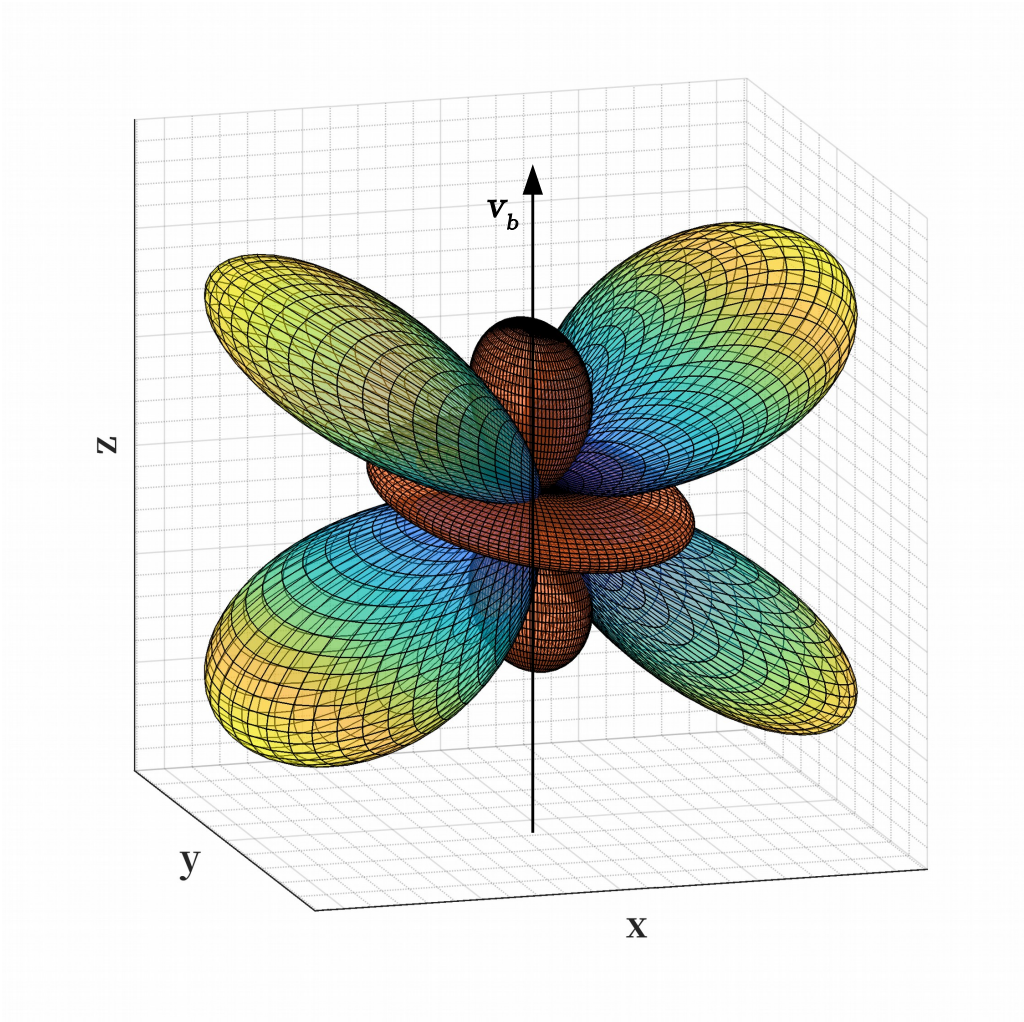

Figure 6.2: A schematic radiation pattern of harmonic EM emission, produced via plasma emission mechanism in homogeneous plasma (multi-colored) and via Langmuir wave coalescence inside density clumps (orange). Here the ratio between homogeneous and inhomogeneous parts is chosen to be 5:1 (Tkachenko et al., 2021).

6.4.3 Radiation intensity in solar corona and solar wind

Observations of type III radio bursts indicate, that fundamental-harmonic pairs comprise the majority of radio bursts in high frequency range. The fundamental usually begins below 100 MHz, while harmonic can begin as high as $\sim$ 500 MHz (Dulk & Suzuki, 1980). At the same time, rarity of fundamental emission in 100-500 MHz remains unexplained, as the absorption due to inverse bremsstrahlung becomes significant only above around 500 MHz for fundamental and above 1 GHz for harmonic emission (Reid & Ratcliffe, 2014). This might indicate that in corona and it's proximity the efficiency of conversion of Langmuir waves into EM radio emission is higher for certain mechanisms of harmonic radiation generation. Further we will formally discuss intensity of the radiation remembering it's simple relation to the energy density of the waves $I \sim W_t$.

We have revisited a well-known result for harmonic emission from homogeneous plasma and obtained an analytical result that is different from one obtained by Willes et al. (1996). We have shown that the assumptions used by Willes et al. (1996) are not always justified and they sufficiently underestimate the EM wave amplitude. We have performed the direct calculations for a general case. According to our result, intensity of such emission is much higher then it was predicted. Such emission is more efficiently produced for larger ratio of v_b to c and smaller electron temperatures T_e (see the left panel of Fig.6.1). As electron temperature is decreasing with heliocentric distance, we can infer a dependence of T_e on radial distance from the Sun, making use of one of solar wind models (e.g. Meyer-Vernet & Issautier (1998)), and make a reference between the scales of domination of harmonic emission from homogeneous plasma and density clumps.

Harmonic emission from density clumps is the most intense at smaller heliocentric distances. Its efficiency of generation is higher for smaller ratios of v_b to c and for smaller level of density fluctuations (see the right panel of Fig.6.1). Here we note that we have applied a constant level of electron temperature T_e and density

fluctuations throughout the whole plasma frequency interval. Recent studies show, that according to *in situ* measurements of *Parker Solar Probe*, the level of density fluctuations at around 36 $R_\odot$ is about 0.06-0.07, and is predicted to grow up to ~ 0.2 to the distance of a few solar radii (Krupar et al., 2020). On the right panel of Fig.6.1 we implied a level of density fluctuations $\langle \Delta n \rangle / n_0 = 0.1$.

As we compare the efficiency of conversion of Langmuir waves into harmonic emission and thus indirectly the relevant intensities, we see that emission from density clumps can become as important as the emission from quasihomogeneous plasma at around a few solar radii, closer to low corona.

6.5 Conclusions

It is widely accepted that relative electron density fluctuations in solar wind affect the propagation of radio emission. At the same time, there are very few studies of the impact of these inhomogeneities on the process of generation of such emission. In current manuscript we have attempted to cover the range of contributions that were already made to the investigation of the various stages of generation of type III emission, such as the excitation of Langmuir waves by an energetic electron beam, generation of the EM emission at a fundamental frequency. In addition, we have considered the generation of harmonic radio emission via $l + l' \rightarrow t$ process under two different circumstances: in a quasihomogeneous plasma (coalescence of two nearly oppositely directed Langmuir waves, which was somewhat already studied before) and inside structures, formed by density fluctuations with increasing density gradient (coalescence of Langmuir wave with it's reflected part in the vicinity of the reflection point). For each of the stages we have provided the spatial scalings and dependencies on the level of the density fluctuations.

We have estimated the efficiency of the conversion of the beam-generated Langmuir waves into harmonic EM emission from both regions of emission. To sum up,

the following conclusions can be made:

(1) direct calculation of the generation of harmonic EM emission via the process of coupling of primary beam-generated Langmuir wave with the reflected wave in quasihomogeneous plasma yields a higher radiation intensity than found previously (e.g. by Willes et al. (1996)),

(2) a new model of generation of harmonic emission inside density clumps close to the region of reflection of Langmuir waves demonstrates the efficiency of conversion of Langmuir waves into EM waves that is under certain conditions comparable with the aforementioned quasihomogeneous plasma emission, and prevails at smaller heliocentric distances,

(3) EM radiation from density clumps may be important for the visibility of the harmonic emissions of type III radio bursts.

We have also analyzed the density fluctuations measured by *Parker Solar Probe* spacecraft during 12 hours within its Encounter 5 phase of orbit. On the given time interval there were series of type III radio bursts observed together with the associated Langmuir waves, which indicates that the spacecraft was performing measurements directly inside the *source region* of the type IIIs. We have estimated the level of the density fluctuations to be around 3% and have shown that the probability density function of the fluctuations manifests rather significant deviations from Gaussian distribution.

6.6 Résumé en français

Il est largement admis que les fluctuations de densité d'électrons relatives dans le vent solaire affectent la propagation des émissions radio. Dans le même temps, il existe très peu d'études sur l'impact de ces inhomogénéités sur le processus de génération de telles émissions. Dans le manuscrit actuel, nous avons tenté de couvrir la gamme des contributions qui ont déjà été apportées à l'étude des différentes

étapes de génération d'émission de type III, telles que l'excitation des ondes de Langmuir par un faisceau d'électrons énergétique, la génération de l'émission électromagnétique à un la fréquence fondamentale. De plus, nous avons considéré la génération d'émission radio harmonique via le processus $l + l' \rightarrow t$ dans deux circonstances différentes: dans un plasma quasi homogène (coalescence de deux ondes de Langmuir presque opposées, ce qui était un peu déjà étudié auparavant) et à l'intérieur des structures, formées par des fluctuations de densité avec un gradient de densité croissant (coalescence de l'onde de Langmuir avec sa partie réfléchie au voisinage du point de réflexion). Pour chacune des étapes, nous avons fourni la mise à l'échelle spatiale et les dépendances sur le niveau des fluctuations de densité.

Nous avons estimé l'efficacité de la conversion des ondes de Langmuir générées par le faisceau en émission électromagnétique harmonique à partir des deux régions d'émission. Pour résumer, les conclusions suivantes peuvent être tirées:

(1) le calcul direct de la génération d'émission EM harmonique via le processus de couplage de l'onde de Langmuir générée par le faisceau primaire avec l'onde réfléchie dans un plasma quasi homogène donne une intensité de rayonnement plus élevée que celle trouvée précédemment (par exemple par Willes et al. (1996)),

(2) un nouveau modèle de génération d'émission harmonique à l'intérieur des amas de densité proches de la région de réflexion des ondes de Langmuir démontre l'efficacité de conversion des ondes de Langmuir en ondes EM qui est dans certaines conditions comparable à l'émission de plasma quasi homogène susmentionnée, et prévaut à distances héliocentriques plus petites,

(3) Le rayonnement électromagnétique des amas de densité peut être important pour la visibilité de l'émission harmonique des sursauts de type III.

Nous avons également analysé les fluctuations de densité mesurées par le vaisseau spatial *Parker Solar Probe* pendant 12 heures au cours de sa phase d'orbite Rencontre 5. Sur l'intervalle de temps donné, des séries de sursauts radio de type III ont été observées avec les ondes de Langmuir associées, ce qui indique que l'engin

spatial effectuait des mesures directement à l'intérieur de la *région source* des types III. Nous avons estimé le niveau des fluctuations de densité à environ 3% et avons montré que les fonctions de densité de probabilité des fluctuations manifestent des écarts assez importants par rapport à la distribution gaussienne.

Bibliography

Artsimovich, L., & Sagdeev, R. 1979, MAtom

Bale, S., Kellogg, P. J., Goetz, K., & Monson, S. 1998, Geophysical research letters, 25, 9

Bardwell, S., & Goldman, M. 1976, The Astrophysical Journal, 209, 912

Breizman, B., & Ryutov, D. 1969, Sov. Phys. JETP, 57, 1401

—. 1971, SOVIET PHYSICS JETP, 33

Brejzman, B., & Pekker, L. 1978, Physics Letters A, 65, 121

Cairns, I. H. 1987, Journal of plasma physics, 38, 179

Cairns, I. H., & Robinson, P. 1997, Geophysical research letters, 24, 369

—. 1999, Physical review letters, 82, 3066

Celnikier, L., Harvey, C., Jegou, R., Moricet, P., & Kemp, M. 1983, Astronomy and Astrophysics, 126, 293

Celnikier, L., Muschietti, L., & Goldman, M. 1987, Astronomy and Astrophysics, 181, 138

Chen, C., Salem, C., Bonnell, J., Mozer, F., & Bale, S. 2012, Physical Review Letters, 109, 035001

Chen, C., Sorriso-Valvo, L., Šafránková, J., & Němeček, Z. 2014, The Astrophysical Journal Letters, 789, L8

Chen, F. F., et al. 1984, Introduction to plasma physics and controlled fusion, Vol. 1 (Springer)

DLMF. 2019, *NIST Digital Library of Mathematical Functions*, http://dlmf.nist.gov/, Release 1.0.25 of 2019-12-15. `http://dlmf.nist.gov/`

Drummond, W., & Pines, D. 1962, Nuclear Fusion Supplements, 3, 1049

Dulk, G., & Suzuki, S. 1980, Astronomy and Astrophysics, 88, 203

Dulk, G. A., Leblanc, Y., Robinson, P. A., Bougeret, J.-L., & Lin, R. P. 1998, Journal of Geophysical Research: Space Physics, 103, 17223

Elderton, W. P. 1906, Frequency-curves and Correlation (Institute of Actuaries)

Ergun, R., Larson, D., Lin, R., et al. 1998, The Astrophysical Journal, 503, 435

Ergun, R., Malaspina, D., Cairns, I. H., et al. 2008, Physical review letters, 101, 051101

Erokhin, N., Moiseev, S., & Mukhin, V. 1974, Nuclear Fusion, 14, 333

Fainberg, Y. B., Shapiro, V., & Shevchenko, V. 1970, Soviet Phys. JETP, 30, 528

Fox, N., Velli, M., Bale, S., et al. 2016, Space Science Reviews, 204, 7

Galeev, A., & Krasnoselskikh, V. 1976, ZhETF Pisma Redaktsiiu, 24, 558

Ginzburg, V., & Zheleznyakov, V. 1958, Soviet Astron. AJ, 2, 235

Goldman, M. V., Reiter, G. F., & Nicholson, D. R. 1980, The Physics of Fluids, 23, 388

Goldstein, M. L., Roberts, D. A., & Matthaeus, W. 1995, Annual review of astronomy and astrophysics, 33, 283

Gurnett, D. A., Anderson, R. R., Scarf, F., & Kurth, W. 1978, Journal of Geophysical Research: Space Physics, 83, 4147

Harding, J. C., Cairns, I. H., & Melrose, D. B. 2020, Physics of Plasmas, 27, 020702

Hinkel-Lipsker, D., Fried, B., & Morales, G. 1992, Physics of Fluids B: Plasma Physics, 4, 559

Horbury, T., Wicks, R., & Chen, C. 2012, Space Science Reviews, 172, 325

Huddleston, D., Woo, R., & Neugebauer, M. 1995, Journal of Geophysical Research: Space Physics, 100, 19951

Kellogg, P. 1980, The Astrophysical Journal, 236, 696

Kellogg, P., Goetz, K., Monson, S., & Bale, S. 1999, Journal of Geophysical Research: Space Physics, 104, 17069

Kellogg, P. J., & Horbury, T. 2005, Annales Geophysicae, 23, 3765

Khotyaintsev, Y. V., Graham, D., Vaivads, A., et al. 2021, arXiv preprint arXiv:2103.17208

Kim, E.-H., Cairns, I. H., & Johnson, J. R. 2013, Physics of Plasmas, 20, 122103

Kim, E.-H., Cairns, I. H., & Robinson, P. A. 2007, Physical review letters, 99, 015003

—. 2008, Physics of Plasmas, 15, 102110

Kim, E.-H., Johnson, J. R., Cairns, I. H., & Lee, D.-H. 2009in , American Institute of Physics, 13–20

Kontar, E. P. 2001, Astronomy & Astrophysics, 375, 629

Kontar, E. P., & Reid, H. A. 2009, The Astrophysical Journal Letters, 695, L140

Krafft, C., & Volokitin, A. 2014, The European Physical Journal D, 68, 370

Krafft, C., Volokitin, A., & Krasnoselskikh, V. 2013, The Astrophysical Journal, 778, 111

Krasnoselskikh, V., de Wit, T. D., & Bale, S. 2011, arXiv preprint arXiv:1107.4439

Krasnoselskikh, V., Lobzin, V., Musatenko, K., et al. 2007, Journal of Geophysical Research: Space Physics, 112

Krasnoselskikh, V., Voshchepynets, A., & Maksimovic, M. 2019, The Astrophysical Journal, 879, 51

Krucker, S., Oakley, P., & Lin, R. 2009, The Astrophysical Journal, 691, 806

Krupar, V., Kontar, E. P., Soucek, J., et al. 2015, Astronomy & Astrophysics, 580, A137

Krupar, V., Szabo, A., Maksimovic, M., et al. 2020, arXiv preprint arXiv:2001.03476

Landau, L. D., & Lifshitz, E. M. 2013, Course of theoretical physics (Elsevier)

Lin, R. 1985, Solar Physics, 100, 537

Lin, R., Levedahl, W., Lotko, W., Gurnett, D., & Scarf, F. 1986, The Astrophysical Journal, 308, 954

Lin, R., Potter, D., Gurnett, D., & Scarf, F. 1981, The Astrophysical Journal, 251, 364

Malaspina, D., & Ergun, R. 2008, Journal of Geophysical Research: Space Physics, 113

Malaspina, D. M., Cairns, I. H., & Ergun, R. E. 2012, The Astrophysical Journal, 755, 45

Mann, G., Breitling, F., Vocks, C., et al. 2018, Astronomy & Astrophysics, 611, A57

Melrose, D. 1980a, Space Science Reviews, 26, 3

—. 1980b, New York, Gordon and Breach Science Publishers, 1980. 430 p

—. 1987, in Particle Acceleration and Trapping in Solar Flares (Springer), 89–101

—. 2008, Proceedings of the International Astronomical Union, 4, 305

Melrose, D., & Stenhouse, J. 1979, Astronomy and Astrophysics, 73, 151

Melrose, D. B., & Melrose, D. B. 1986, Instabilities in space and laboratory plasmas (Cambridge University Press)

Meyer-Vernet, N., & Issautier, K. 1998, Journal of Geophysical Research: Space Physics, 103, 29705

Mjølhus, E. 1983, Journal of plasma physics, 30, 179

—. 1990, Radio science, 25, 1321

Musatenko, K., Lobzin, V., Soucek, J., Krasnoselskikh, V., & Décréau, P. 2007, Planetary and Space Science, 55, 2273

Neugebauer, M. 1975, Journal of Geophysical Research, 80, 998

—. 1976, Journal of Geophysical Research, 81, 2447

Nishikawa, K., & Ryutov, D. 1976, Journal of the Physical Society of Japan, 41, 1757

Papadopoulos, K., & Freund, H. 1978, Geophysical Research Letters, 5, 881

Podladchikova, O., Lefebvre, B., Krasnoselskikh, V., & Podladchikov, V. 2003, Nonlinear Processes in Geophysics, 10, 323

Prudnikov, A. P., Brychkov, Y. A., & Marichev, O. I. 1986, Integrals and series: special functions, Vol. 2 (CRC Press)

Pulupa, M., Bale, S. D., Badman, S. T., et al. 2020, The Astrophysical Journal Supplement Series, 246, 49

Ratcliffe, H. 2013, PhD thesis, University of Glasgow (United Kingdom)

Reid, H. A., & Kontar, E. P. 2010, The Astrophysical Journal, 721, 864

—. 2013, Solar Physics, 285, 217

Reid, H. A. S., & Ratcliffe, H. 2014, Research in Astronomy and Astrophysics, 14, 773

Robinson, P. 1992, Solar Physics, 139, 147

—. 1995, Physics of Plasmas, 2, 1466

Robinson, P., & Cairns, I. 1993, The Astrophysical Journal, 418, 506

—. 1998, Solar Physics, 181, 363

Robinson, P., Cairns, I., & Gurnett, D. 1992, The Astrophysical Journal, 387, L101

—. 1993, The Astrophysical Journal, 407, 790

Robinson, P., Cairns, I., & Willes, A. 1994, The Astrophysical Journal, 422, 870

Ryutov, D. 1969, Sov. Phys. JETP, 30, 131

Schleyer, F., Cairns, I. H., & Kim, E.-H. 2013, Physics of Plasmas, 20, 032101

—. 2014, Journal of Geophysical Research: Space Physics, 119, 3392

Shaikh, D., & Zank, G. 2010, Monthly Notices of the Royal Astronomical Society, 402, 362

Smith, D., & Sime, D. 1979, The Astrophysical Journal, 233, 998

Stix, T. H. 1992, Waves in plasmas (Springer Science & Business Media)

Sturrock, P. 1964, NASA Special Publication, 50, 357

Thejappa, G., MacDowall, R., & Kaiser, M. 2007, The Astrophysical Journal, 671, 894

Tikhonov, W. 1966, Sov. Radio. Moscow, 678

Tkachenko, A., Krasnoselskikh, V., & Voshchepynets, A. 2021, The Astrophysical Journal, 908, 126

Tsytovich, V. 2012, Nonlinear effects in plasma (Springer Science & Business Media)

Vedenov, A., & Ryutov, D. 1975, RvPP, 6, 1

Vedenov, A., Velikhov, E., & Sagdeev, R. 1961, Nuclear Fusion, 1, 82

—. 1962a, Nuclear Fusion Supplements, 2, 465

Vedenov, A. A., Velikhov, E. P., & Sagdeev, R. Z. 1962b, Quasi-linear theory of plasma oscillations, Tech. rep., Kurchatov Inst. of Atomic Energy, Moscow

Vidojević, S., Zaslavsky, A., Maksimović, M., Dražić, M., & Atanacković, O. 2011, Open Astronomy, 20, 596

Volokitin, A. S., & Krafft, C. 2016, The Astrophysical Journal, 833, 166, doi: 10.3847/1538-4357/833/2/166

—. 2018, The Astrophysical Journal, 868, 104, doi: 10.3847/1538-4357/aae7cc

—. 2020, The Astrophysical Journal Lettersl, 893, L47, doi: 10.3847/2041-8213/ab74de

Voshchepynets, A., & Krasnoselskikh, V. 2013in , Copernicus GmbH, 1379–1385

Voshchepynets, A., & Krasnoselskikh, V. 2015, Journal of Geophysical Research: Space Physics, 120, 10

Voshchepynets, A., Krasnoselskikh, V., Artemyev, A., & Volokitin, A. 2015, The Astrophysical Journal, 807, 38

Voshchepynets, A., Volokitin, A., Krasnoselskikh, V., & Krafft, C. 2017, Journal of Geophysical Research: Space Physics, 122, 3915

Wasow, W. 2018, Asymptotic expansions for ordinary differential equations (Courier Dover Publications)

Willes, A., Robinson, P., & Melrose, D. 1995, Publications of the Astronomical Society of Australia, 12, 197

—. 1996, Physics of Plasmas, 3, 149

Woo, R., & Armstrong, J. 1979, Journal of Geophysical Research: Space Physics, 84, 7288

Zaitsev, V., Mityakov, N., & Rapoport, V. 1972, Solar Physics, 24, 444

Zakharov, V. E. 1972, Sov. Phys. JETP, 35, 908

Zheleznyakov, V., & Zaitsev, V. 1970, Soviet Astronomy, 14, 250

Ziebell, L., Gaelzer, R., Pavan, J., & Yoon, P. 2008, Plasma Physics and Controlled Fusion, 50, 085011

Ziebell, L., Yoon, P., Pavan, J., & Gaelzer, R. 2011, Plasma Physics and Controlled Fusion, 53, 085004

Anna Tkachenko

Le rôle des fluctuations aléatoires de densité dans la génération des sursauts radio solaires de type III

Résumé :

Les sursauts radio solaires de type III font partie des émissions radio les plus intenses du système solaire et sont produites par un processus en plusieurs étapes, qui comprend la génération d'ondes de Langmuir par un faisceau d'électrons et leur conversion en émission électromagnétique fondamentale ou harmonique. Les fluctuations aléatoires de densité du vent solaire jouent un rôle important à chaque étape de ce processus et nous essayons de le couvrir de la manière la plus complète. Nous commençons par la théorie de l'interaction faisceau-plasma, montrant que les fluctuations de densité modifient fortement cette interaction. Le modèle probabiliste récent permet d'obtenir des prédictions bien confirmées par observations. Après avoir examiné les mécanismes suggérés pour expliquer la génération de l'émission fondamentale de type III on a conclu que la conversion de mode linéaire provenant de la réflexion de l'onde de Langmuir par les inhomogénéités peut être un processus dominant. La génération d'une émission harmonique nécessite la présence des ondes de Langmuir se déplaçant vers l'avant et vers l'arrière, donc les réflexions par des inhomogénéités sont cruciales. Nous révisons le mécanisme fonctionnant dans un plasma quasi homogène et suggérons un autre mécanisme qui opère au voisinage immédiat du point de réflexion. Nous comparons l'efficacité de la conversion des ondes de Langmuir en émission harmonique et les diagrammes de rayonnement pour les deux mécanismes. Enfin, nous analysons les fluctuations de densité, mesurées à l'intérieur des régions sources des sursauts radio de type III par la sonde spatiale Parker Solar Probe et étudions leurs propriétés statistiques.

Mots clés : émission radio, vent solaire, fluctuations de densité, électrons énergétiques

On the role of the random density fluctuations in the generation of the type III solar radio bursts

Summary :

Type III solar radio bursts are among the most intense radio emissions in the solar system and are produced via multi-stage process, that includes generation of Langmuir waves by an energetic electron beam and their further conversion into electromagnetic emission at fundamental frequency or its harmonic. Ubiquitous random density fluctuations in solar wind play an important role on each stage of this process and we attempt to cover this role in the most complete manner. We start with the theory of beam-plasma interaction, showing that density fluctuations alter the interaction of the electron beam and plasma waves. We emphasize that recent probabilistic model of beam-plasma interaction allows to obtain predictions that are well confirmed by the observations. After we consider in detail the mechanisms suggested to explain a subsequent generation of a fundamental type III emission and show that the linear mode conversion that occurs during the reflection of Langmuir wave from density inhomogeneities may be a prevailing process. The generation of a harmonic emission requires the presence of the forwards and backwards moving Langmuir waves, thus the reflections from inhomogeneities are crucial. We revise the mechanism operating in a quasihomogeneous plasma and suggest another mechanism which operates in the close vicinity of the reflection point. We evaluate and compare the efficiency of Langmuir wave conversion into harmonic emission and radiation patterns for both mechanisms. And finally, we analyze the density fluctuations, measured inside the source regions of the type III radio bursts by a Parker Solar Probe spacecraft and investigate their statistical properties.

Keywords : radio emission, solar wind, density fluctuations, energetic electrons

UNIVERSITE D'ORLEANS

Laboratoire de Physique et Chimie de l'Evironnement et de l'Espace (LPC2E), 3A Avenue de la Recherche Scientifique, 45071, Orléans, CEDEX 02, France

LPC2E